

Outline

Surface, interface, and nanoscience—short introduction

Some surface concepts and techniques→photoemission

Synchrotron radiation: experimental aspects

Electronic structure—a brief review

**The basic synchrotron radiation techniques:
more experimental and theoretical details**

Core-level photoemission



Valence-level photoemission

Microscopy with photoemission (Later lecturers)

Outline



- Valence-band spectra: low-energy UPS limit and high-energy XPS limit
- Core-level chemical shifts: the potential model
- Core-level chemical shifts: equivalent-core ($Z+1$) and thermochemical energies
- Multiplet splittings
- Spin-orbit splitting, the Fano effect, and spin-polarized outgoing electrons
- Magnetic circular dichroism (MCD) in core-level emission
- Non-magnetic circular dichroism in core-level emission: a.k.a. circular dichroism in angular distributions (CDAD)
- Various other final state effects providing information in core-level spectra

PHOTOELECTRON EMISSION - BASIC MATRIX ELEMENTS + SELECTION RULES:

• ATOMIC-LIKE (LOCALIZED) STATES \Rightarrow CORE:

$$\Psi_i(\vec{r}) = \Psi_{n_i l_i m_i}(r, \theta, \phi) = R_{n_i l_i}(r) Y_{l_i m_i}(\theta, \phi)$$



$$\Psi_f(\vec{r}, \vec{k}_f) = \Psi_{E_f}(\vec{r}, \vec{k}_f)$$

= $4\pi \sum_{l_f m_f} i^{l_f} e^{-i\delta_{l_f}} Y^*_{l_f m_f}(\theta, \phi) Y_{l_f m_f}(\theta, \phi) R_{E_f l_f}(r)$

PHASE SHIFT OF l_f WAVE IN $V(r)$

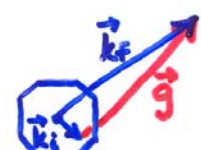
DIPOLE APPROX.: $\text{INT.} \propto |\langle \Psi_f | \hat{\epsilon} \cdot \vec{r} | \Psi_i \rangle|^2 = |\hat{\epsilon} \cdot \langle \Psi_f | \vec{r} | \Psi_i \rangle|^2 \Rightarrow$

EQUIVALENT WITHIN CONSTANT FACTOR

$\Delta l = l_f - l_i = \pm 1$
 TWO CHANNELS
 $\Delta m = m_f - m_i = 0, \pm 1$
 LINEAR POLARIZ.
 $\Delta m = \pm 1$, CIRCULAR POLARIZATION

VALENCE BANDS IN SOLIDS:

• BLOCH-FUNCTION (DELOCALIZED) STATES \Rightarrow VALENCE:



$$\Psi_i(\vec{r}) = u_{\vec{k}_i}(\vec{r}) e^{i\vec{k}_i \cdot \vec{r}}$$

$$\Psi_f(\vec{r}) = u_{\vec{k}_f}(\vec{r}) e^{i\vec{k}_f \cdot \vec{r}}; E_f = \frac{p_f^2}{2m} = \frac{\hbar^2 k_f^2}{2m}$$

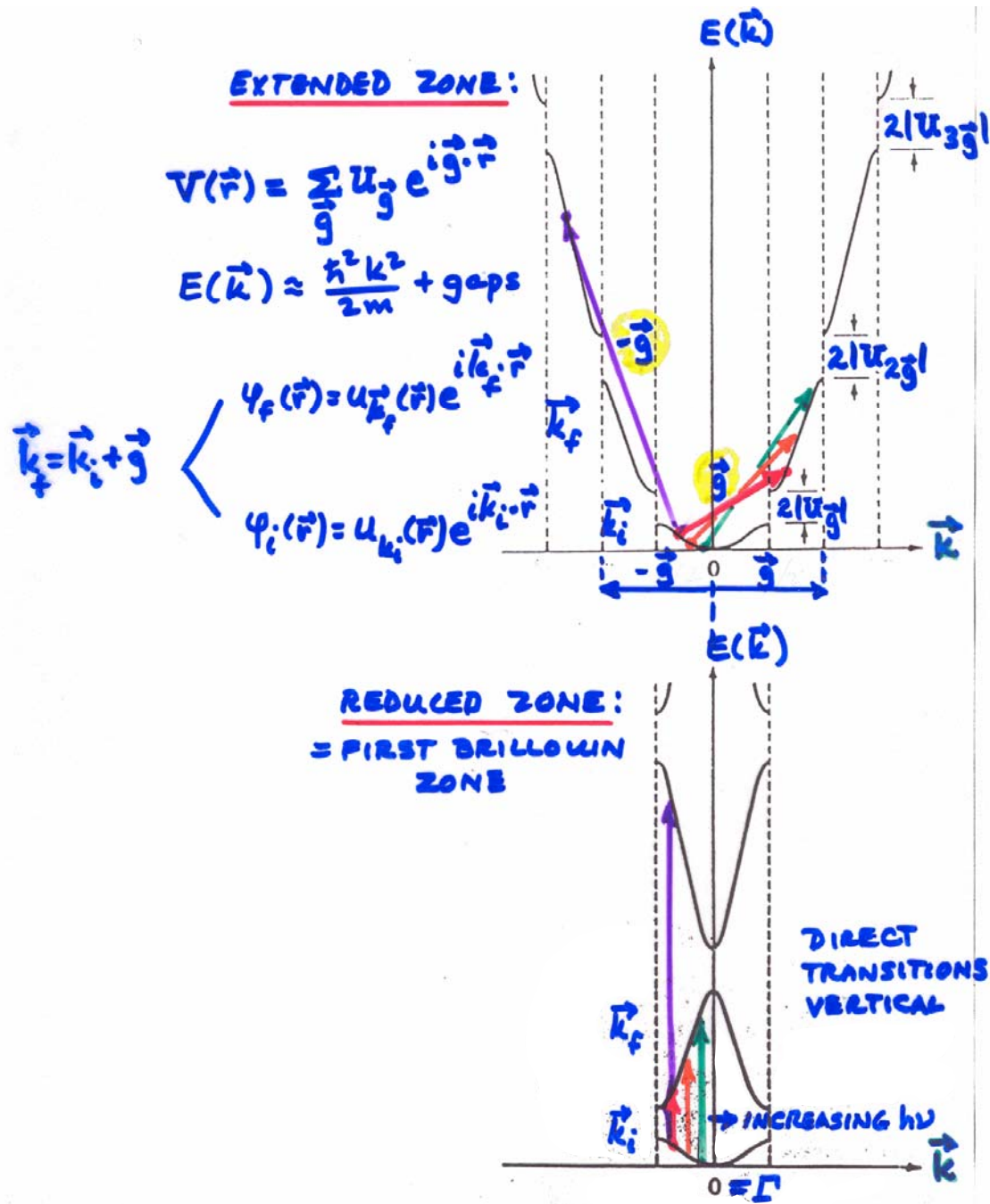
USUALLY NEGIG.

$$|\langle \Psi_f | \hat{\epsilon} \cdot \vec{p} | \Psi_i \rangle|^2 = |\hat{\epsilon} \cdot \langle \Psi_f | \vec{p} | \Psi_i \rangle|^2 \Rightarrow \Delta \vec{k} = \vec{k}_f - \vec{k}_i - \vec{k}_{\text{LW}} + \vec{k}_{\text{PHON-ON}} = \vec{g}_{\text{BULK}} \text{ (or } \vec{g}_{\text{SURF}} \text{)}$$

"DIRECT" TRANSITIONS

BUT LATTICE VIBRATIONS \Rightarrow SUM OVER \vec{k}_{PHONON}
 \Rightarrow FRACTION DIRECT \approx DEBYE-WALLER FACTOR
 $= \exp[-g^2 \bar{u}^2]$

NEARLY-FREE ELECTRONS IN A WEAK PERIODIC POTENTIAL—1 DIM.



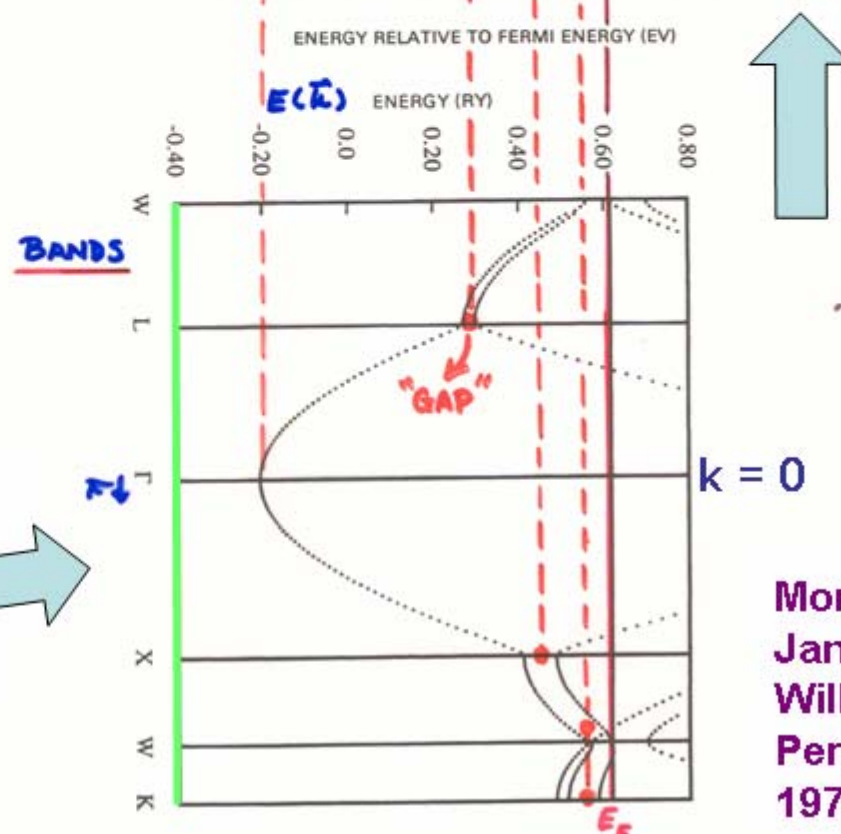
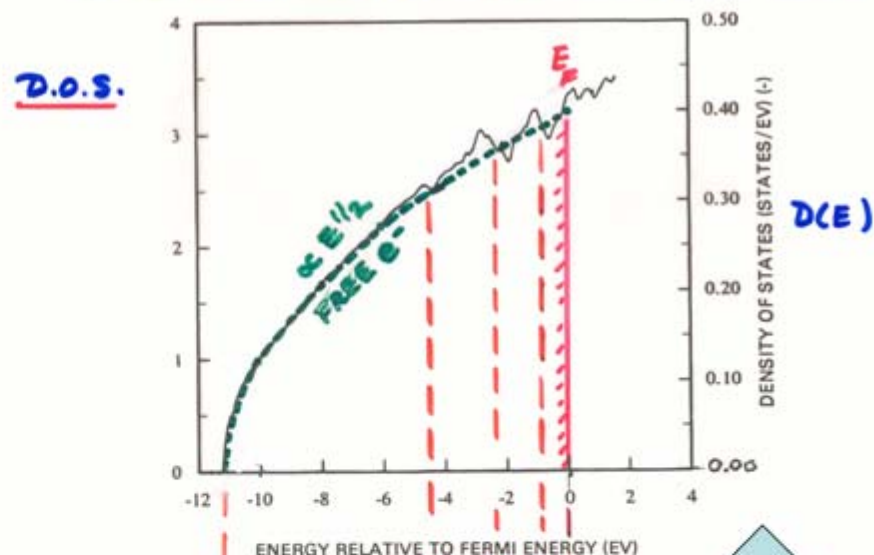
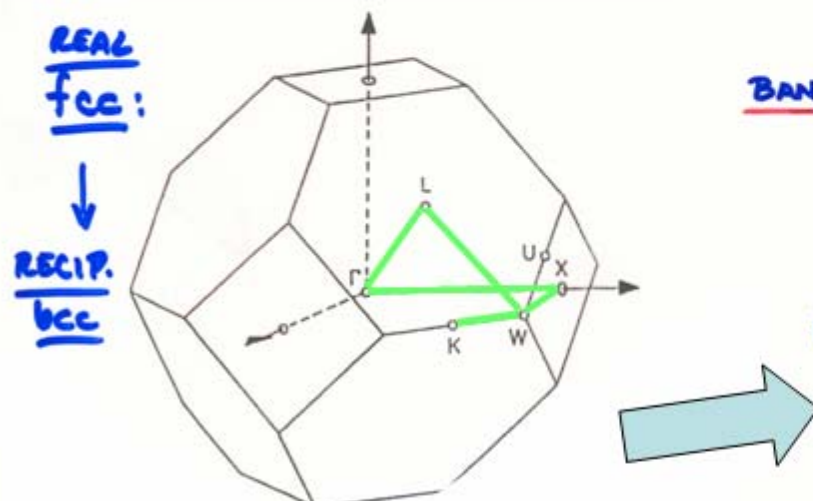
ALUMINUM - ELECTRONIC BANDS + D.O.S.

The electronic structure
of a nearly free-electron
metal—fcc Al

$$\phi(\vec{r}) = u_{\vec{k}}(\vec{r}) e^{i\vec{k}\cdot\vec{r}}; E(\vec{k}) \approx \frac{\hbar^2 \vec{k}^2}{2m}$$

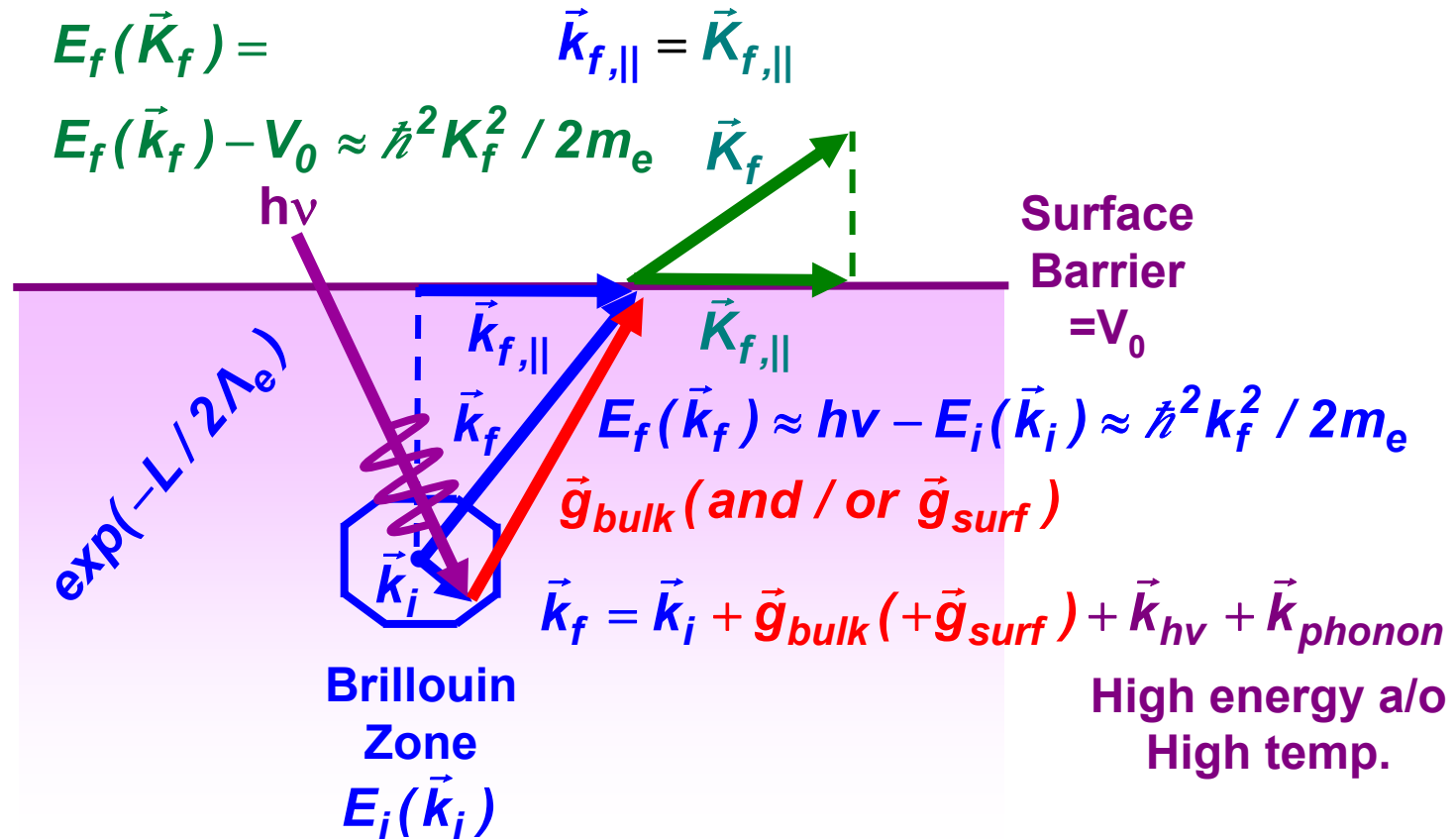
(Bloch)

3D Brillouin zone



Moruzzi,
Janak,
Williams,
Pergamon,
1978

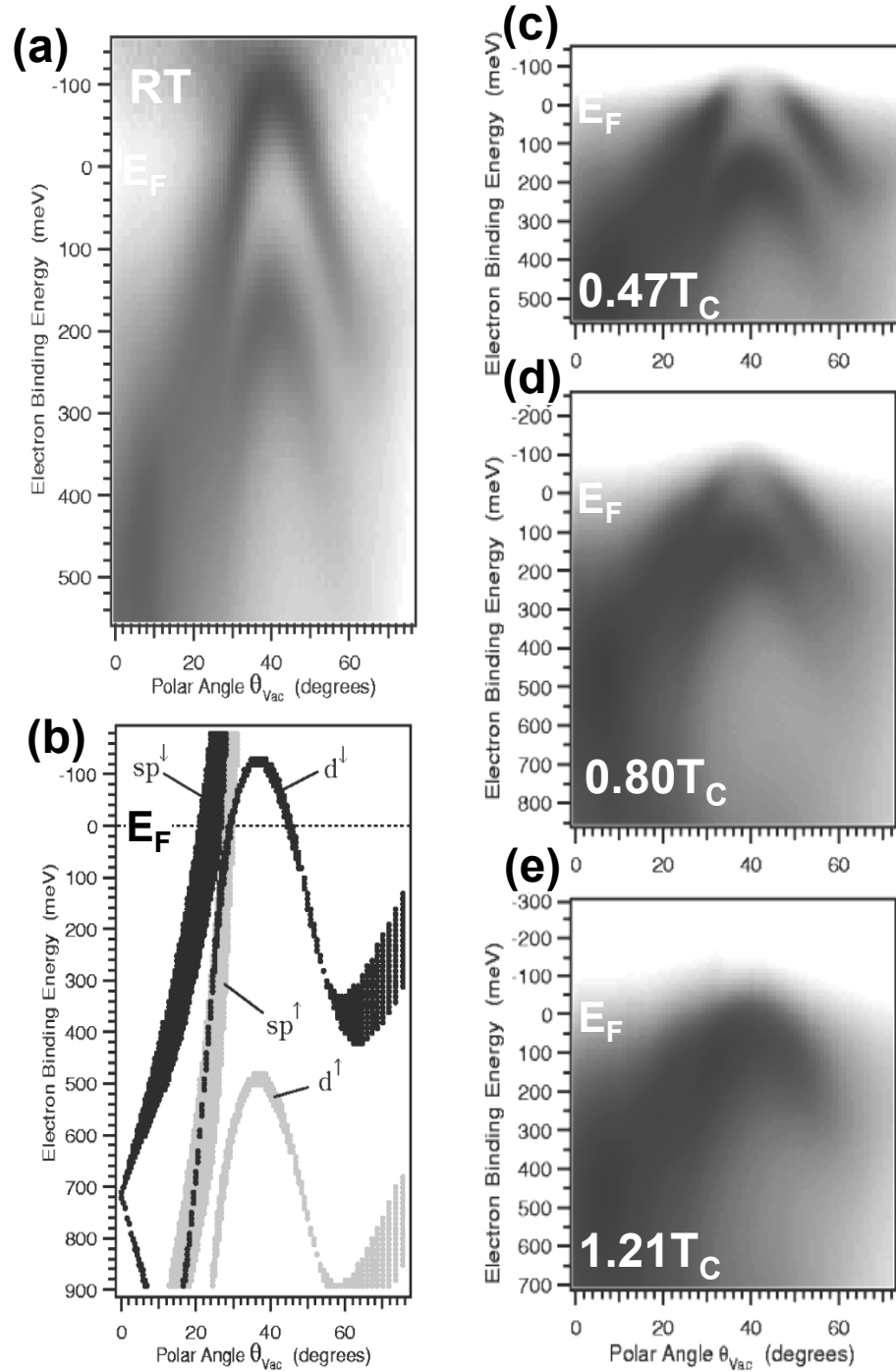
Valence-band photoemission: Angle-Resolved Photoemission (ARPES)



$$I(E_f, \vec{k}_f) \propto \left| \hat{\varepsilon} \bullet \langle \varphi_{photoe}(E_f = h\nu + E_i, \vec{k}_f = \vec{k}_i + \vec{g}) | \vec{r} | \varphi(E_i, \vec{k}_i) \rangle \right|^2$$

“Direct” or k -conserving transitions

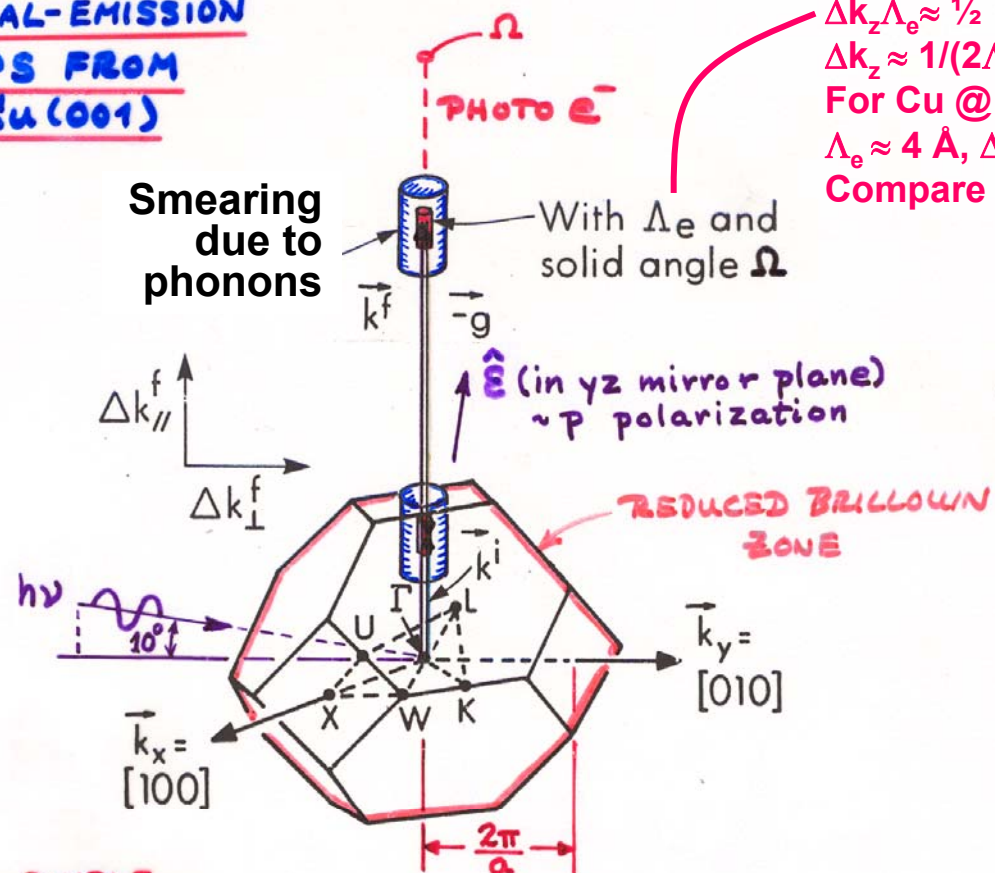
**Angle-Resolved
Photoemission
from ferromagnetic
Ni(111)
 $h\nu = 21.2$ eV
Spin-split
bands**



Kreutz et al.,
Phys. Rev. B 58 (1998) 1300

EXAMPLE:
NORMAL-EMISSION
UPS FROM
Cu(001)

Smearing
due to
phonons



SIMPLE DT MODEL: Direct: $\vec{k}^f = \vec{k}^i + \vec{g} + \vec{k}_{hv}$ ~~\times~~

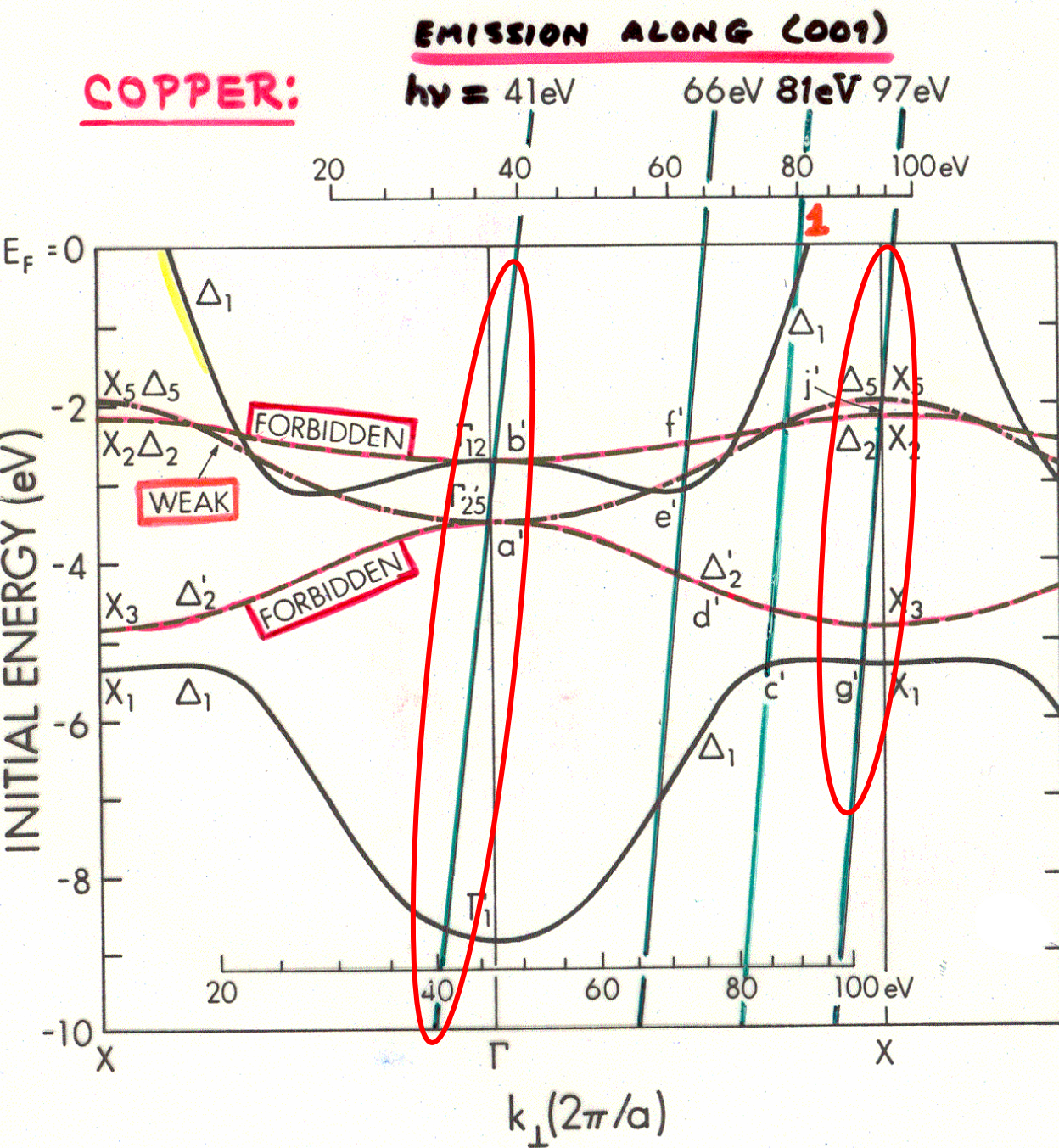
$E^i(\vec{k}^i)$ = initial band structure

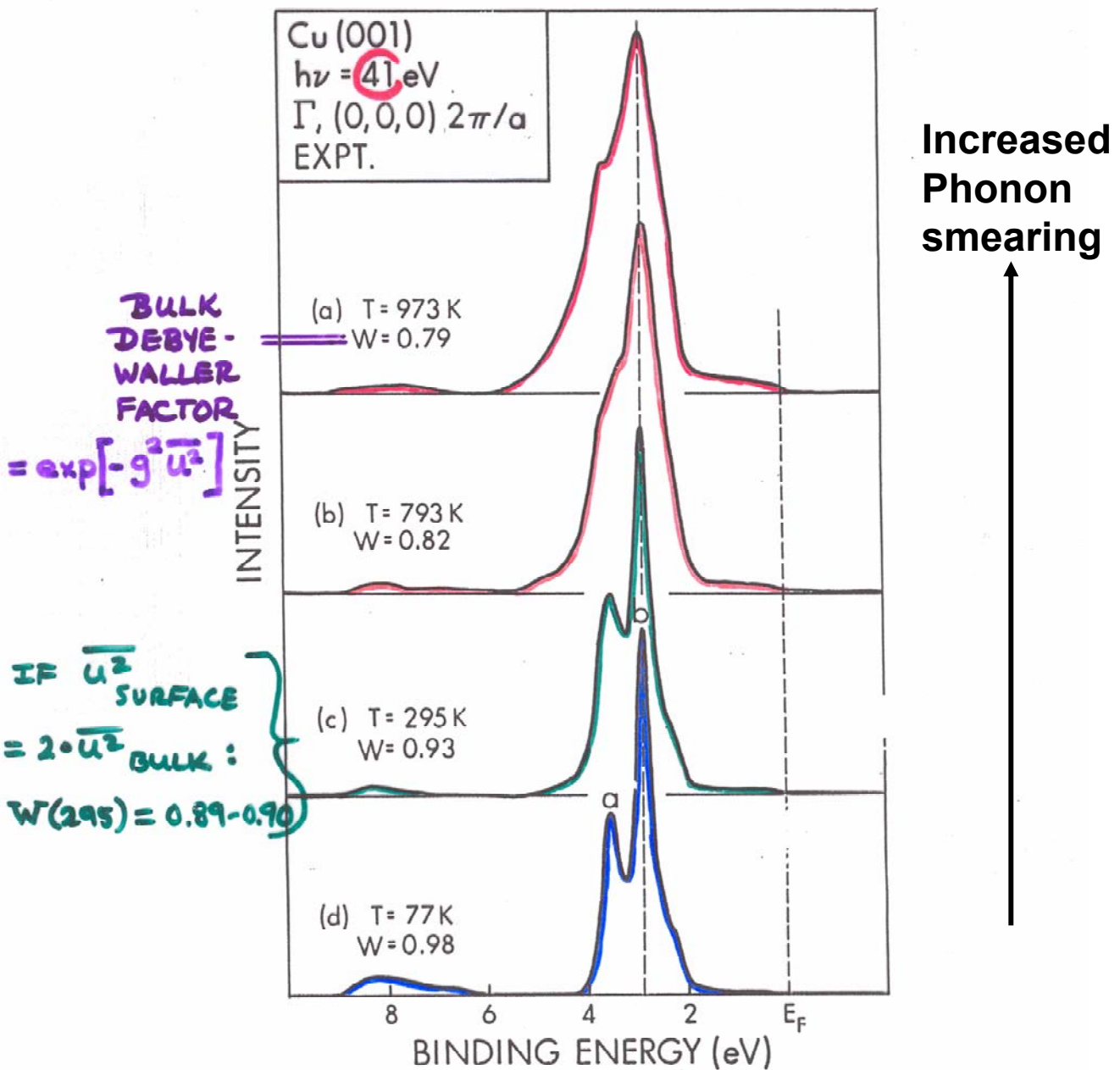
$$E^f(\vec{k}^f) \approx \hbar^2 (\vec{k}^f)^2 / 2m$$

Constant matrix
elements

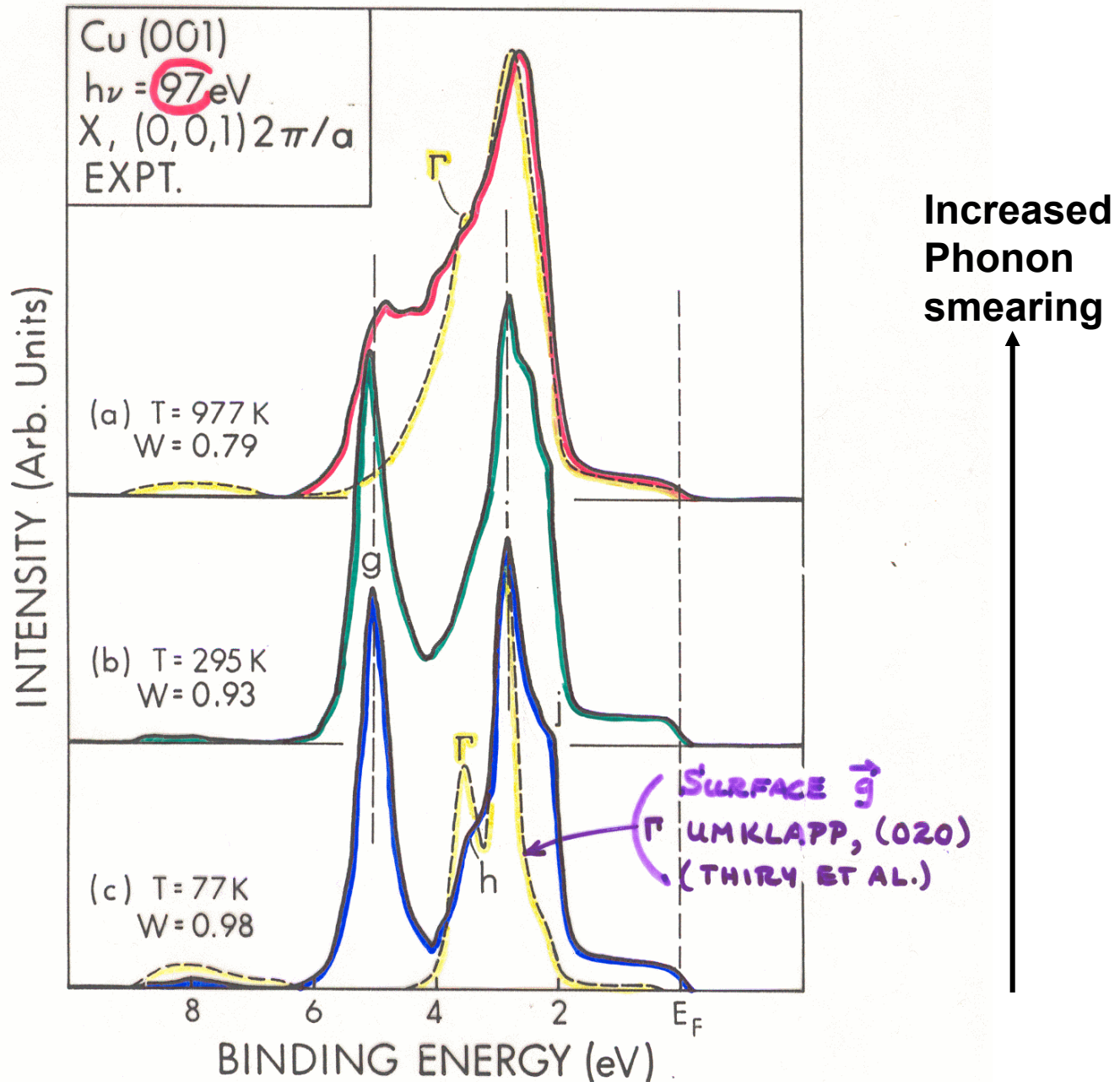
$$\begin{aligned} \Delta p_z \Delta z &\approx \hbar / 2 \\ \Delta k_z \Lambda_e &\approx 1/2 \\ \Delta k_z &\approx 1/(2\Lambda_e) \\ \text{For Cu @ } E_{\text{kin}} &\approx 80 \text{ eV,} \\ \Lambda_e &\approx 4 \text{ \AA}, \Delta k_z \approx 0.12 \text{ \AA}^{-1} \\ \text{Compare } 2\pi/a &= 0.98 \text{ \AA}^{-1} \end{aligned}$$

Expectations from simple direct-transition theory + symmetry considerations in matrix elements





R.C. WHITE ET AL., PHYS. REV. B 35, 1147 (1987)



Cu: ANGLE-RESOLVED PHOTOEMISSION AND BAND-MAPPING ALONG (001)

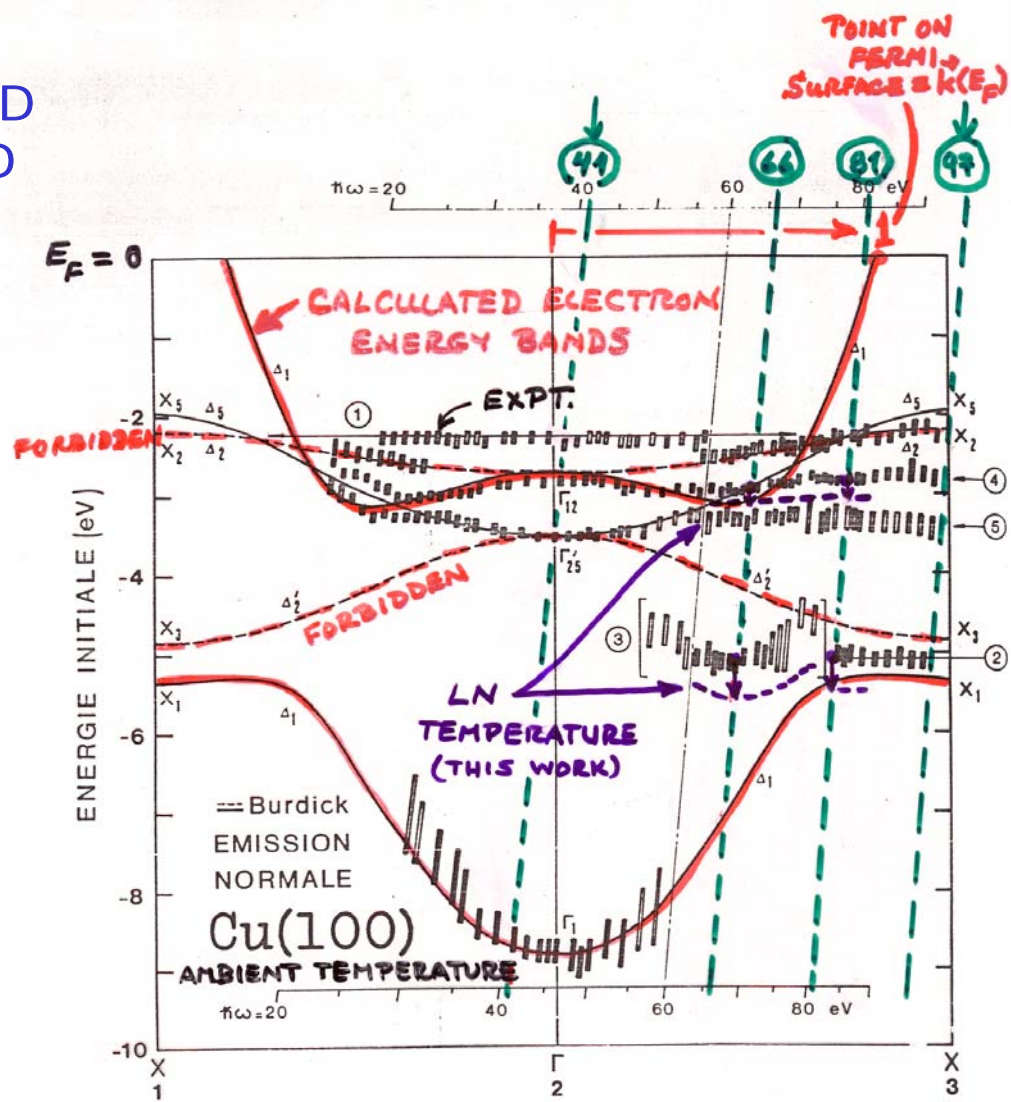


FIG.56

Cu: ANGLE-RESOLVED PHOTOEMISSION AND BAND-MAPPING ALONG (110)

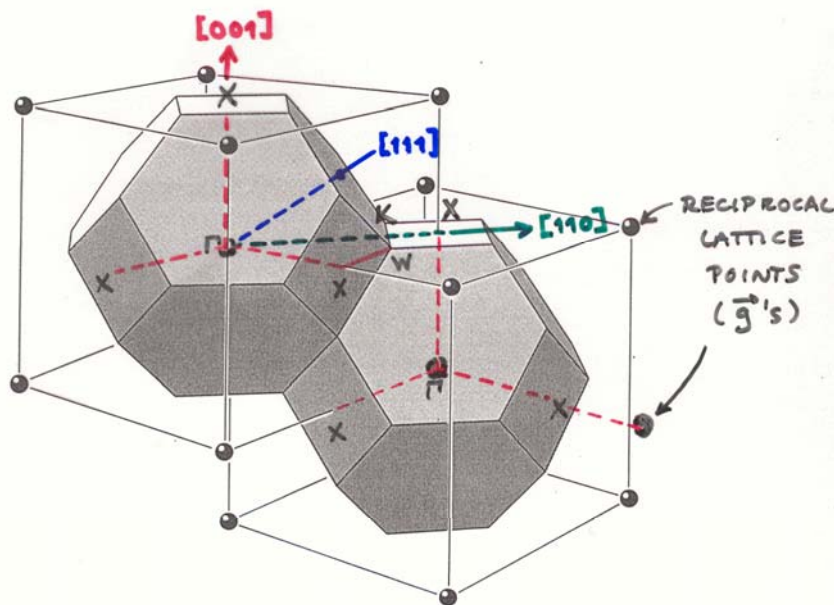
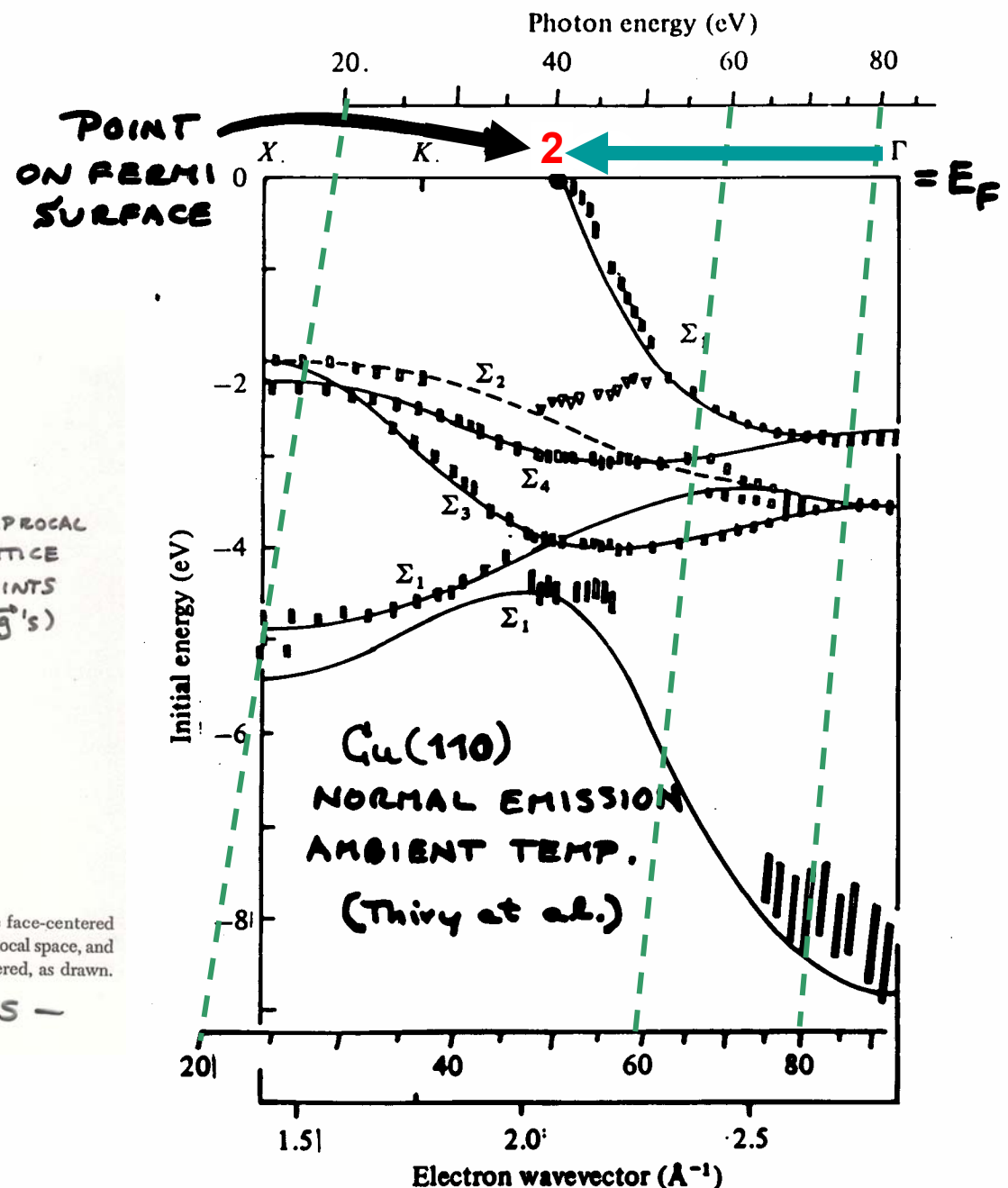


Figure 28 Brillouin zones of the face-centered cubic lattice. The cells are in reciprocal space, and the reciprocal lattice is body-centered, as drawn.

- STACKING OF fcc BRILLOUIN ZONES -

P.Thiry, Ph.D.
thesis, Univ.
of Paris (1980)



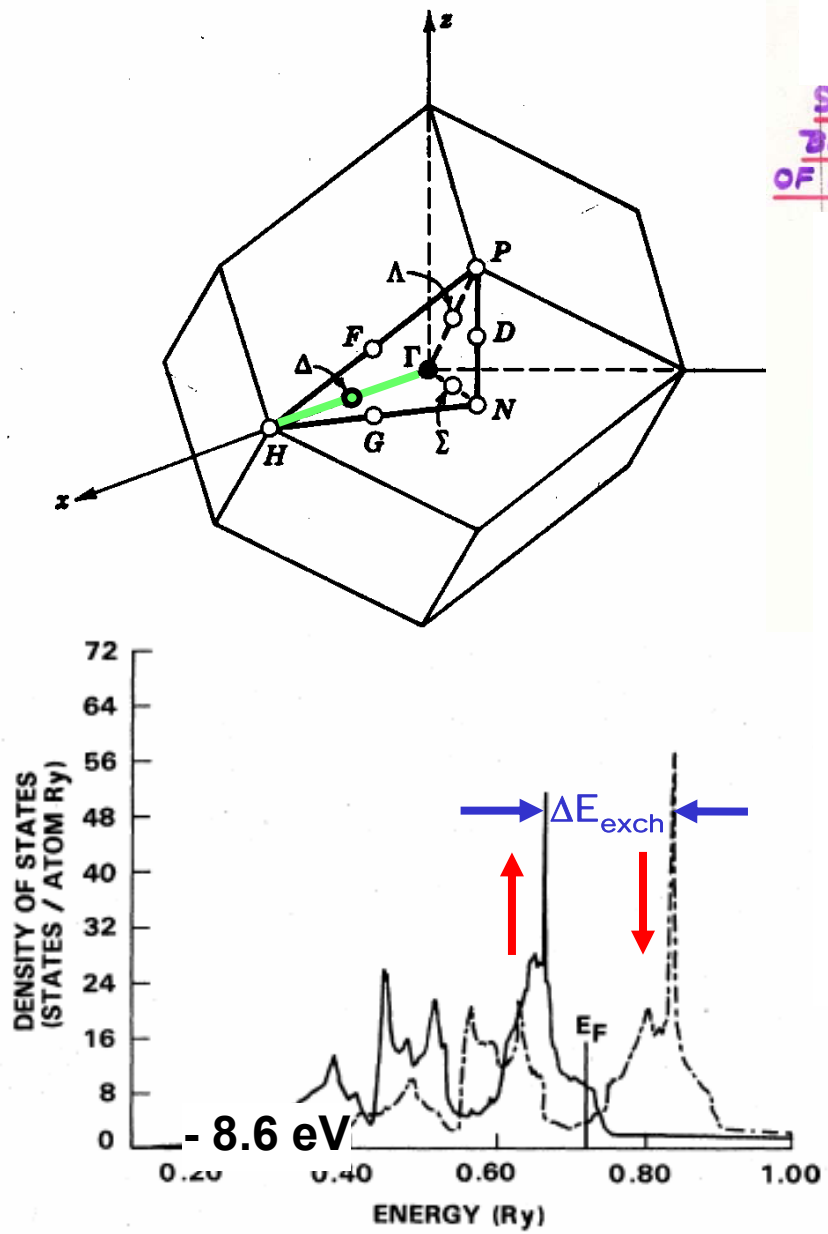
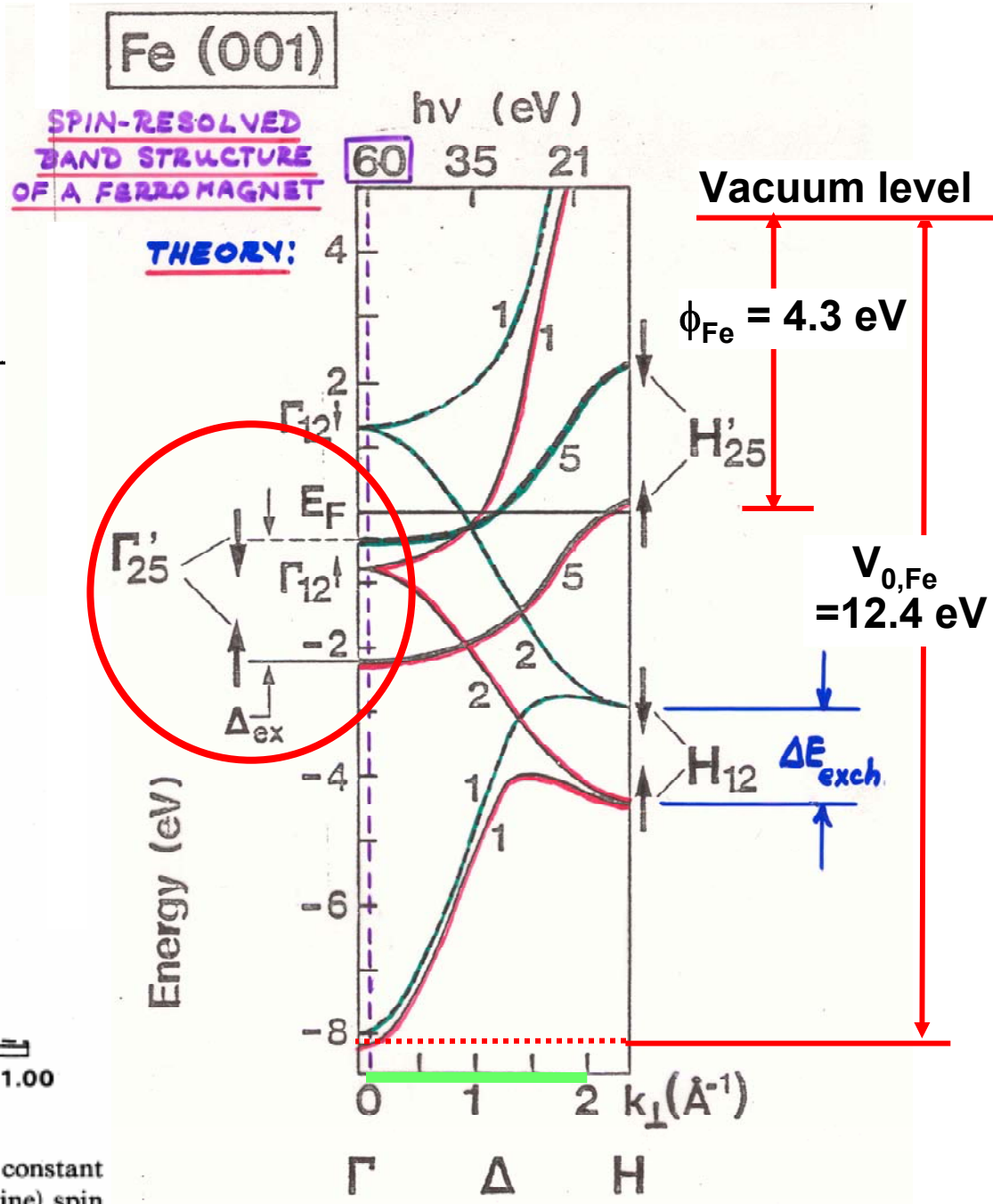


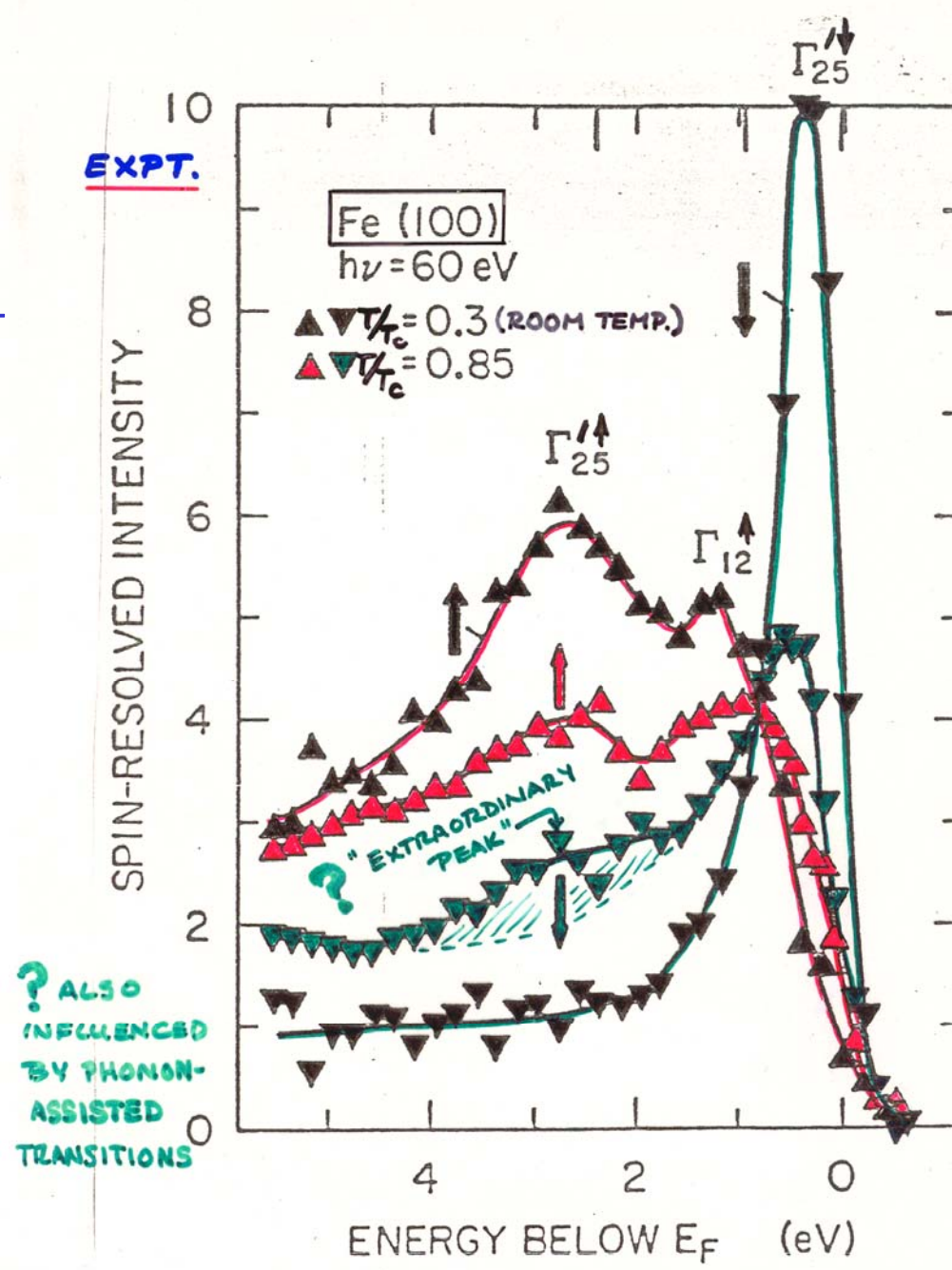
FIG. 4. Density of states at the equilibrium lattice constant of Fe for majority- (solid line) and minority- (broken line) spin states.

Hathaway et al., Phys. Rev. B 31, 7603 ('85)



E. KISKER ET AL., PHYS. REV. B
31, 329 (1985)

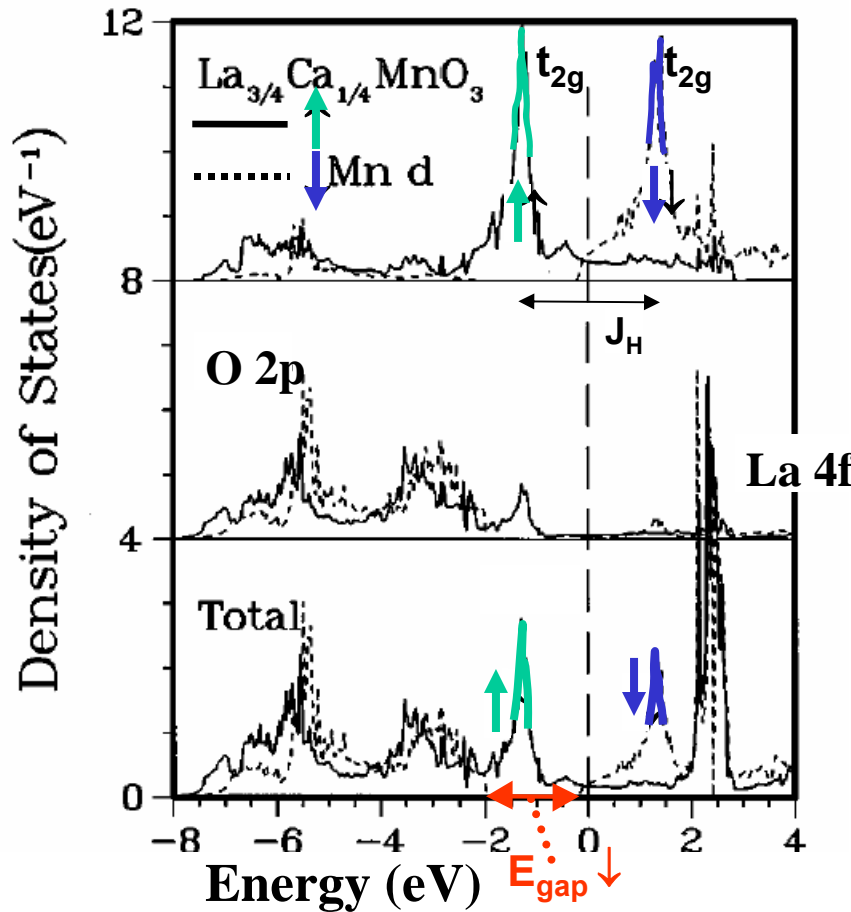
Fe: ANGLE AND SPIN-RESOLVED SPECTRA AT Γ POINT



E. KISKER ET AL., PHYS. REV. B
31, 329 (1985)

Half-Metallic Ferromagnetism

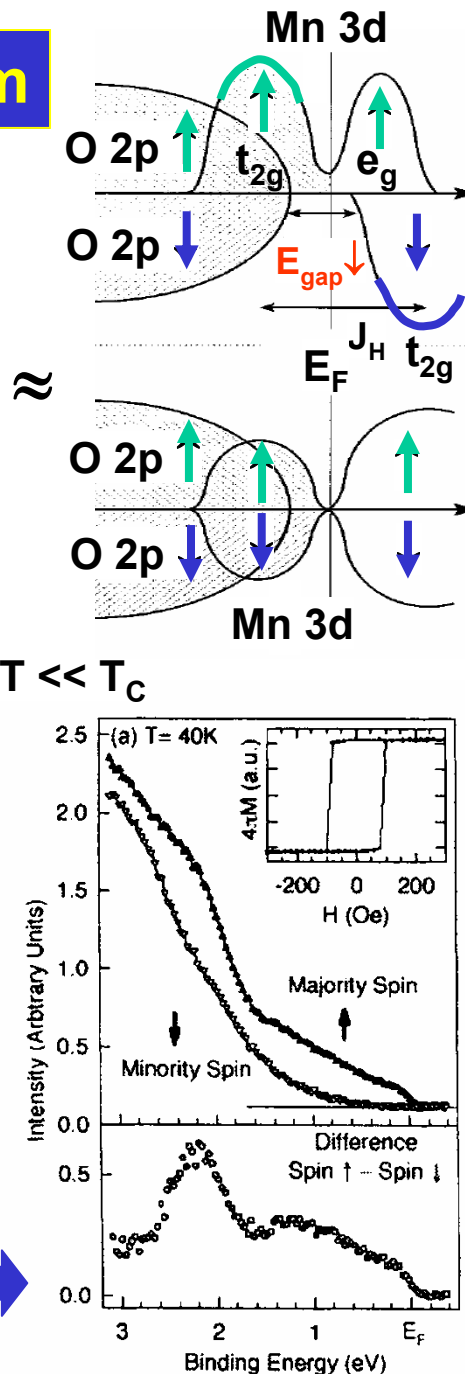
LDA theory- FM $\text{La}_{0.75}\text{Ca}_{0.25}\text{MnO}_3$



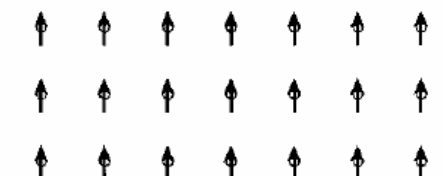
Pickett and Singh, PRB 53, 1146 (1996)

Experiment- spin-resolved PS
 $\text{La}_{0.70}\text{Sr}_{0.30}\text{MnO}_3$ as thin film

Park et al., Nature, PRB 392, 794 (1998)



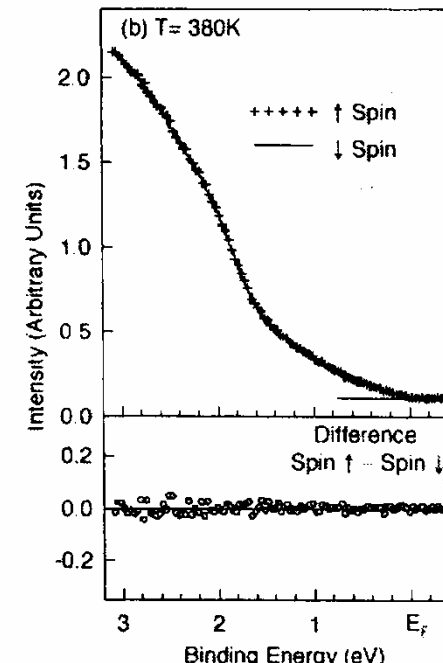
FM : $T \ll T_c$



PM : $T > T_c$



$T > T_c$



Vacuum level

The electronic structure of a transition metal—fcc Cu

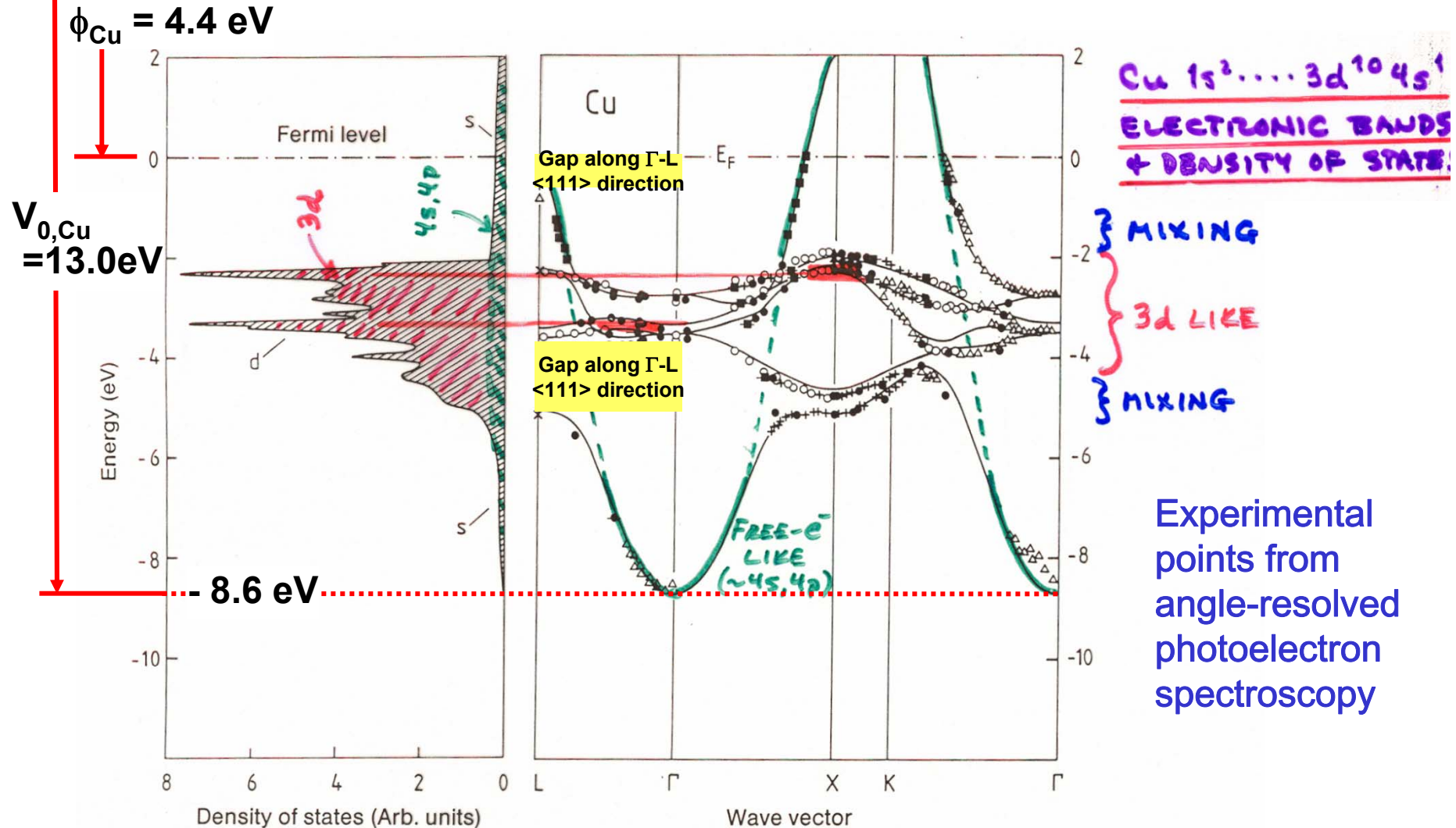


Fig. 7.12. Bandstructure $E(k)$ for copper along directions of high crystal symmetry (right). The experimental data were measured by various authors and were presented collectively by Courths and Hüfner [7.4]. The full lines showing the calculated energy bands and the density of states (left) are from [7.5]. The experimental data agree very well, not only among themselves, but also with the calculation

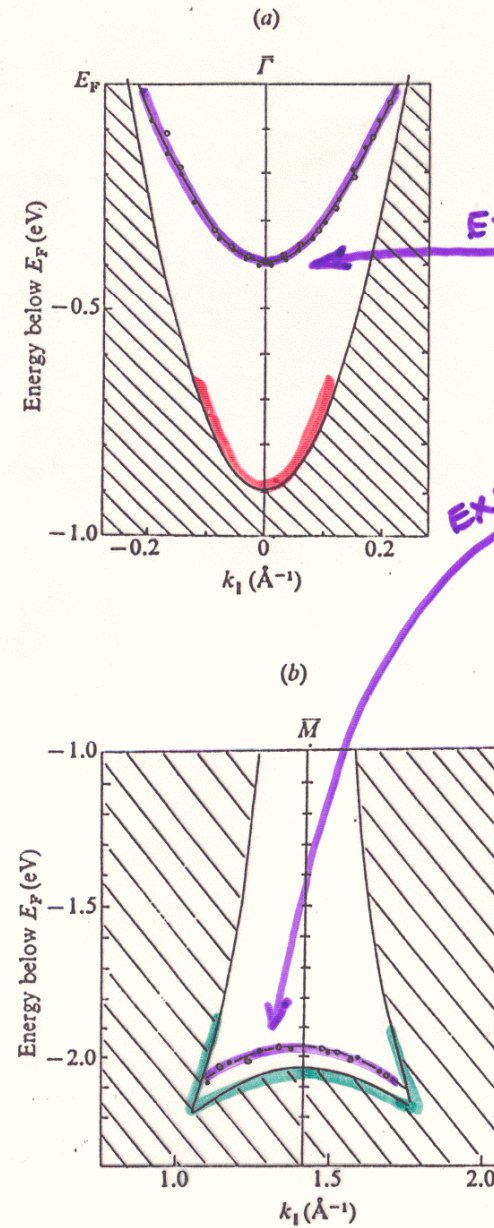
Surface states on Cu(111)

**Shockley
surface
state**

**Tamm
surface
state**

Zangwill,
Surface Physics,

Fig. 4.21. Experimental dispersion of Cu(111) surface states plotted with a projection of the bulk bands: (a) Shockley state near the zone center (Kevan, 1983); (b) Tamm state near the zone boundary (Heimann, Hermanson, Miosga and Neddermeyer, 1979). Compare with Fig. 4.17.



THEORY

Fig. 4.17. Surface states (dashed curves) and bulk projected bands for Cu(111) surface according to a six-layer surface band structure calculation (Euceda, Bylander & Kleinman, 1983).

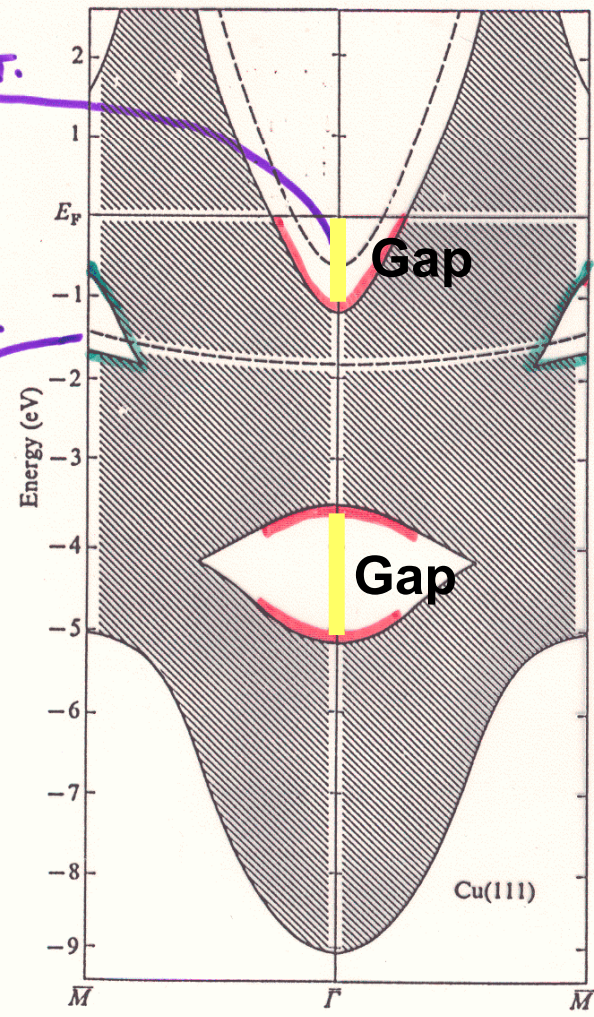
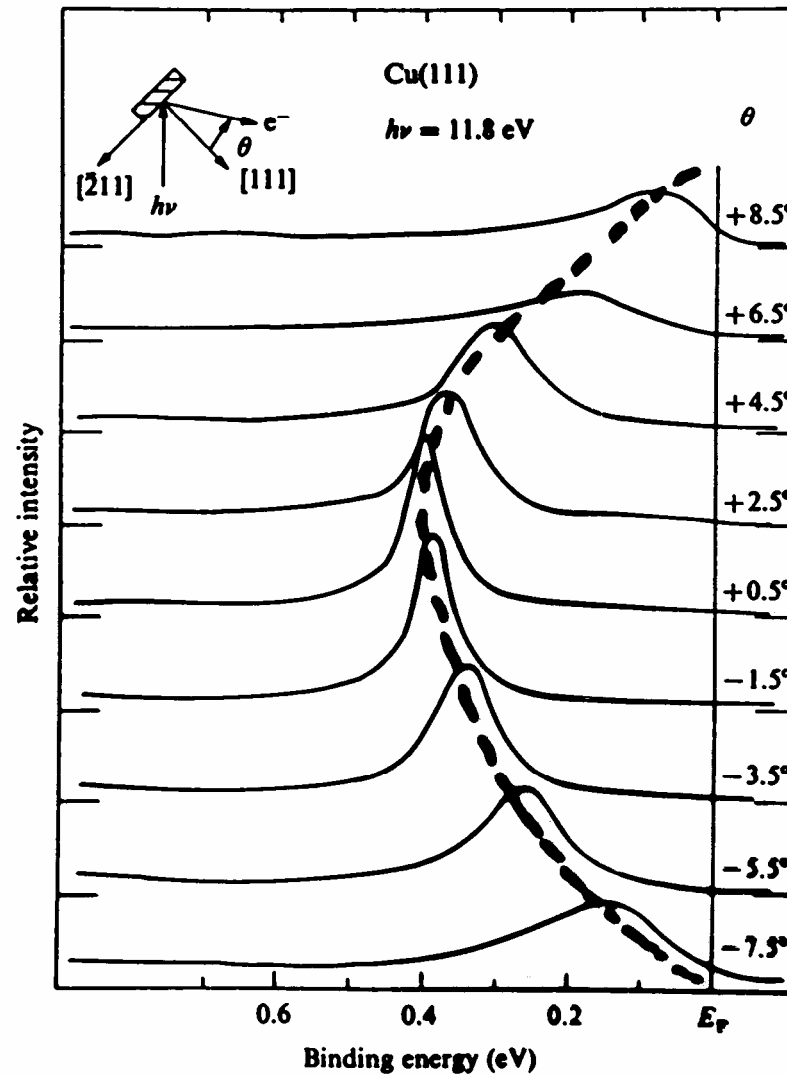
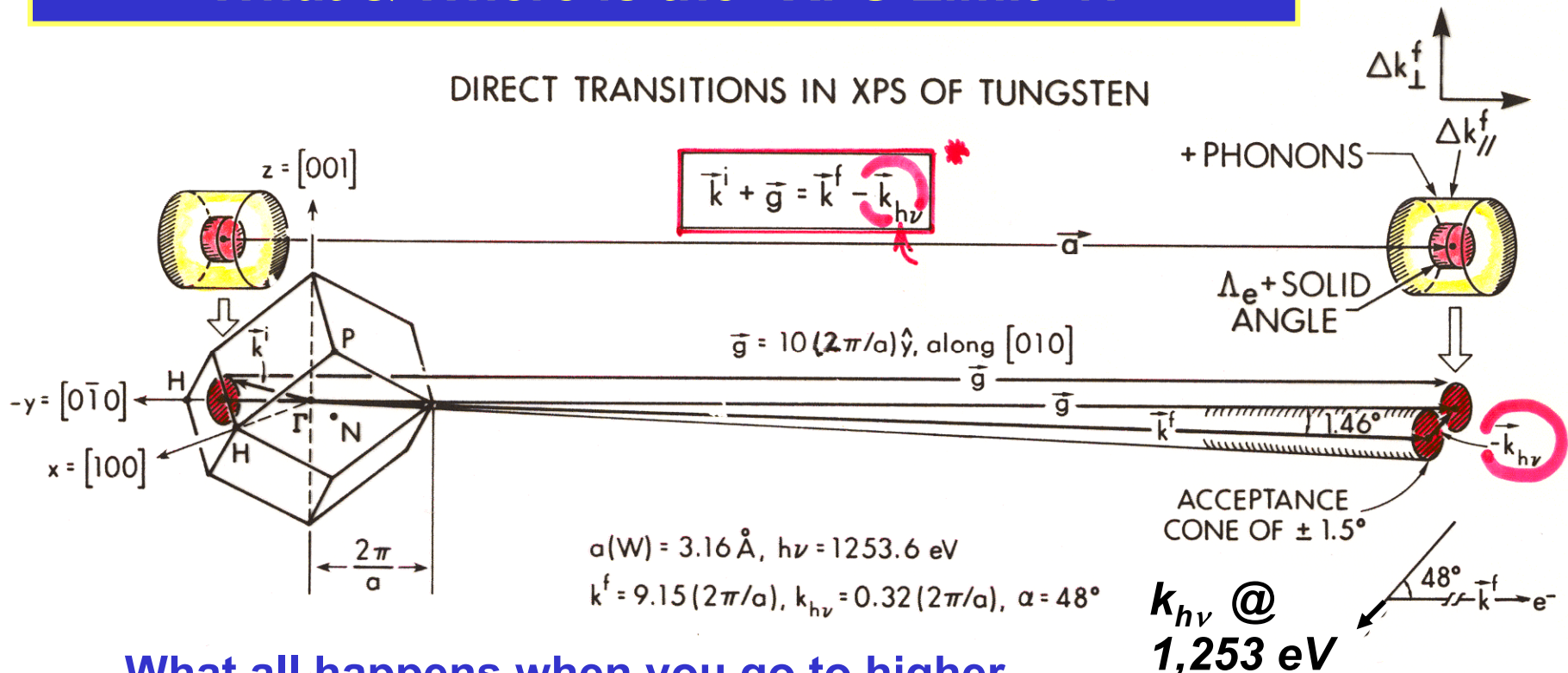


Fig. 4.20. Photoemission energy distribution curves from Cu(111) at different collection angles. Equation (4.32) has been used to express the electron kinetic energy in terms of the binding energy of the electron state (Kevan, 1983).



Zangwill,
Surface Physics,

Valence-Band Photoemission at High Energy-- What & Where is the “XPS Limit”?:

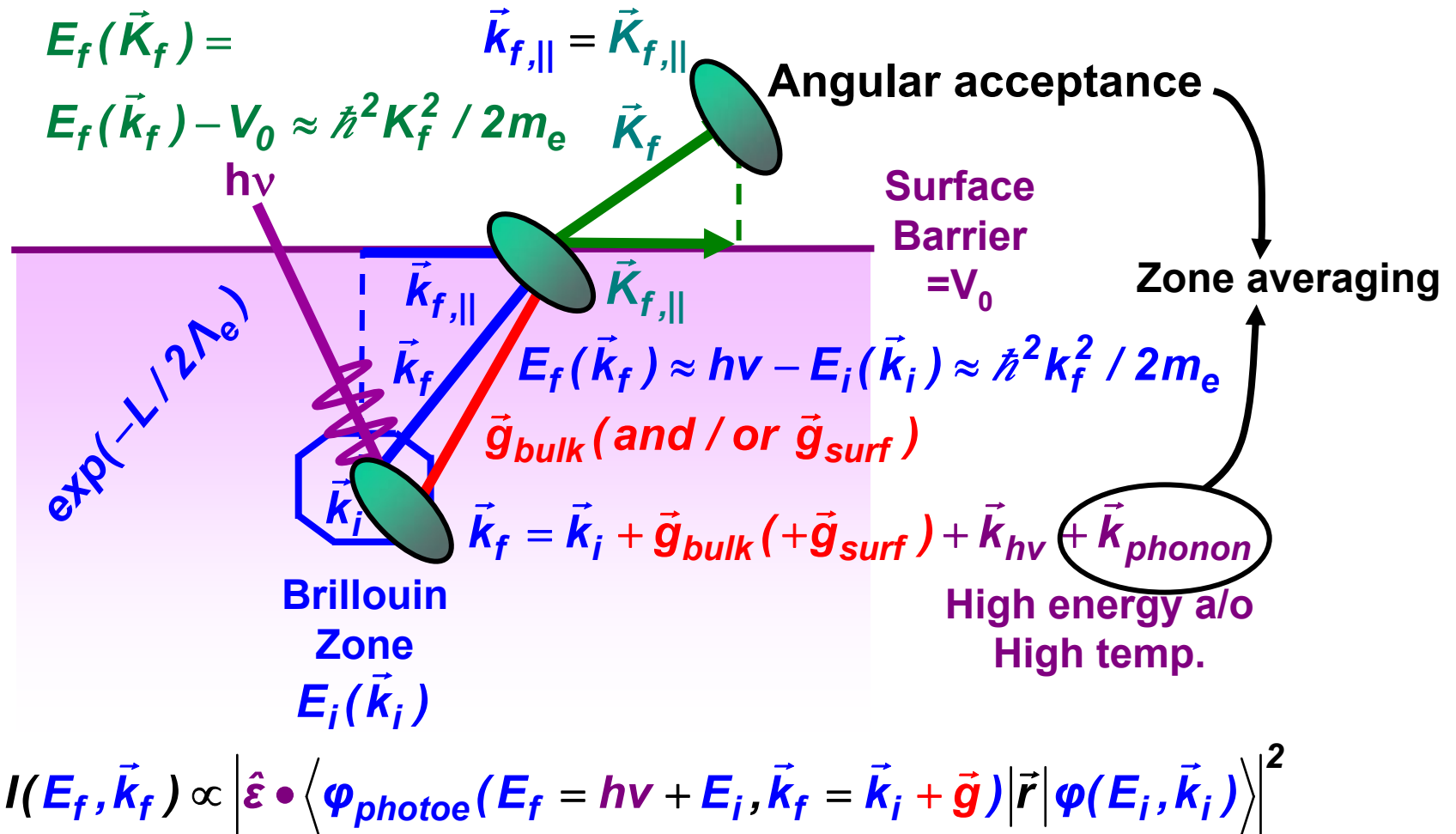


What all happens when you go to higher photon energies?

- non-dipole effect → the photon momentum
 - angular acceptance → B.Z. averaging
 - lattice recoil, phonon creation → more Brillouin Zone averaging
- The XPS limit of full B.Z. averaging and D.O.S. sensitivity

Hussain et al., Phys. Rev. B 22, 3750 ('80)

Valence-band photoemission—at higher energy



$$h\nu = 1487 \text{ eV}$$

Estimating phonon effects: 1st approx.

$$W(T) = \text{Debye-Waller factor} = \exp\left(-\frac{1}{3}g^2 \langle U^2(T) \rangle\right)$$

$$I(E, T) = W(T) I_{DT} + [1 - W(T)] I_{NDT}$$

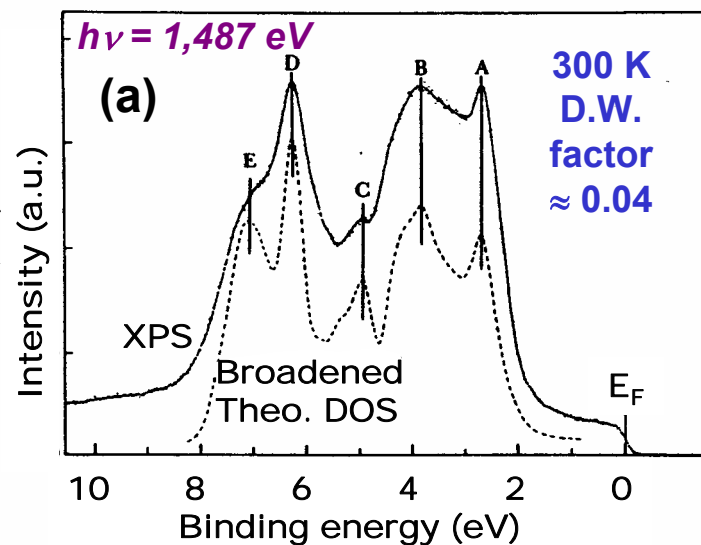
Shevchik, Phys. Rev. B 20, 3020 ('79);
 Hussain et al., Phys. Rev. 22, 3750 ('80)

TABLE I. Tabulation of thermal displacements ($\langle U^2 \rangle$) and Debye-Waller factors [$W(T) = \exp(-\frac{1}{3}\langle U^2 \rangle g^2)$] in the XPS regime ($E_{\text{kin}} = 1482 \text{ eV}$) for various elements. The Debye temperatures are taken from Ref. 30. The solid line divides the Debye-Waller factors so as to indicate when $\frac{1}{2}$ of the transitions will be direct. Elements are in order of Z .

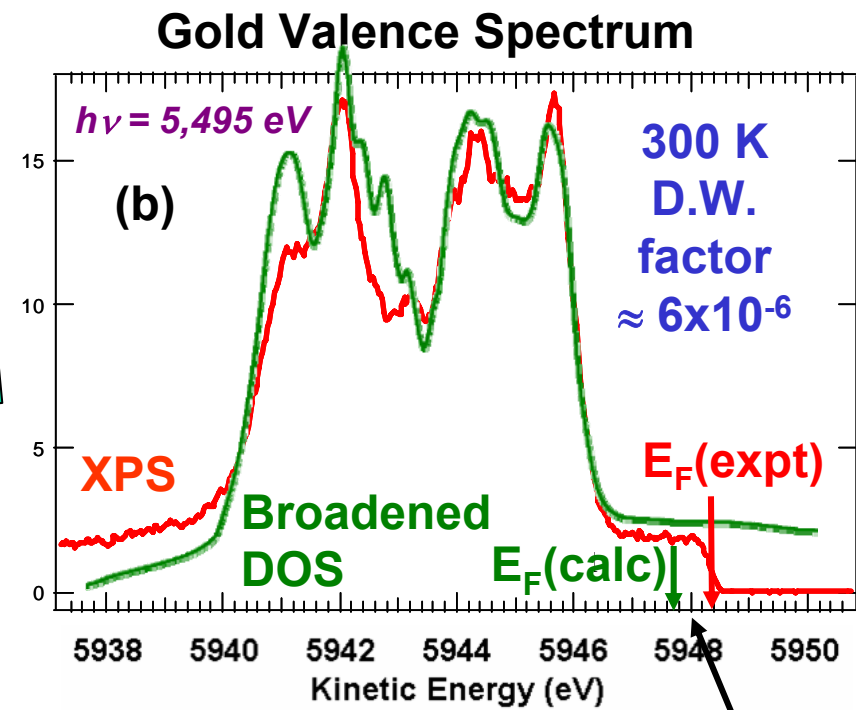
Element	Θ_D (K)	A (amu)	$T = 4 \text{ K}$		$T = 77 \text{ K}$		$T = 300 \text{ K}$		$T = 1000 \text{ K}$	
			$\langle U^2 \rangle$ (10^{-18} cm^2)	W	$\langle U^2 \rangle$ (10^{-18} cm^2)	W	$\langle U^2 \rangle$ (10^{-18} cm^2)	W	$\langle U^2 \rangle$ (10^{-18} cm^2)	W
B	1449	9.012	0.84	0.84	0.86	0.83	1.07	0.23	2.47	0.04
C	2230	12.001	0.41	0.53	0.41	0.53	0.46	0.53	0.83	0.34
Mg	400	24.212	1.15	0.29	1.15	0.16	0.52	0.01		
Al	428	26.981	0.35	0.29	1.15	0.22	2.79	0.03		
Si	645	23.086	0.60	0.46	0.56	0.42	1.26	0.19	3.07	0.02
Ca	230	40.08	1.19	0.21	1.94	0.06	6.24	0.0		
Ti	420	47.9	0.54	0.49	0.66	0.42	1.63	0.12	3.16	0.0
V	380	50.942	0.56	0.48	0.72	0.39	1.85	0.09	5.93	0.0
Cr	630	51.996	0.39	0.65	0.37	0.62	0.71	0.40	2.15	0.06
Mn	410	54.935	0.48	0.56	0.60	0.46	1.49	0.14	4.72	0.0
Fe	470	55.817	0.42	0.58	0.43	0.53	1.13	0.23	3.58	0.01
Co	443	55.933	0.42	0.58	0.56	0.52	1.19	0.21	3.74	0.0
Ni	450	58.71	0.41	0.59	0.49	0.59	1.17	0.22	3.67	0.01
Cu	243	63.54	0.50	0.52	0.67	0.42	1.82	0.69	5.84	0.0
Zn	327	65.37	0.51	0.51	0.70	0.40	1.92	0.68		
Ge	374	72.59	0.46	0.59	0.61	0.51	1.34	0.17	4.28	0.0
As	382	74.922	0.52	0.51	0.77	0.37	2.26	0.05	7.32	0.0
Zr	291	81.22	0.41	0.58	0.60	0.46	1.74	0.10	5.65	0.0
Nb	275	92.906	0.42	0.57	0.65	0.43	1.90	0.08	6.21	0.0
Mo	450	95.94	0.26	0.78	0.59	0.69	0.71	0.32	2.25	0.05
Ru	600	101.07	0.15	0.76	0.23	0.77	0.40	0.60	1.21	0.21
Rh	450	102.995	0.22	0.75	0.26	0.71	0.59	0.46	1.84	0.09
Pd	274	106.4	0.37	0.61	0.57	0.48	1.68	0.11	5.46	0.0
Ag	225	107.57	0.45	0.56	0.75	0.38	2.44	0.04	5.00	0.0
Cd	209	112.49	0.47	0.55	0.81	0.35	2.70	0.03		
Sn	200	118.63	0.46	0.53	0.83	0.34	2.55	0.04		
Sb	211	121.75	0.42	0.57	0.79	0.35	2.46	0.04		
Hf	252	178.49	0.24	0.73	0.38	0.60	1.18	0.22	3.85	0.01
Ta	240	180.948	0.25	0.73	0.42	0.68	1.28	0.19	4.19	0.0
W	400	182.83	0.17	0.59	0.15	0.79	0.47	0.55	1.48	0.14
Re	630	188.2	0.19	0.51	0.27	0.31	0.40	0.50	1.23	0.19
Os	500	190.2	0.11	0.58	0.15	0.56	0.30	0.63	0.92	0.38
Ir	420	192.2	0.14	0.54	0.17	0.51	0.41	0.35	1.29	0.19
Pt	240	195.09	0.23	0.74	0.39	0.60	1.19	0.21	3.88	0.01
Au	165	196.267	0.24	0.65	0.52	0.35	2.46	0.04	8.14	0.0
Pb	105	207.19	0.51	0.32	1.54	0.13	3.73	0.0		

Greater than 50% direct transitions

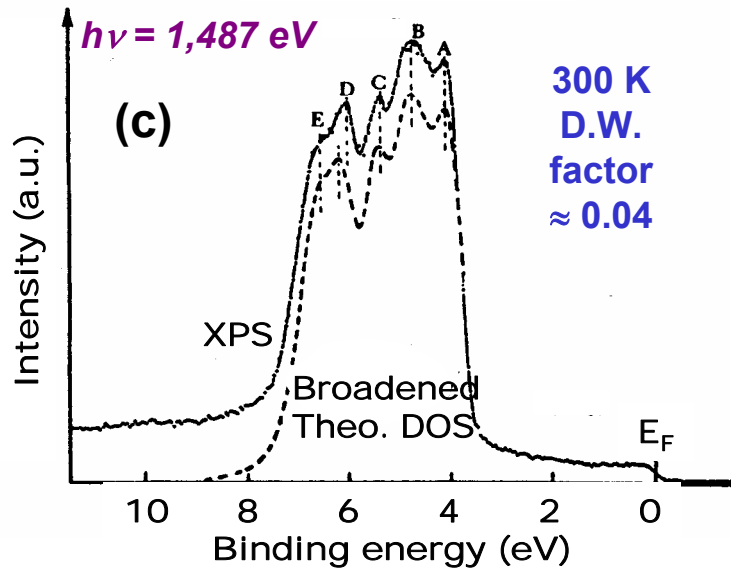
Gold Valence Spectrum



Valence spectra in the XPS Limit

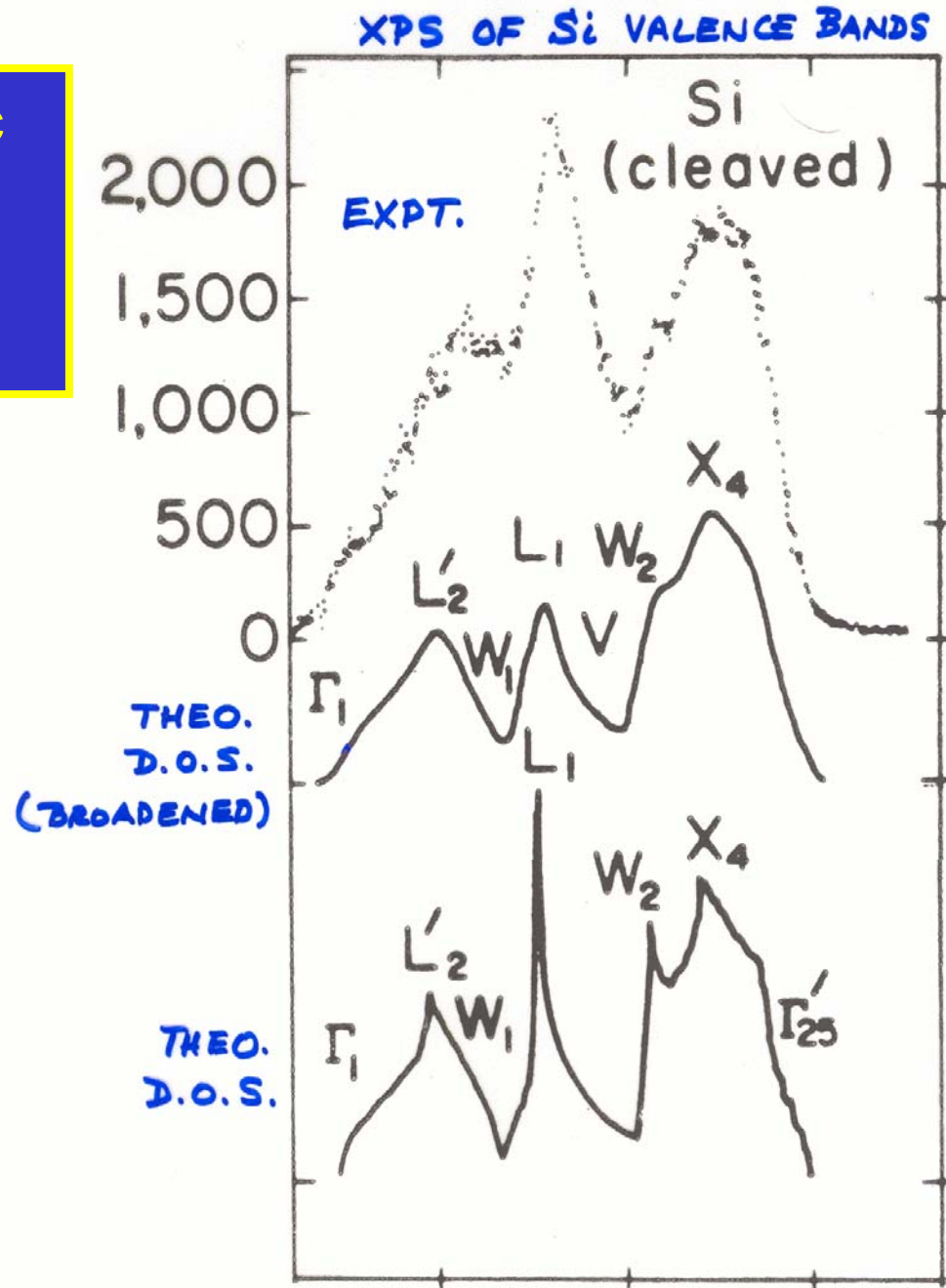


Silver Valence Spectrum



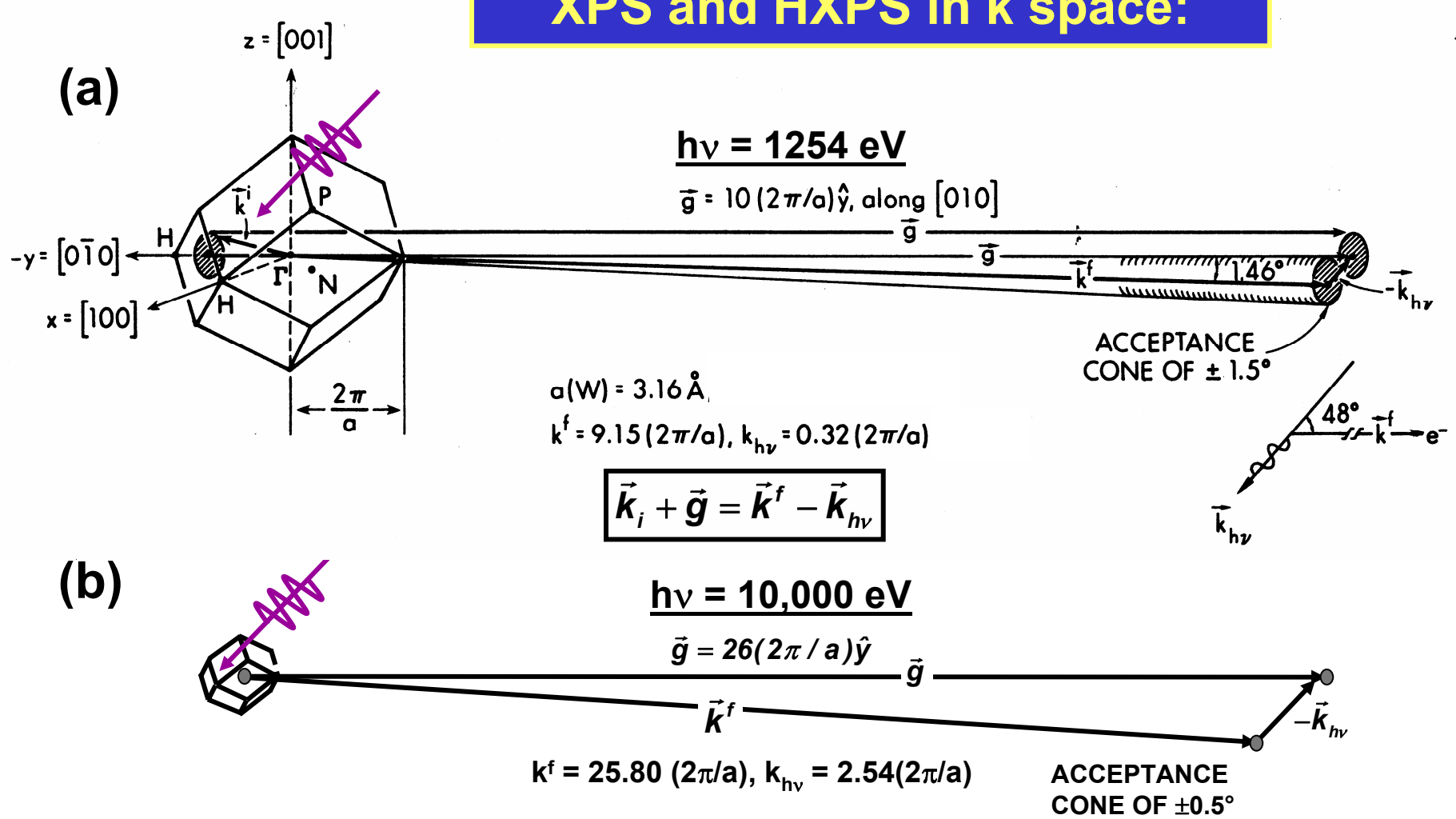
Screening/
self-energy
correction

Some classic cases in the XPS limit:



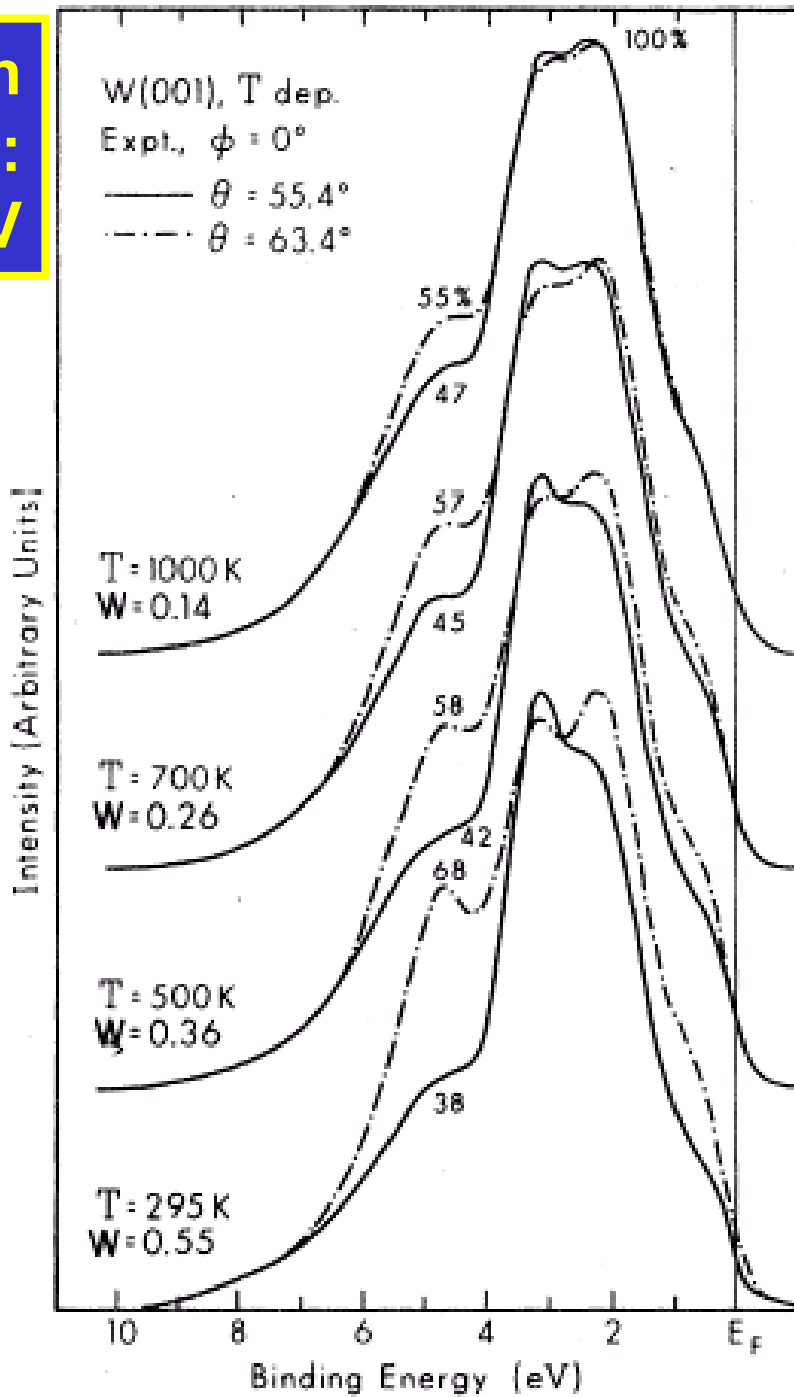
"Basic Concepts of XPS"
Figure 14

XPS and HXPS in k space:



Phonon effects: Approximate fraction of “good” direct transitions
 \approx Debye-Waller factor = $W(T) \approx \exp[-g^2 \langle u^2(T) \rangle]$
 $=$ Mean-squared
 vibrational displacement

Direct-transition effects in XPS: W(110) at 1253.6 eV

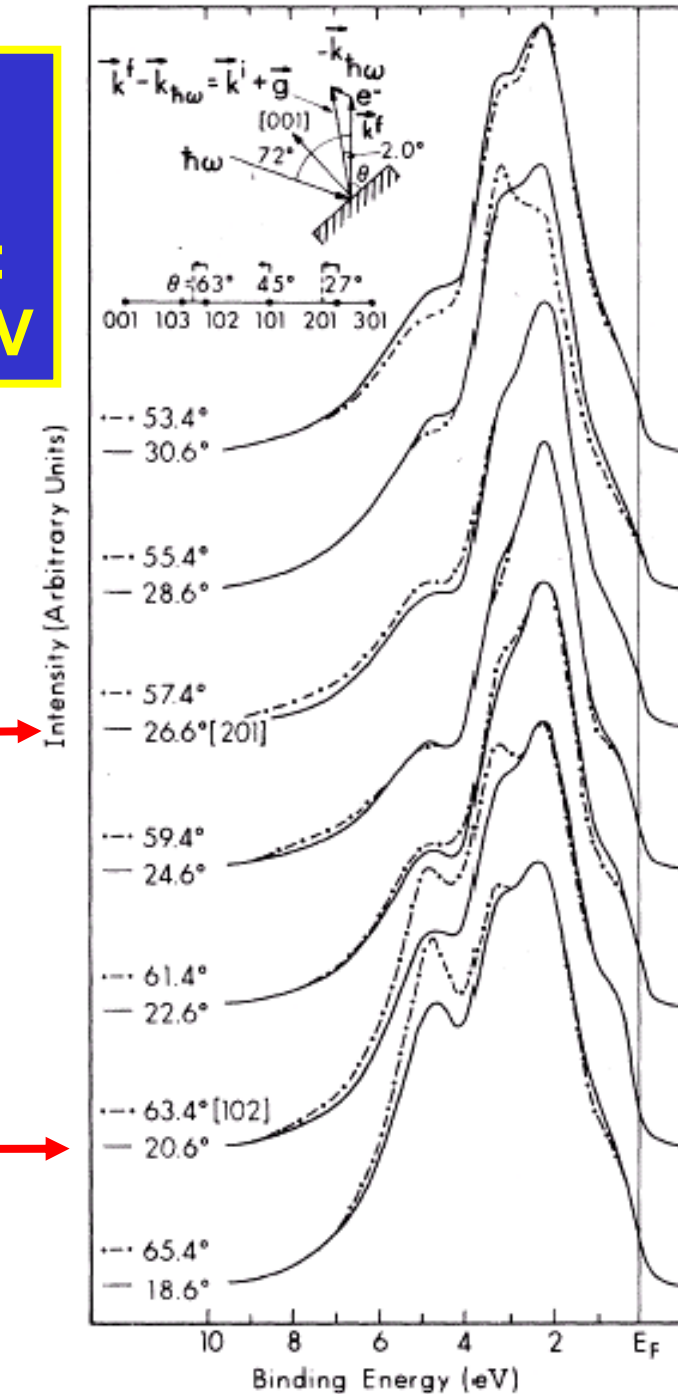


Present if vibrations stiff enough (Debye T high enough), but suppressed as temperature is raised.

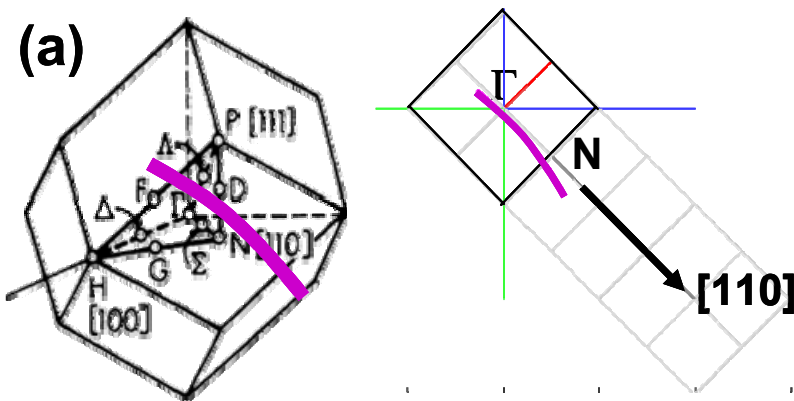
Hussain et al.,
Phys. Rev. 22,
3750 (1980)

Effect of photon momentum on k conservation: W(110) at 1253.6 eV

Symmetry-related spectra shifted by 6.0° for best match.
Theoretical 4.8° due to k_{hv}

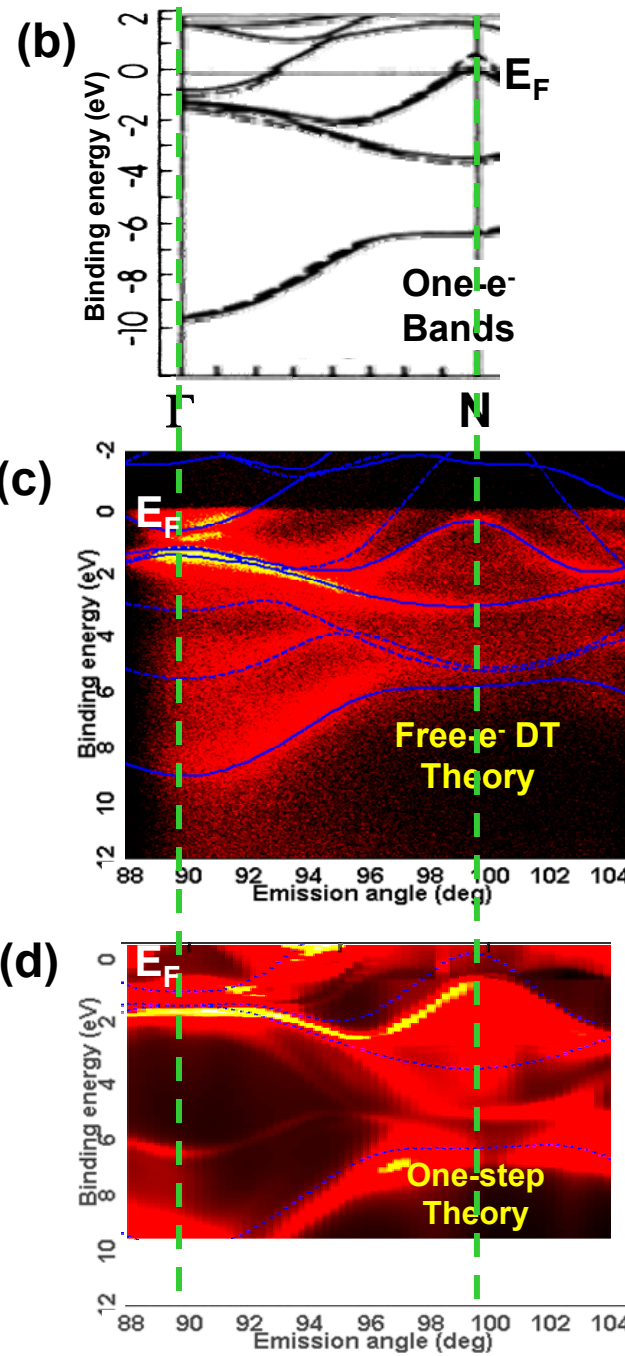


Hussain et al.,
Phys. Rev. 22,
3750 (1980)



**Angle-Resolved
Photoemission
from W(110)**
 $h\nu = 260 \text{ eV}$
 $90^\circ = \text{normal}$
 $\Theta_{\text{Debye}} = 400 \text{ K}$

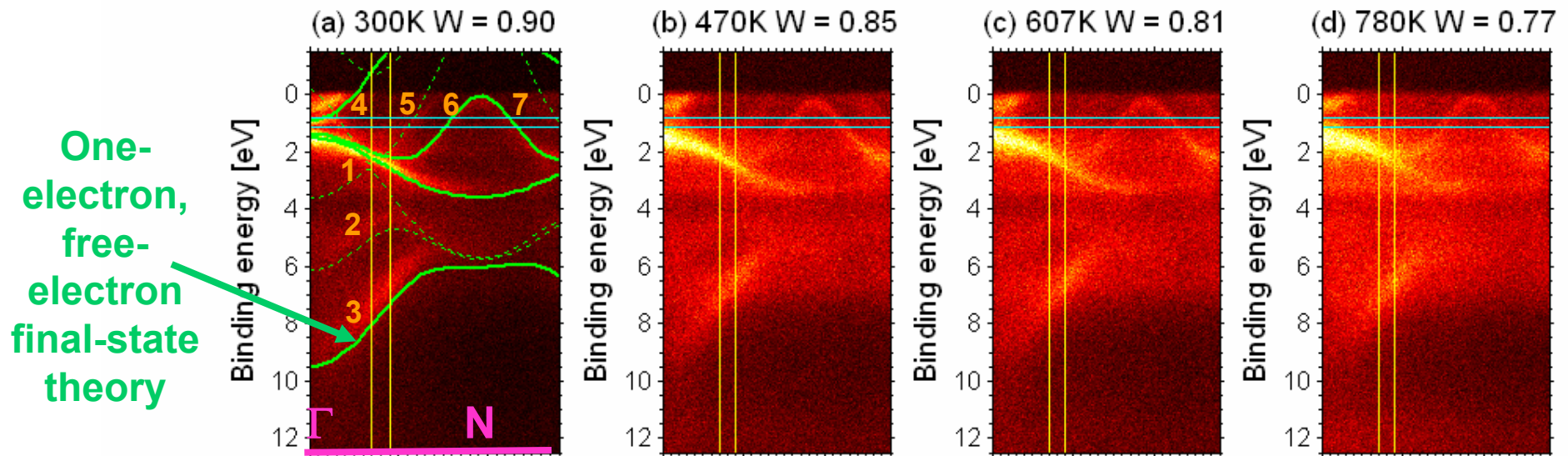
Plucinski et al., Phys.
Rev. B, submitted



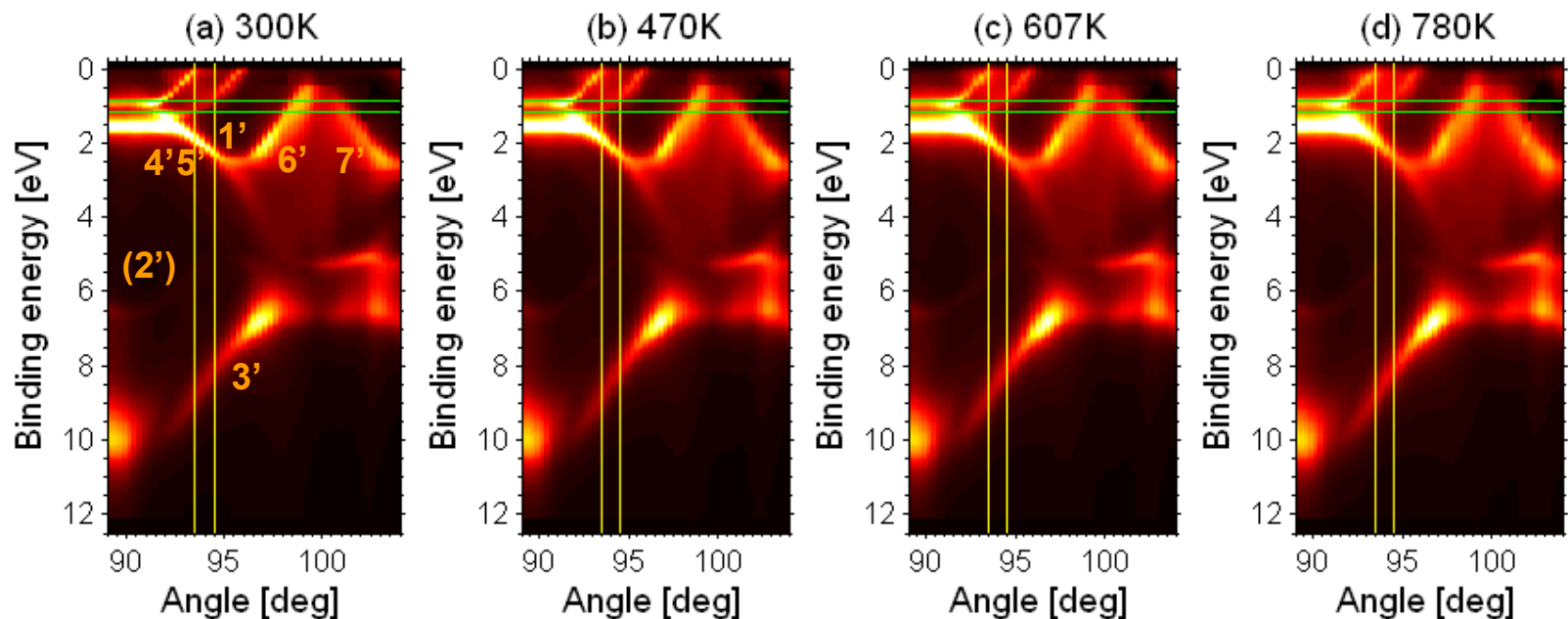
Plucinski

Braun, Minar,
Ebert

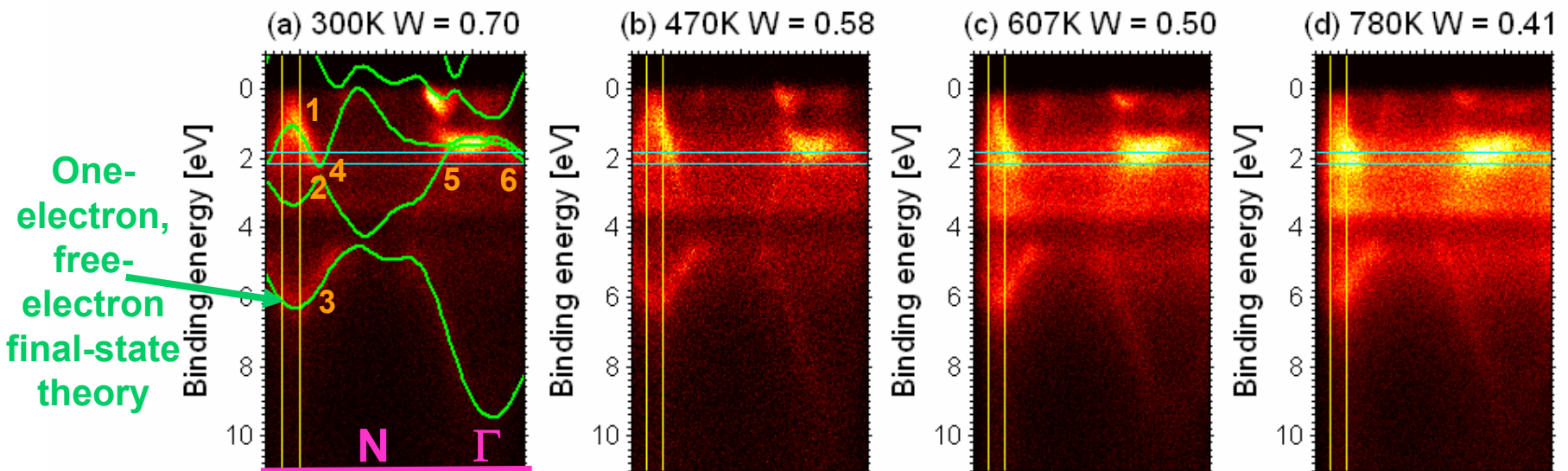
ARPES from W(110): Expt, $h\nu = 260$ eV, near-normal emission, $\Theta_{\text{Debye}} = 400$ K



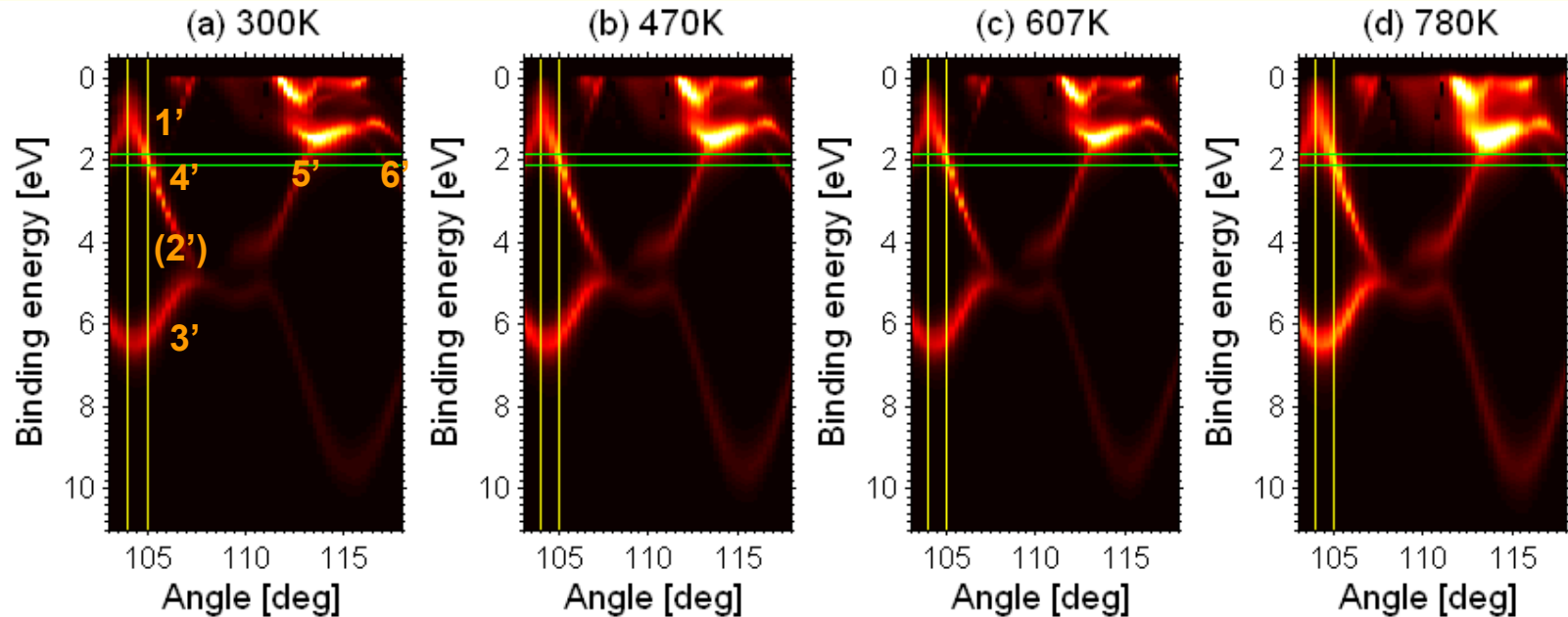
ARPES from W(110): 1-Step Theory, $h\nu = 260$ eV, near-normal emission, $\Theta_{\text{Debye}} = 400$ K



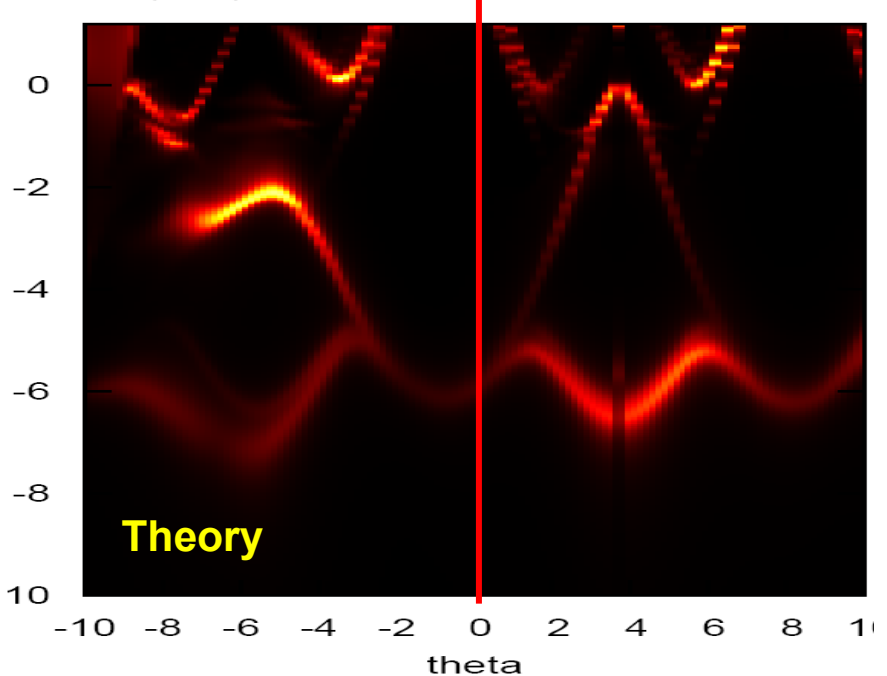
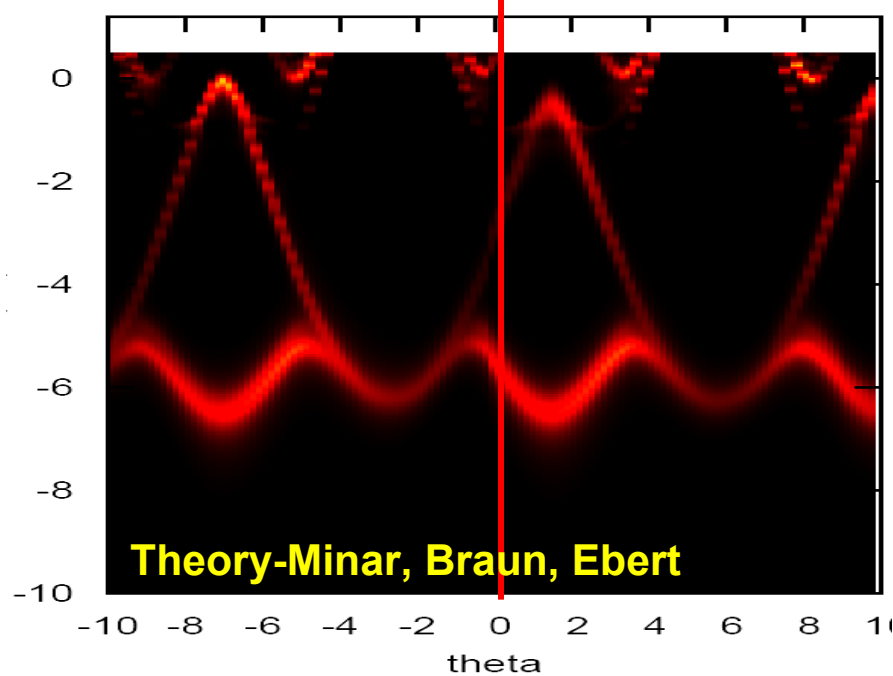
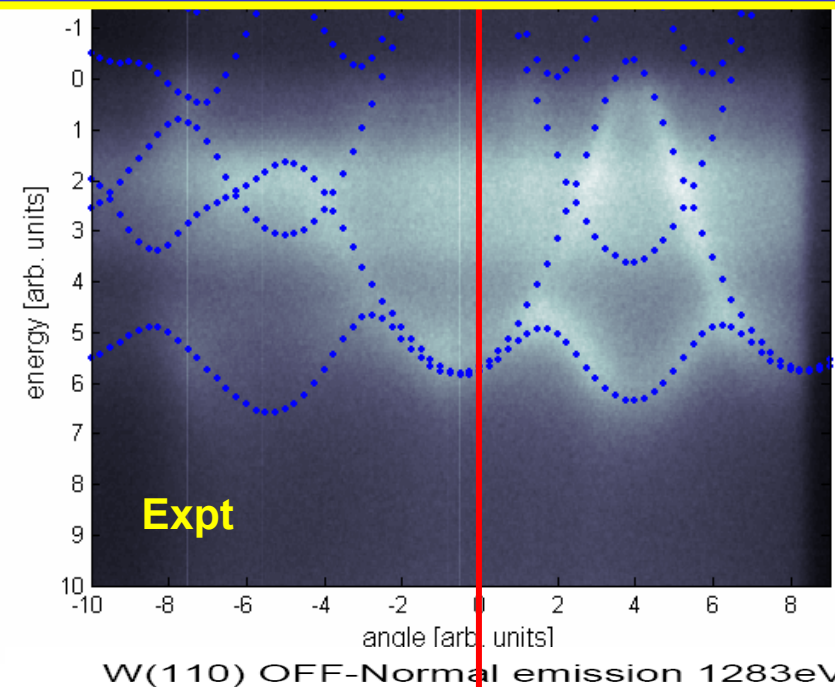
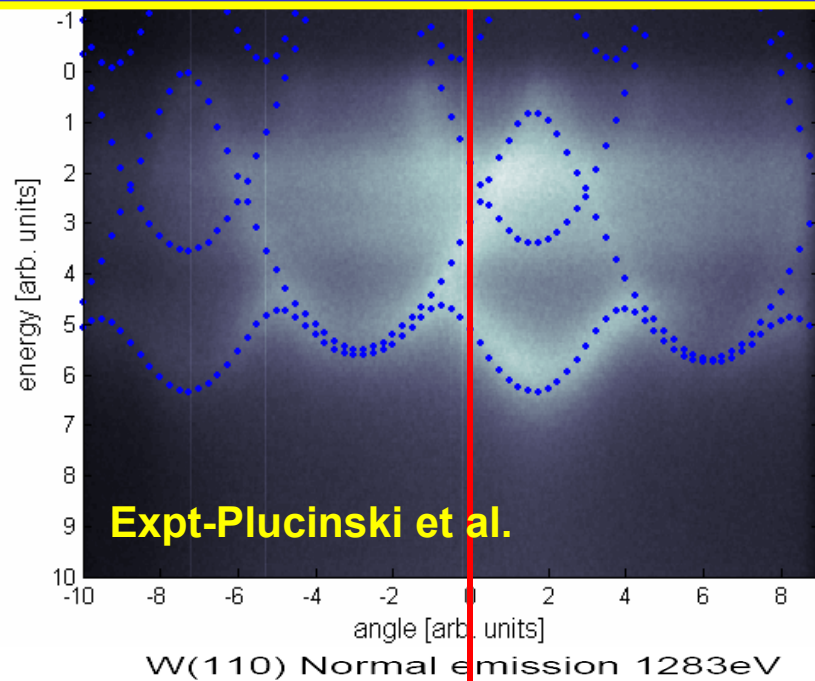
ARPES from W(110): Expt, $h\nu = 860$ eV, near-normal emission, $\Theta_{\text{Debye}} = 400$ K

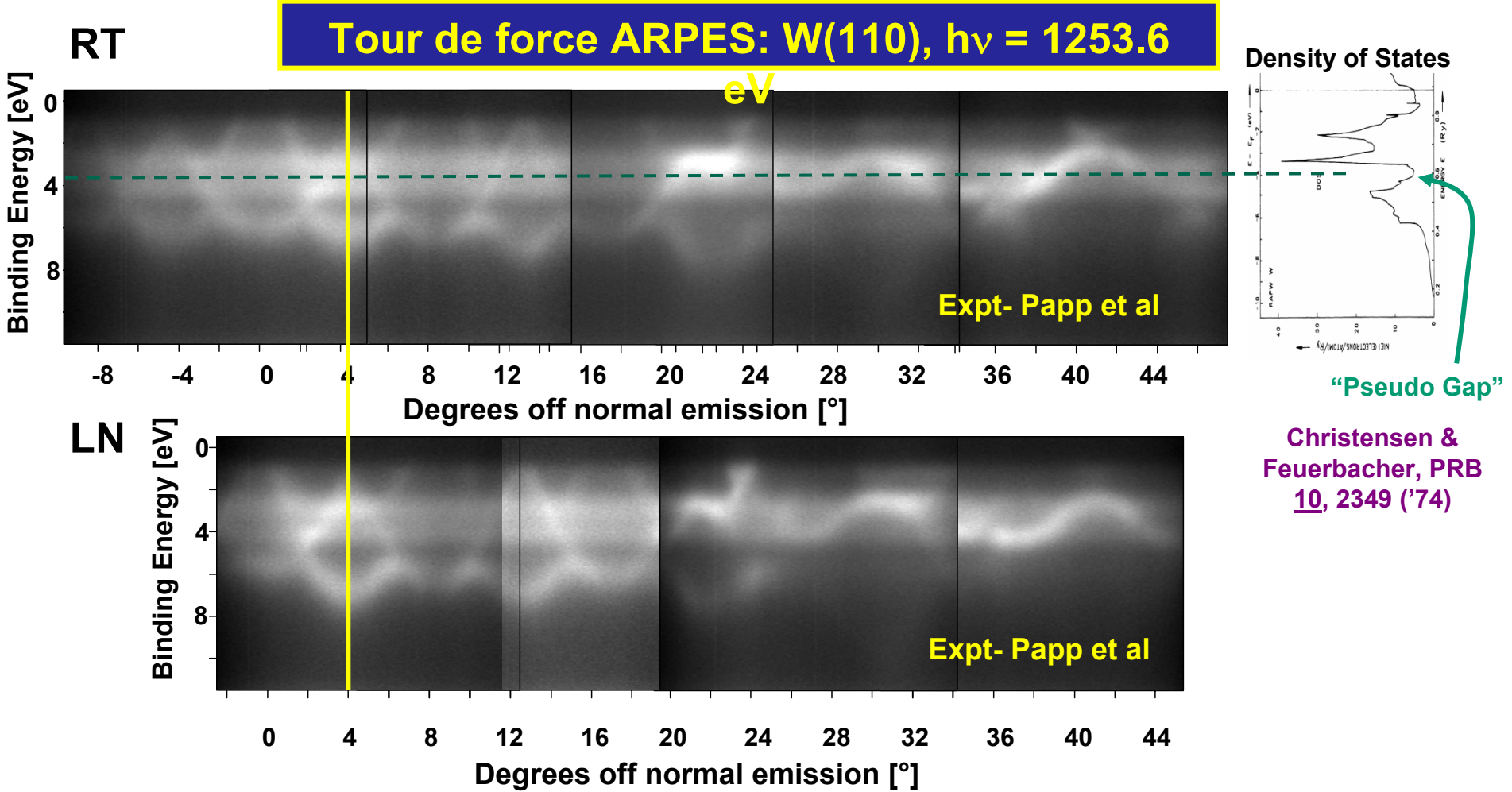


ARPES from W(110): 1-Step Theory, $h\nu = 870$ eV, near-normal emission, $\Theta_{\text{Debye}} = 400$ K



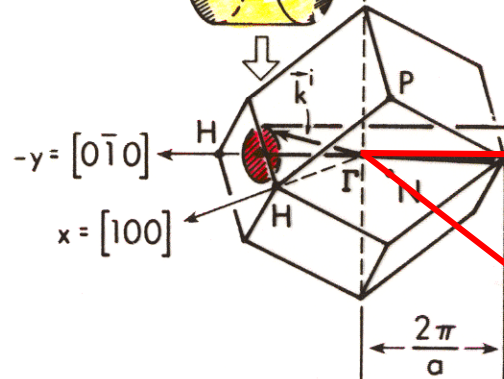
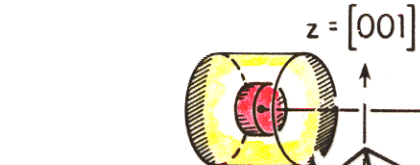
ARPES with a non-monochromatized lab. x-ray source: $h\nu = 1253.6$ eV, $T = \sim 77$ K





Tour de force ARPES: W(110), $h\nu = 1253.6$

DIRECT TRANSITIONS eV IN XPS OF TUNGSTEN

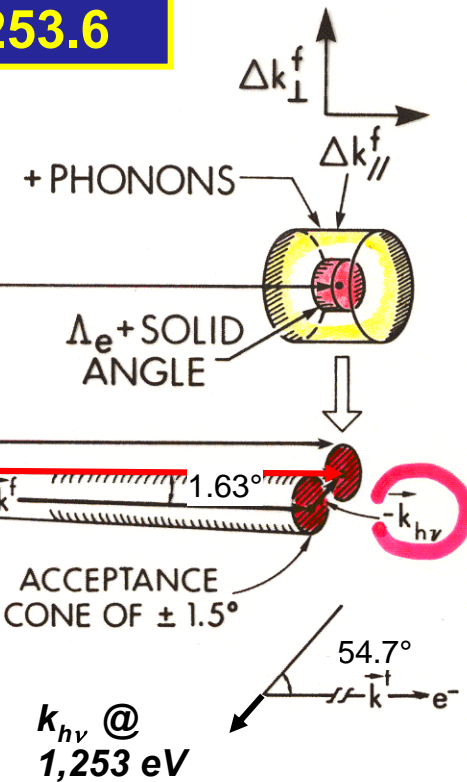


$$\vec{k}^i + \vec{g} = \vec{k}^f - \vec{k}_{hv}$$

$$\vec{g} = 10(2\pi/a)\hat{y}, \text{ along } [010]$$

$$a(W) = 3.16 \text{ \AA}, h\nu = 1253.6 \text{ eV}$$

$$k^f = 9.16(2\pi/a), k_{hv} = 0.32(2\pi/a), \alpha = 54.7^\circ$$

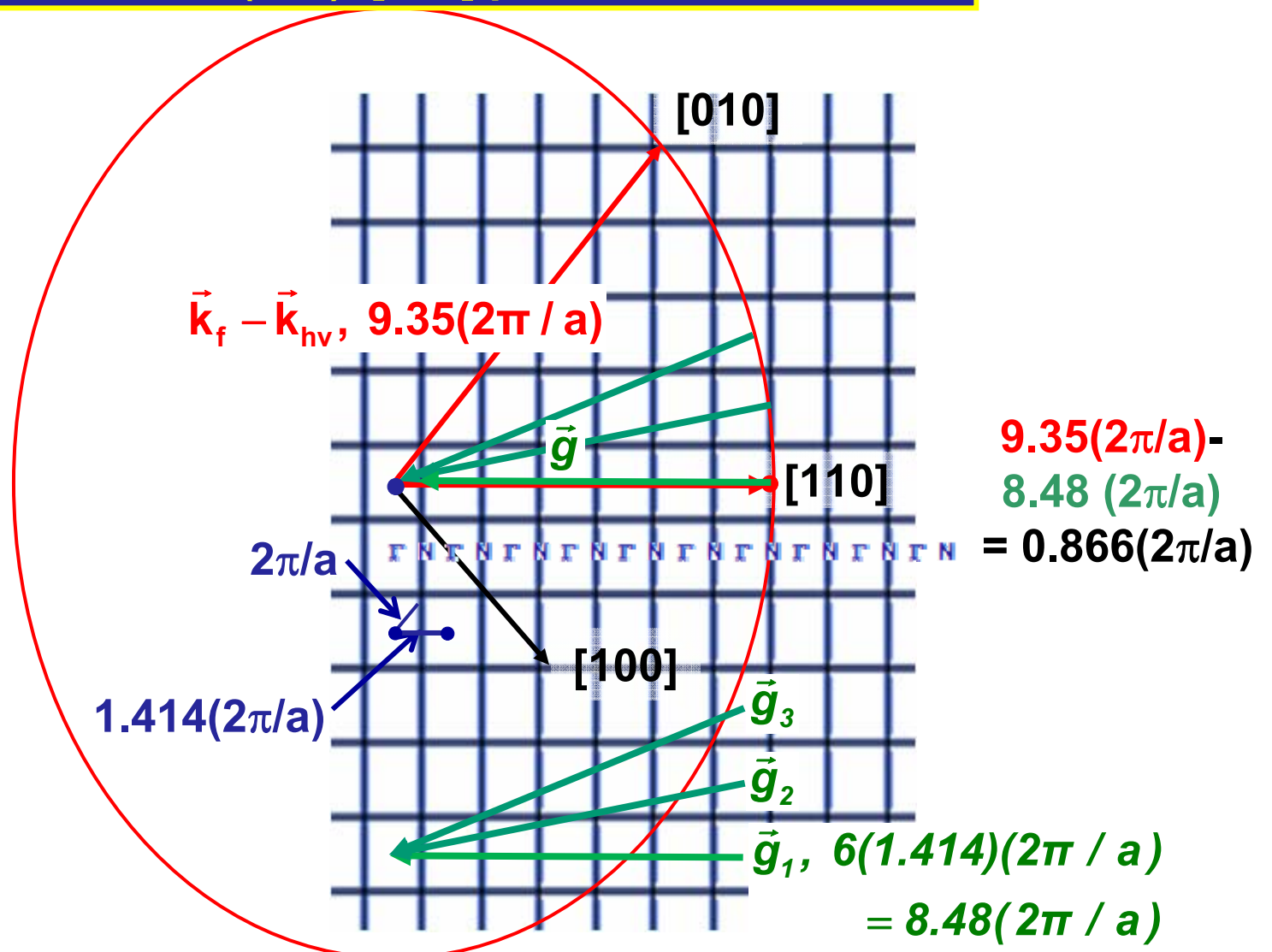


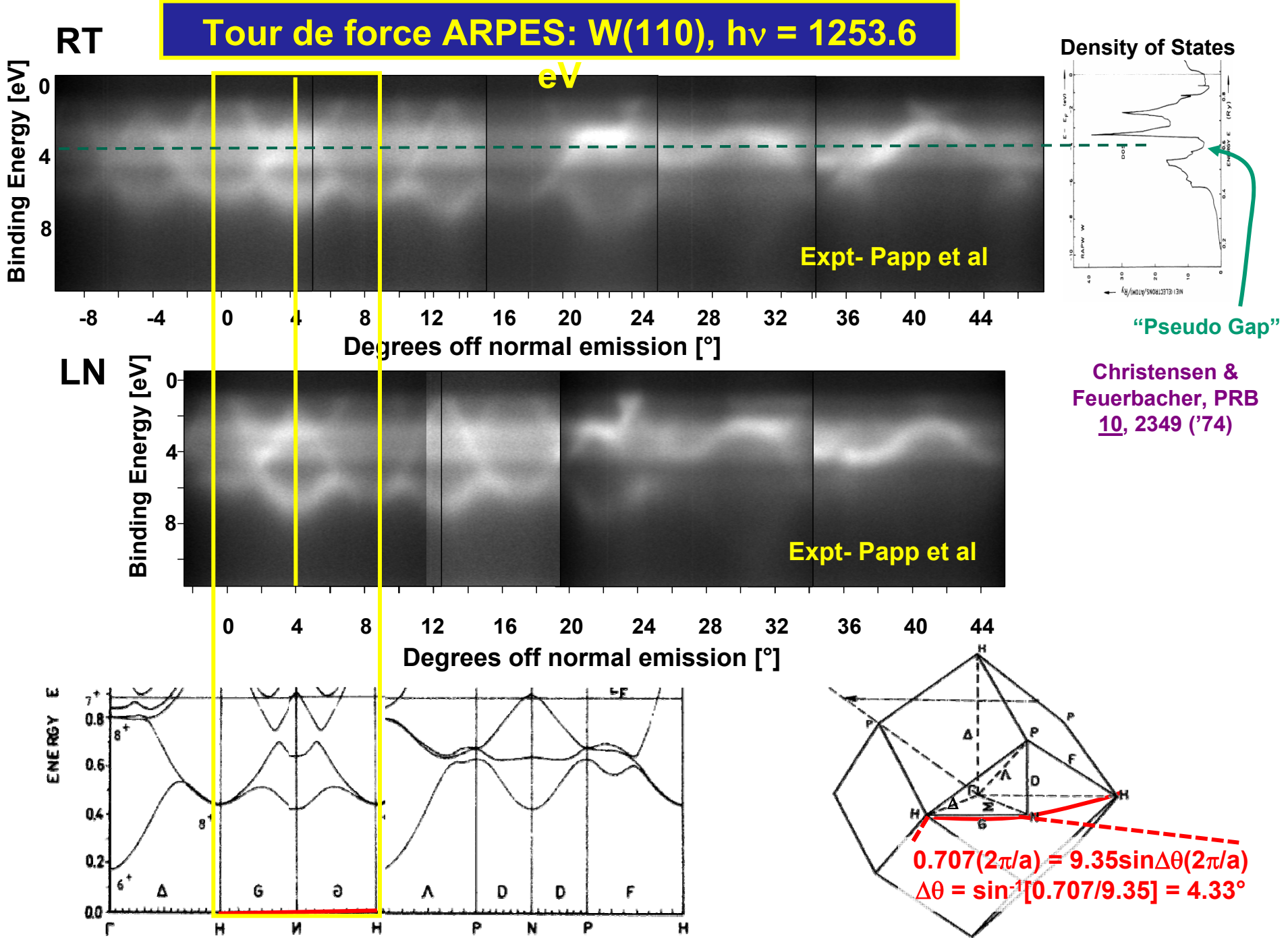
$$\vec{k}_f - \vec{k}_{hv}, \text{ with } |\vec{k}_f - \vec{k}_{hv}| = 9.35 2\pi/a$$

$[110]$
 $[010] \rightarrow [110] \rightarrow [100] \rightarrow [001]$ plane
 $\sim -9^\circ$ $+46^\circ$

Scan emission in $[001]$ plane

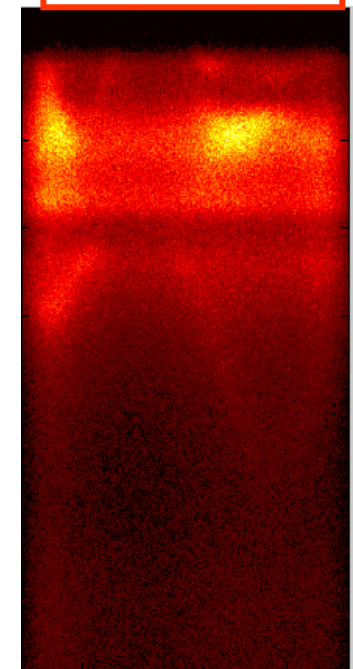
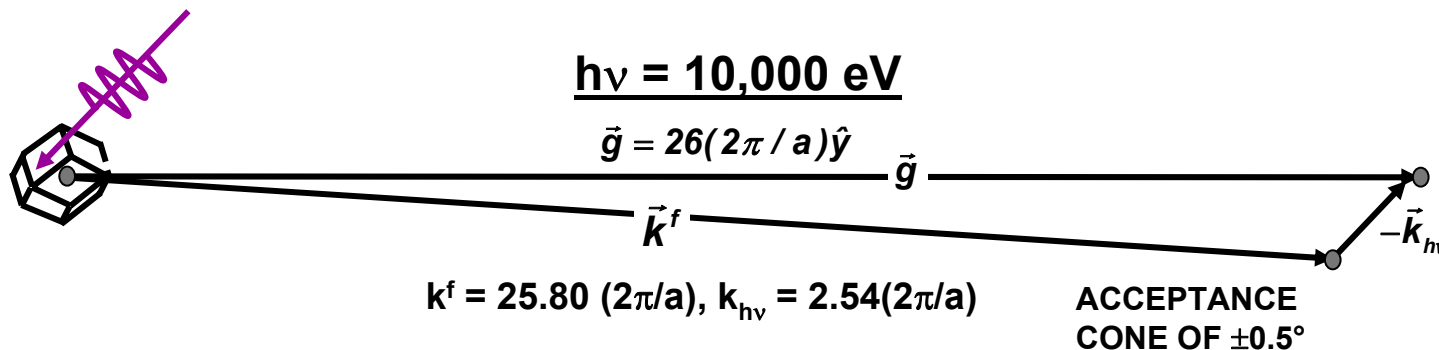
Tour de force ARPES in an extended zone
scheme: W(110), [001] plane, $h\nu = 1253.6$ eV





And what would happen at 10 keV?:

$h\nu = 870 \text{ eV}$
 $T = 780\text{K}$
 $W \approx 0.41$



$$\Theta_{\text{Debye}} = 310\text{K}, \langle u^2 \rangle (10^{-20} \text{ cm}^2) = 5.34 + 0.0583T \xrightarrow{\text{High } T} 0.0583T$$

Debye-Waller Factor = $W(T) \approx \exp(-k_e^2 \langle u^2(T) \rangle)$

$$= \exp(-C_1 E_{\text{kin}} \langle u^2(T) \rangle) \xrightarrow{\text{High } T} \exp(-C_2 E_{\text{kin}} T)$$

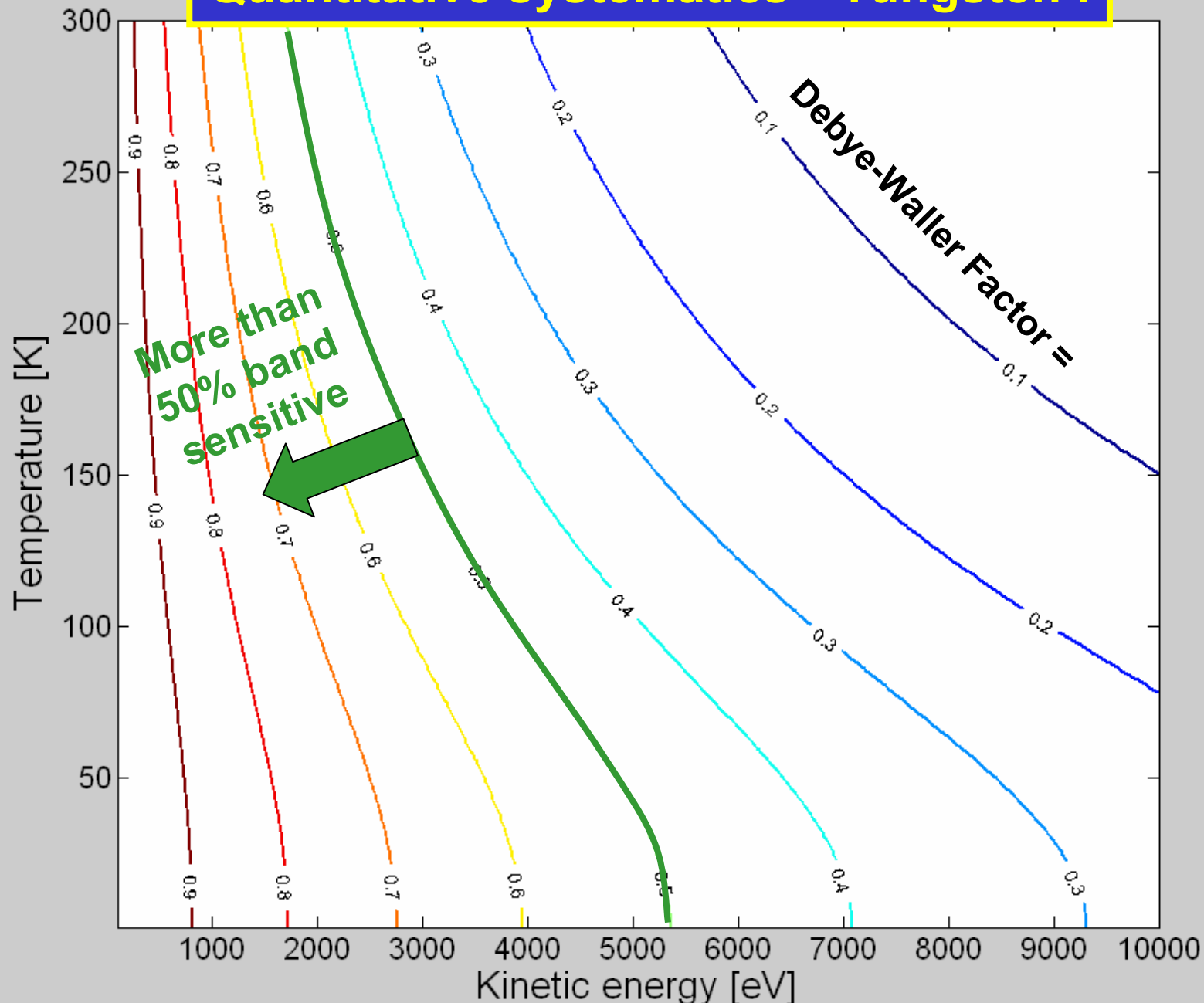
W at 4K: $W \approx 0.27$, $\approx 27\%$ direct

at 77K: $W \approx 0.20$, $\approx 20\%$ direct

at 300K: $W \approx 0.017$, $\approx 2\%$ direct

Correlated vibrations and better theory (e.g. Phys. Rev. B 35, 1147 ('87) and 53, 7524 ('96) + 54, 14703 ('96)) may yield different DT percentages, but needs further experimental and theoretical study

Quantitative systematics—Tungsten :



Outline

Surface, interface, and nanoscience—short introduction

Some surface concepts and techniques→photoemission

Synchrotron radiation: experimental aspects

Electronic structure—a brief review

**The basic synchrotron radiation techniques:
more experimental and theoretical details**



Core-level photoemission

Valence-level photoemission

Microscopy with photoemission

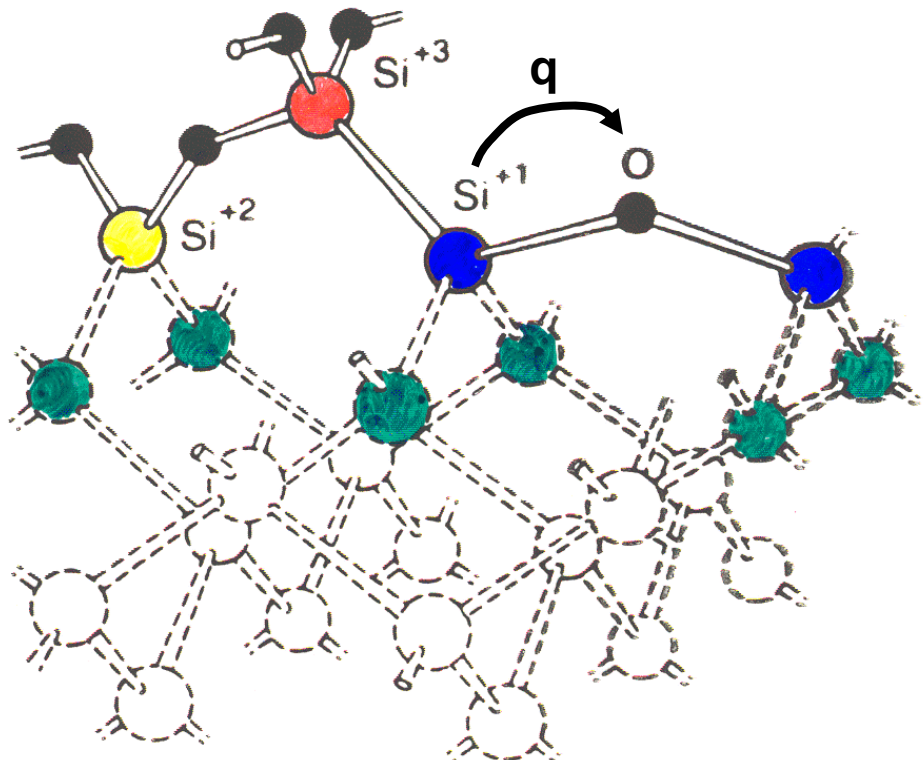
Outline

- Valence-band spectra: low-energy UPS limit and high-energy XPS limit
- Core-level chemical shifts: the potential model
- Core-level chemical shifts: equivalent-core ($Z+1$) and thermochemical energies
- Multiplet splittings
- Spin-orbit splitting, the Fano effect, and spin-polarized outgoing electrons
- Magnetic circular dichroism (MCD) in core-level emission
- Non-magnetic circular dichroism in core-level emission: a.k.a. circular dichroism in angular distributions (CDAD)
- Various other final state effects providing information in core-level spectra

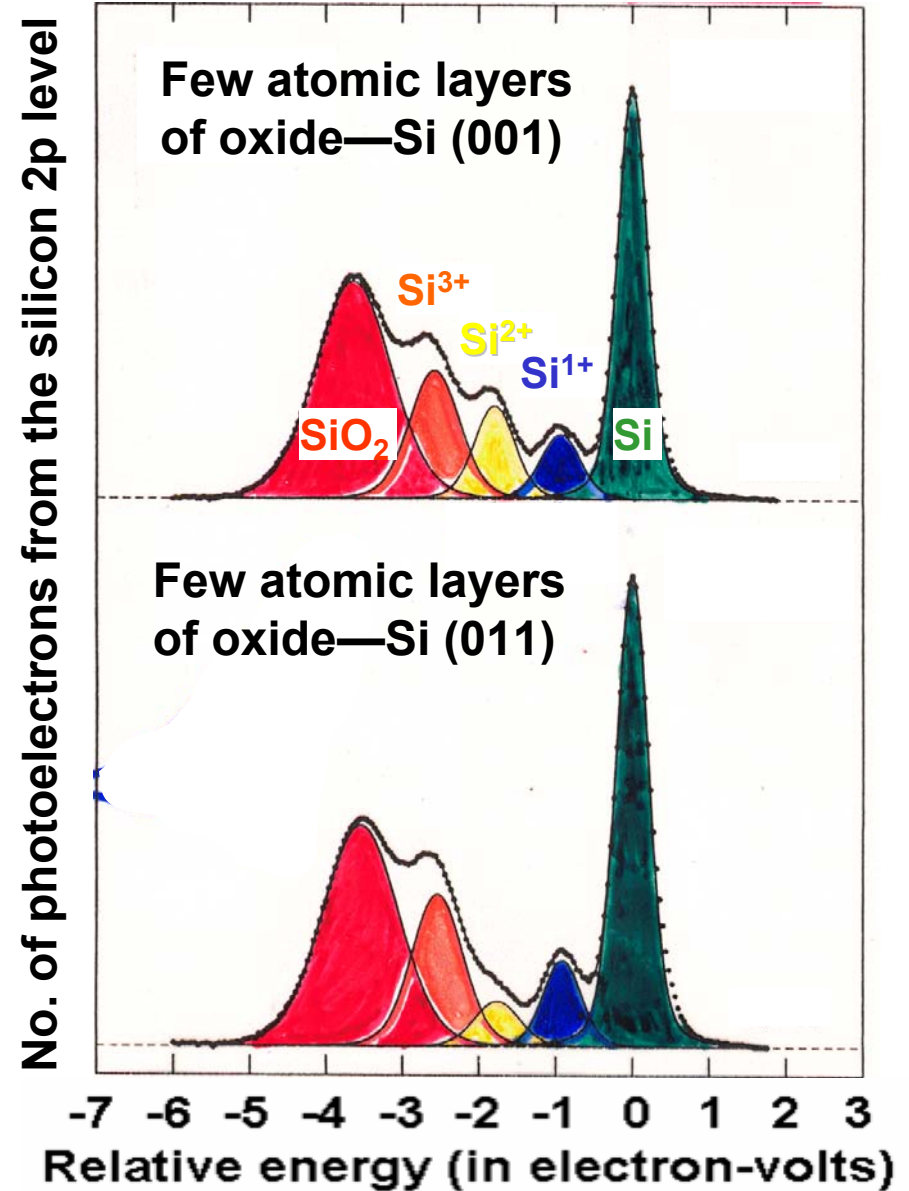
Looking into the silicon dioxide layer with photoelectron spectroscopy

Charge transfer, $e^- - e^-$ coulomb integral:

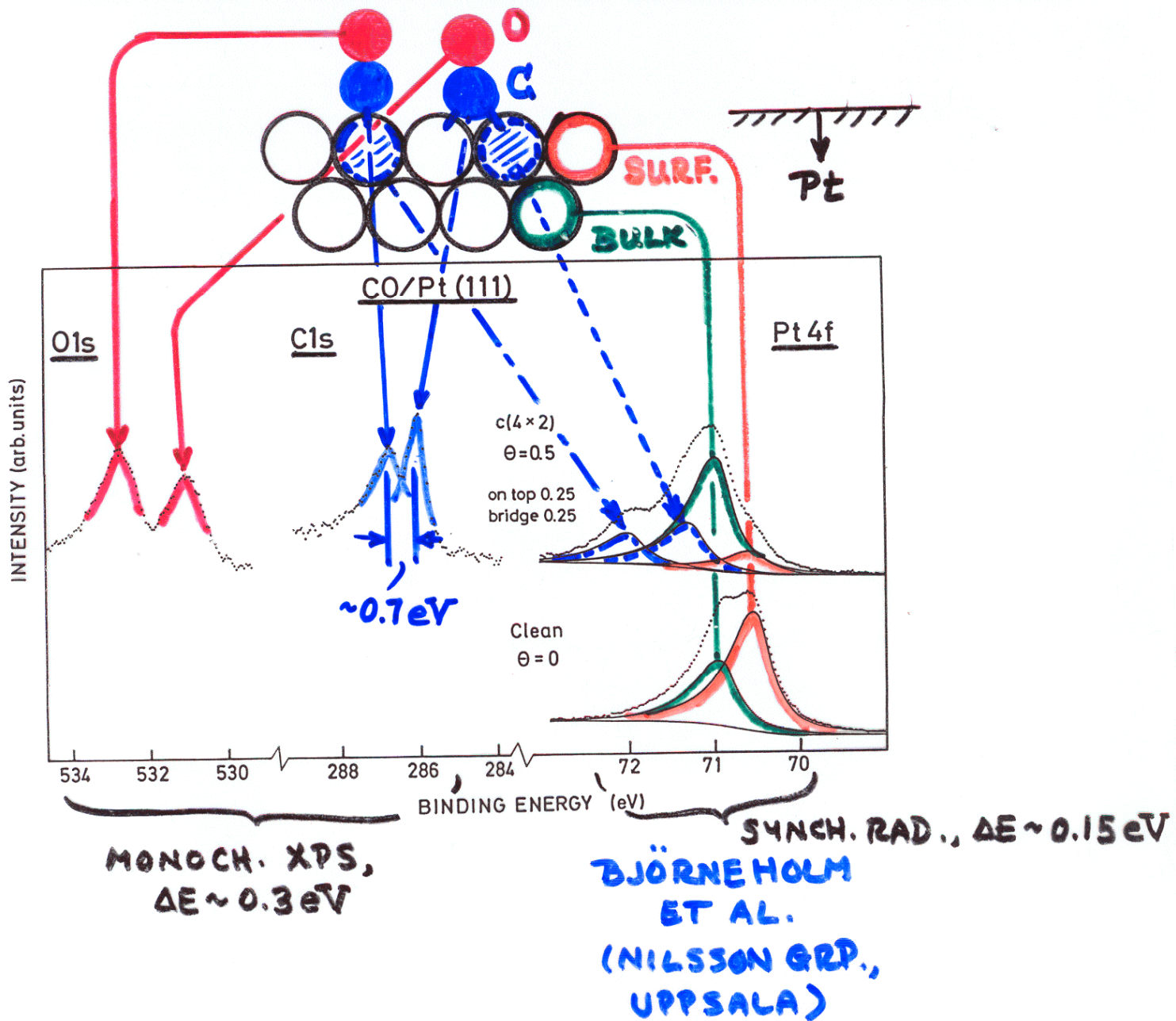
$$\text{Shift} \approx q_{Si} J_{Si2p, Si3p} = \int \varphi_{2p}^*(\vec{r}_1) \varphi_{3p}^*(\vec{r}_2) \frac{e^2}{r_{12}} \varphi_{2p}(\vec{r}_1) \varphi_{3p}(\vec{r}_2) dV_1 dV_2$$

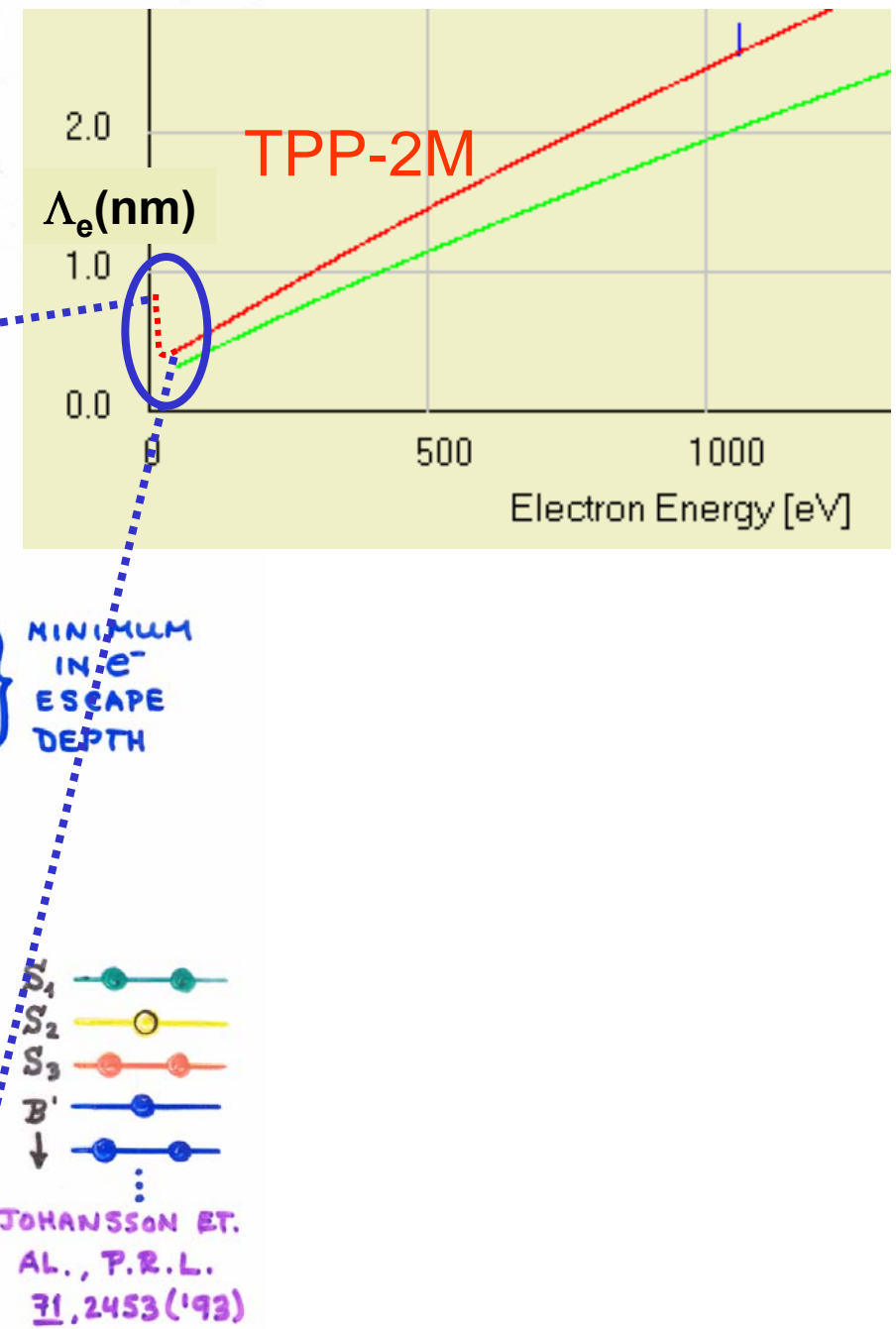
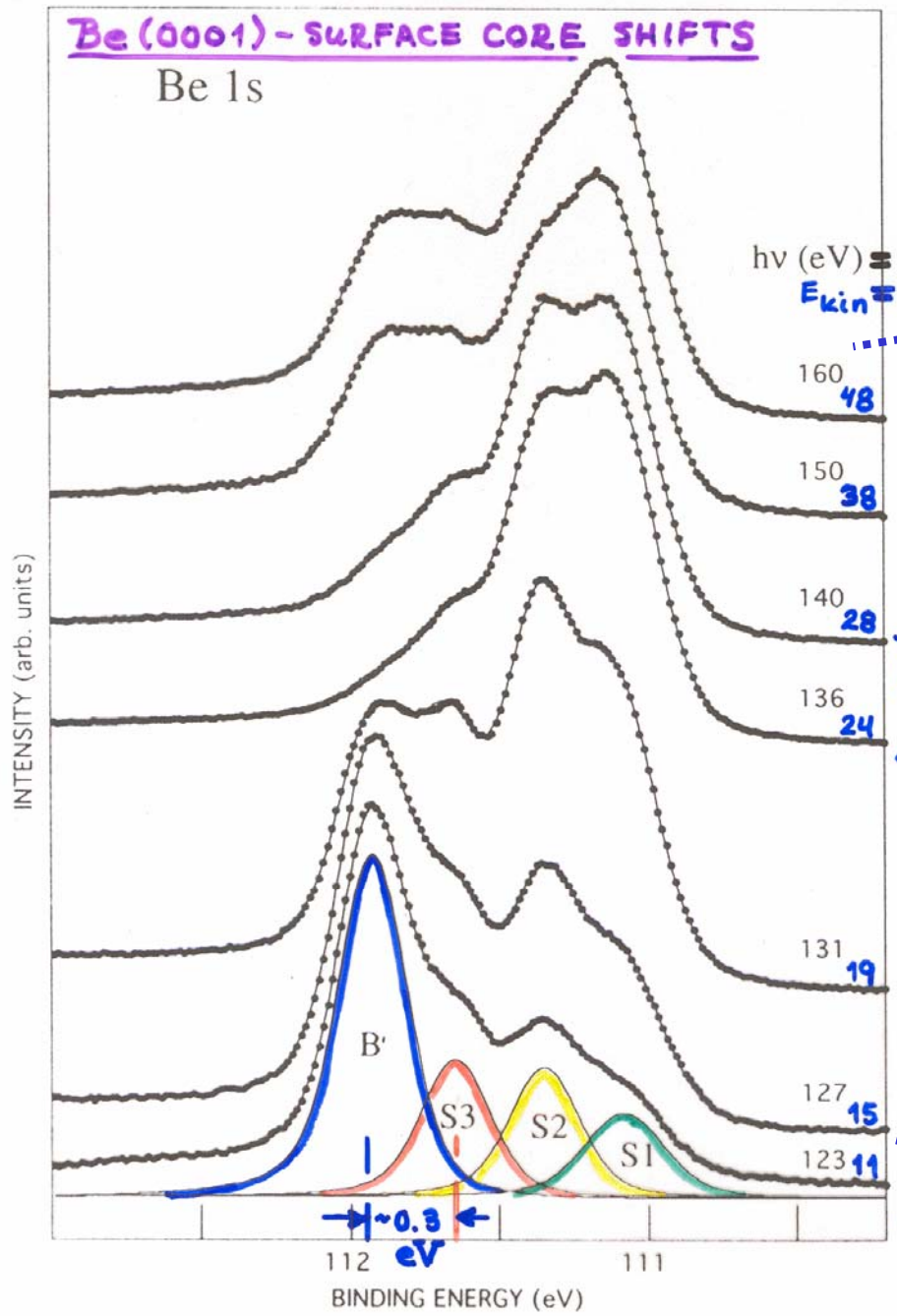


Himpsel et al., Phys. Rev. B 38, 6086 ('88)



CHEMICAL SHIFTS IN ADSORBATE + SUBSTRATE





What does the hole do?

BINDING ENERGIES & KOOPMANS' THEOREM:

$N-e^-$ SCH. EQN. — $\hat{H}(N)\Psi_j(N) = E_j(N)\Psi_j(N), j=1, 2, \dots$

MINIMIZE $E_j(N)$ $\downarrow \Psi_j \approx \Phi_j = \text{SLATER DET.}$

$N-1-e^-$ HARTREE-FOCK EQNS. — $\hat{H}(1)\Psi_k(1) = \varepsilon_k(1)\Psi_k(1)$

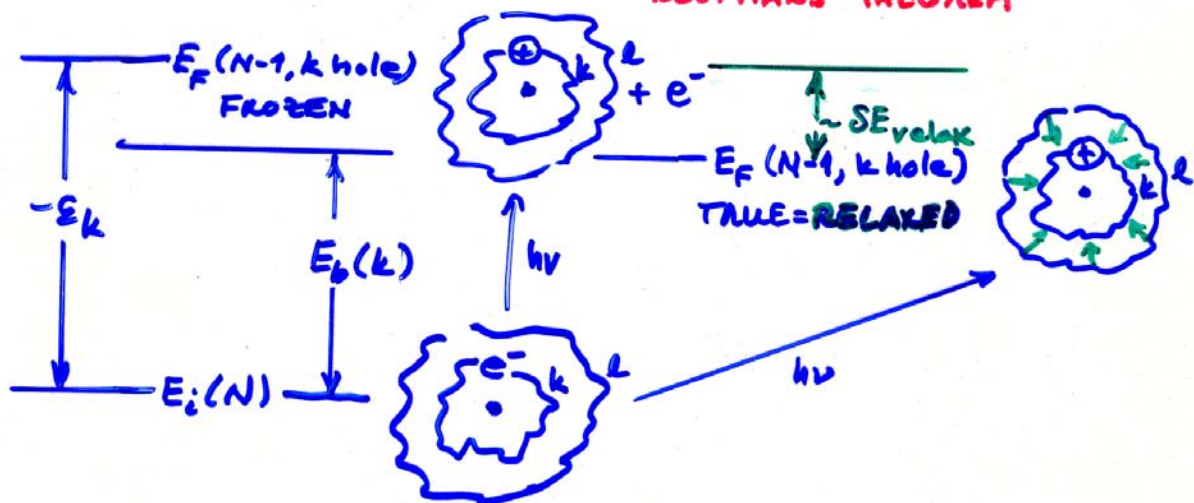
- COUPLED INTEGRO-DIFF.
- COULOMB + EXCHANGE

$E_b(k) = k^{\text{th}}$ BINDING ENERGY = $E_f(N-1, k \text{ hole}) - E_i(N)$

(+) EXACT

OR $E_b(k) = -\varepsilon_k$ IF $\Psi_{ki} = \Psi_{kf}$ (FROZEN ORBITAL)

KOOPMANS' THEOREM



⇒ RELAXATION, SCREENING, CONFIGURATION INTERACTION, SELF-ENERGY EFFECT ALWAYS PRESENT; ANDERSON IMPURITY MODEL ETC.

KOOPMANS' THEOREM CALCULATION OF SHIFTS

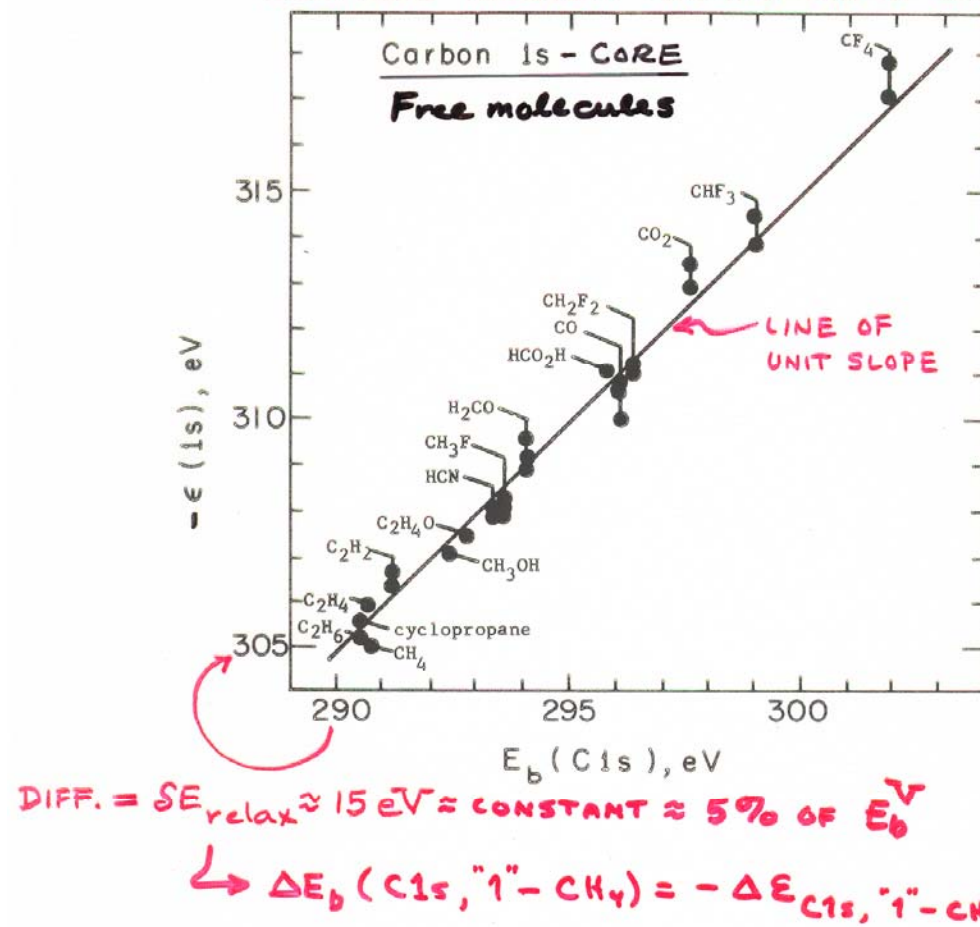
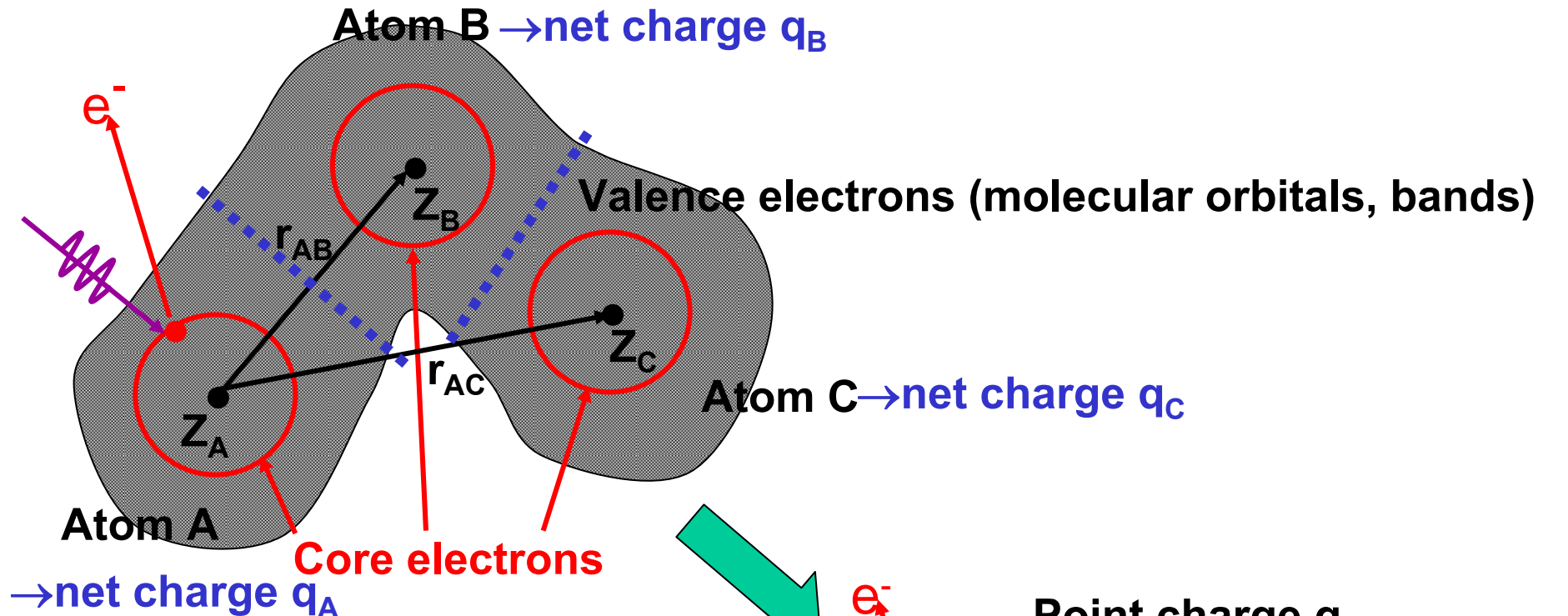


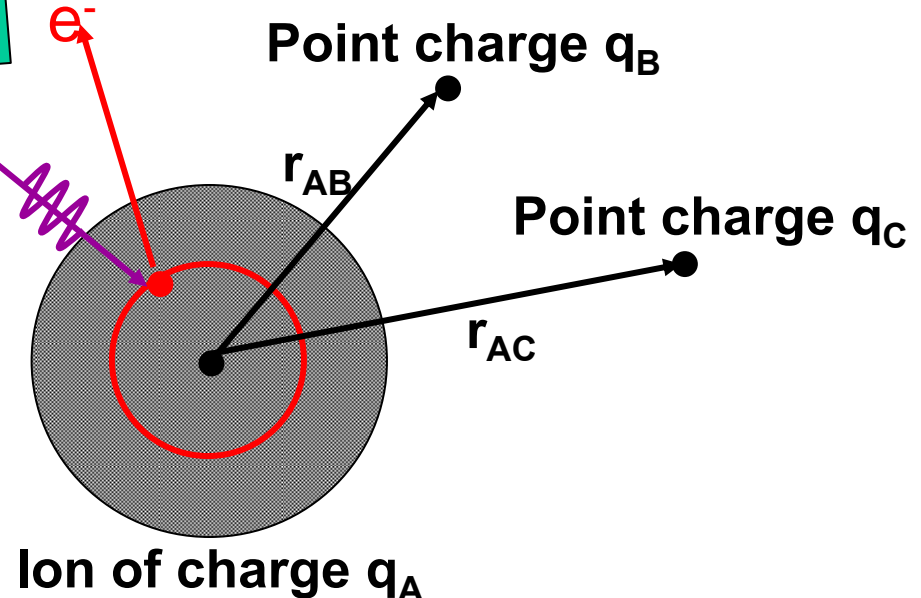
Figure 18 -- Plot of carbon 1s binding energies calculated via Koopmans' Theorem against experimental binding energies for several carbon-containing gaseous molecules. For some molecules, more than one calculated value is presented. The slope of the straight line is unity. The two scales are shifted with respect to one another by 15 eV, largely due to relaxation effects. All of the theoretical calculations were of roughly double-zeta accuracy or better. (From Shirley, reference 7.)

"Basic Concepts of XPS"
Figure 18

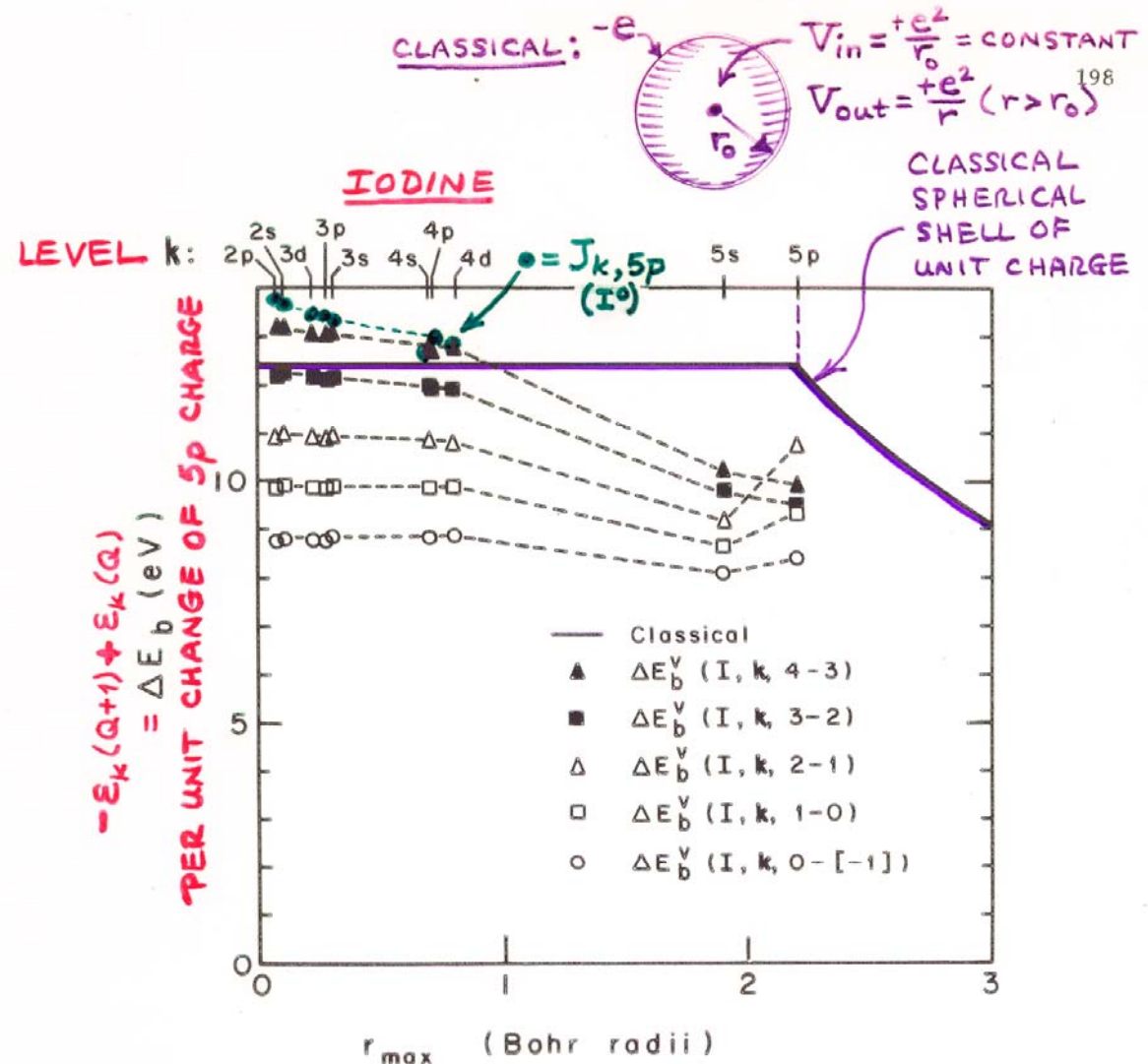
POTENTIAL MODEL FOR CORE-LEVEL CHEMICAL SHIFTS



Core binding energy on A in
molecule ABC =
Core binding energy of *free ion A*
with charge q_A
+ $q_B e^2/r_{AB} + q_C e^2/r_{AC}$
(+ relaxation corrections)



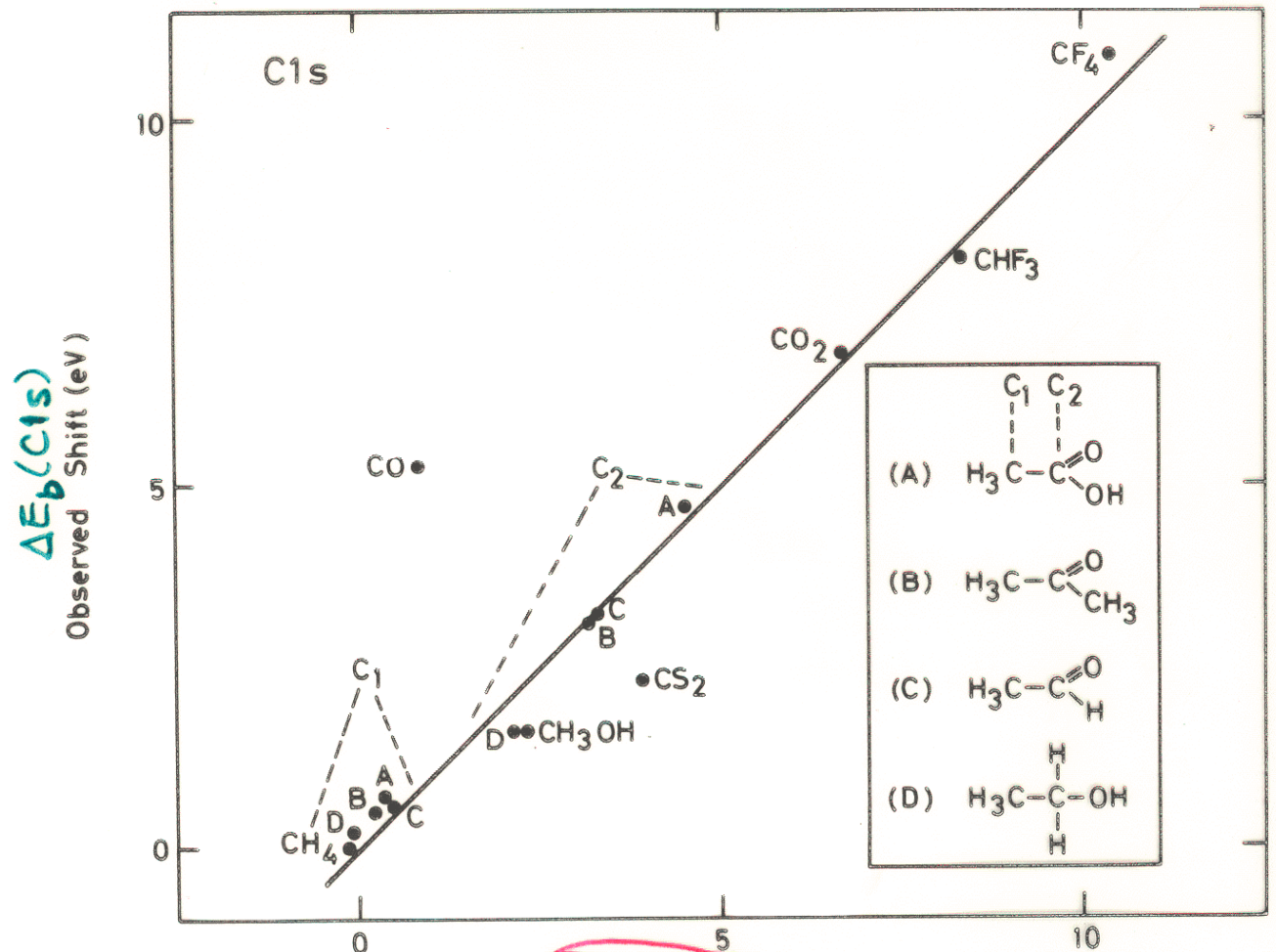
FREE-ION (INTRAATOMIC) ASPECTS OF SHIFTS: KOOPMANS' THEOREM & CLASSICAL CHARGED SHELL



→ REMOVAL/ADDITION OF VALENCE e^- CHARGE IN BONDING SHIFTS ALL INNER $e^- E_b$'s $\approx E_k$'s BY SAME AMOUNT

"Basic Concepts of XPS"
Figure 19

POTENTIAL MODEL CALCULATION OF CARBON CHEMICAL SHIFTS



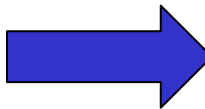
EMPIRICAL:
 $C_A = 21.9 \text{ eV}$
 $\approx J_{1s, \text{valence}}$
 $\ell \approx 0.80 \text{ eV}$

THEORY
 $C_A q_A + V + \ell \text{ (eV)}$
 $(\sum \frac{q_i}{r_{AL}}, q_i \text{'s FROM CNDO MO})$

"Basic Concepts of XPS"

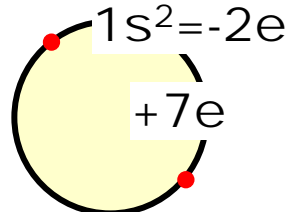
Figure 24

Outline

- Valence-band spectra: low-energy UPS limit and high-energy XPS limit
- Core-level chemical shifts: the potential model
- Core-level chemical shifts: equivalent-core ($Z+1$) and thermochemical energies 
- Multiplet splittings
- Spin-orbit splitting, the Fano effect, and spin-polarized outgoing electrons
- Magnetic circular dichroism (MCD) in core-level emission
- Non-magnetic circular dichroism in core-level emission: a.k.a. circular dichroism in angular distributions (CDAD)
- Various other final state effects providing information in core-level spectra

CORRELATION OF THERMOCHEMICAL DATA WITH CHEMICAL SHIFTS: EQUIVALENT-CORE OR (Z+1) MODEL

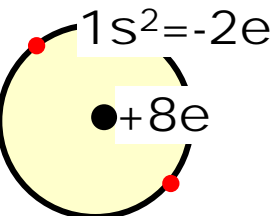
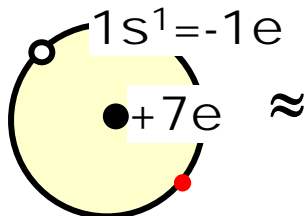
$$N \text{ core} = N 1s^2 = N^{5+}$$



Assume:

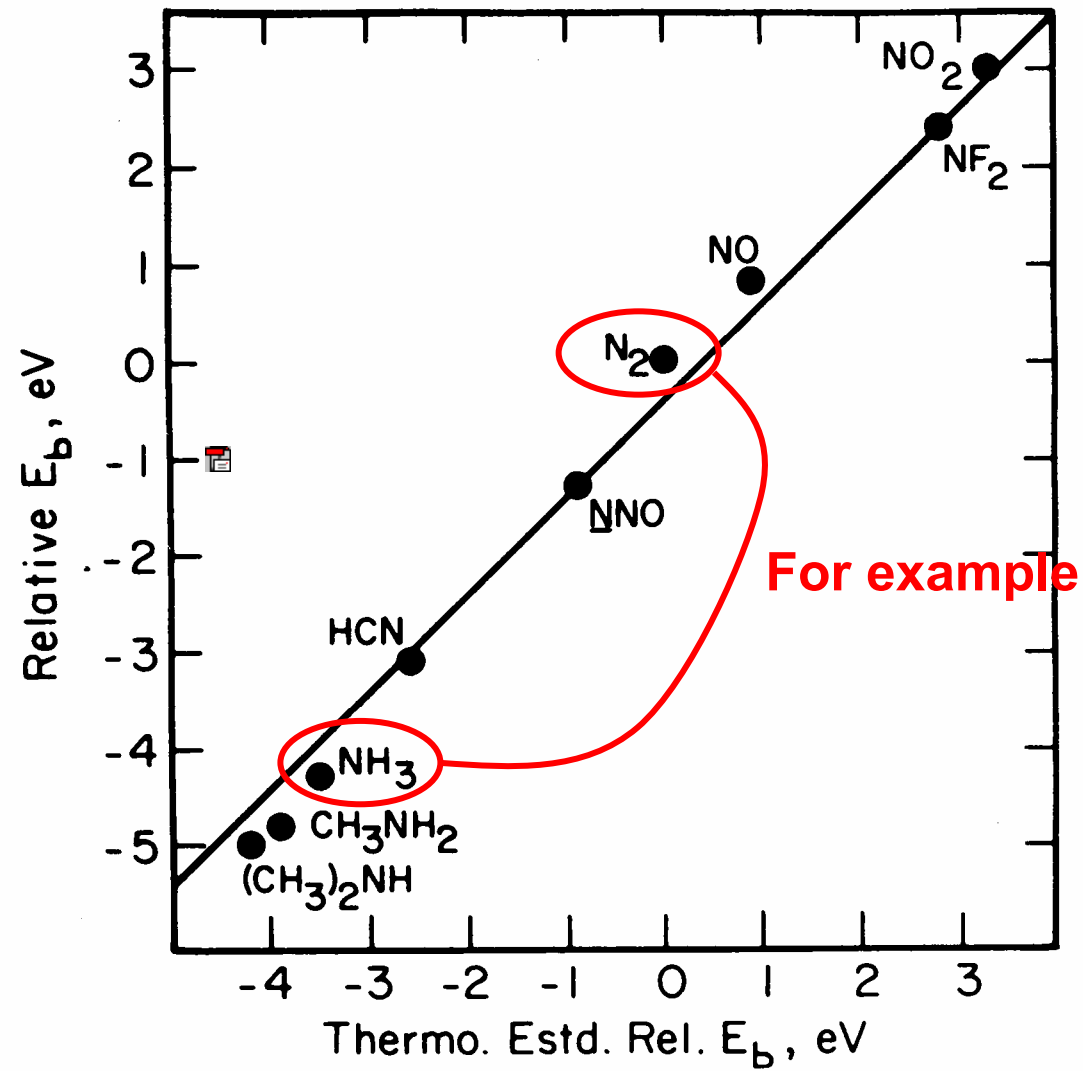
N^{6+*} core with

$1s$ hole = N^{6+*} =



= O^{6+} core

Plus see pp. 92-93
in "Basic Concepts
of XPS"



Jolly et al.

Binding energies: ${}^* = \text{N } 1\text{s core hole present}$

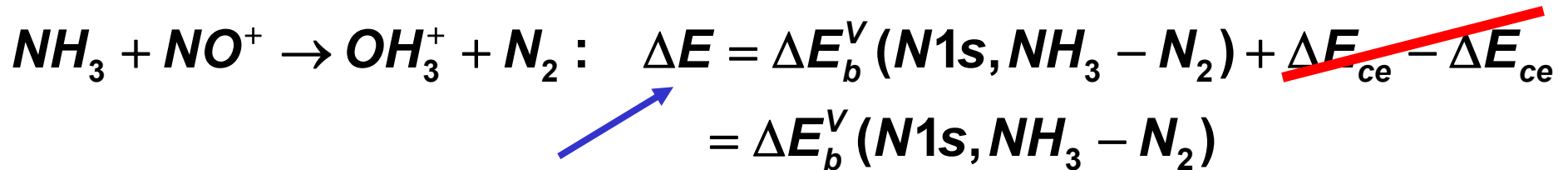


Adding and subtracting:

$$\begin{aligned}\text{NH}_3 + \text{N}_z^{+*} \rightarrow \text{NH}_3^{+*} + \text{N}_2 : \quad \Delta E &= \Delta E_1 - \Delta E_2 \\ &= E_b^V(\text{N } 1\text{s}, \text{NH}_3) - E_b^V(\text{N } 1\text{s}, \text{N}_2) \\ &= \Delta E_b^V(\text{N } 1\text{s}, \text{NH}_3 - \text{N}_2)\end{aligned}$$

The chemical shift

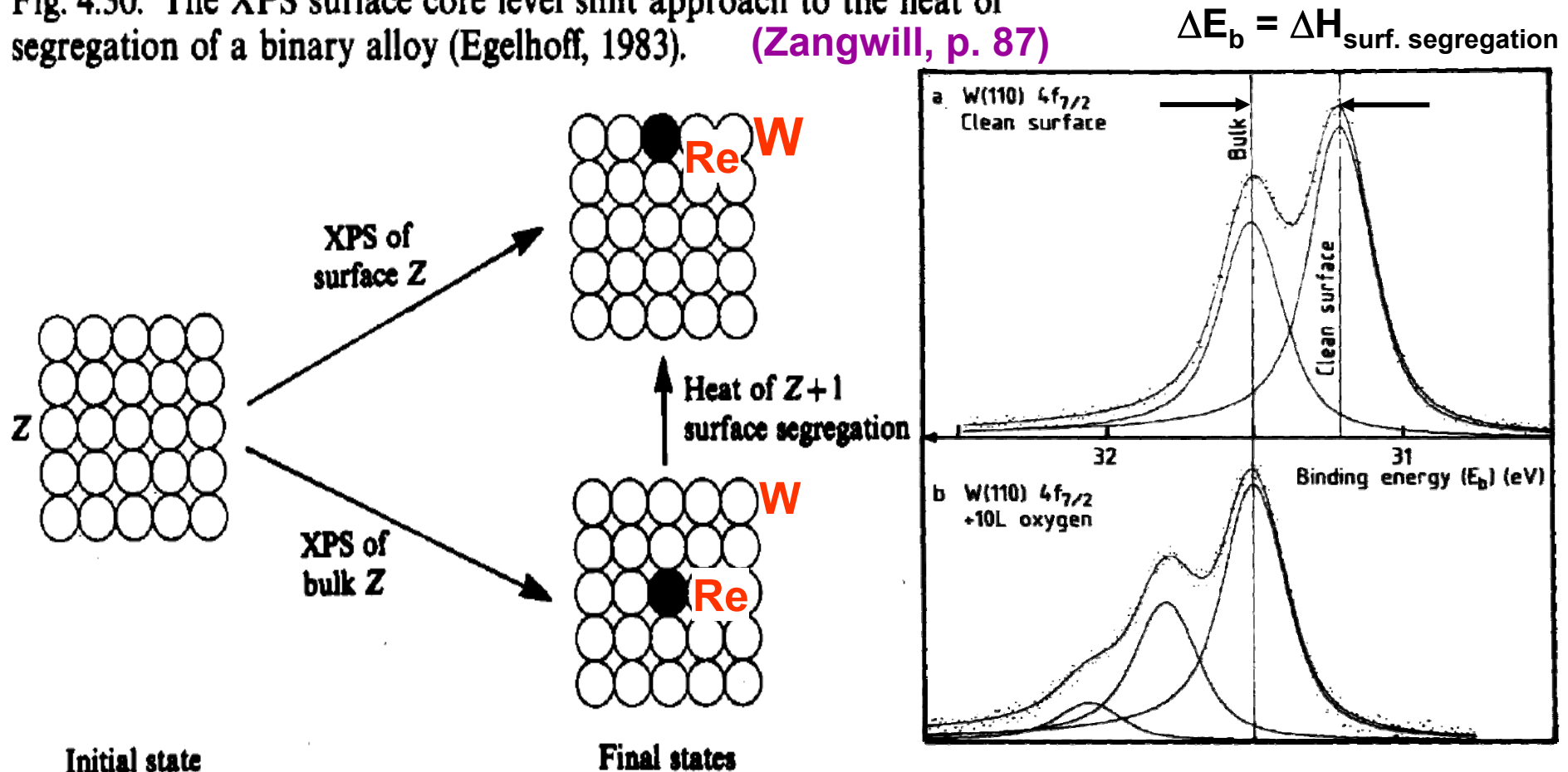
Replacing real N 1s core with equivalent O 1s core:



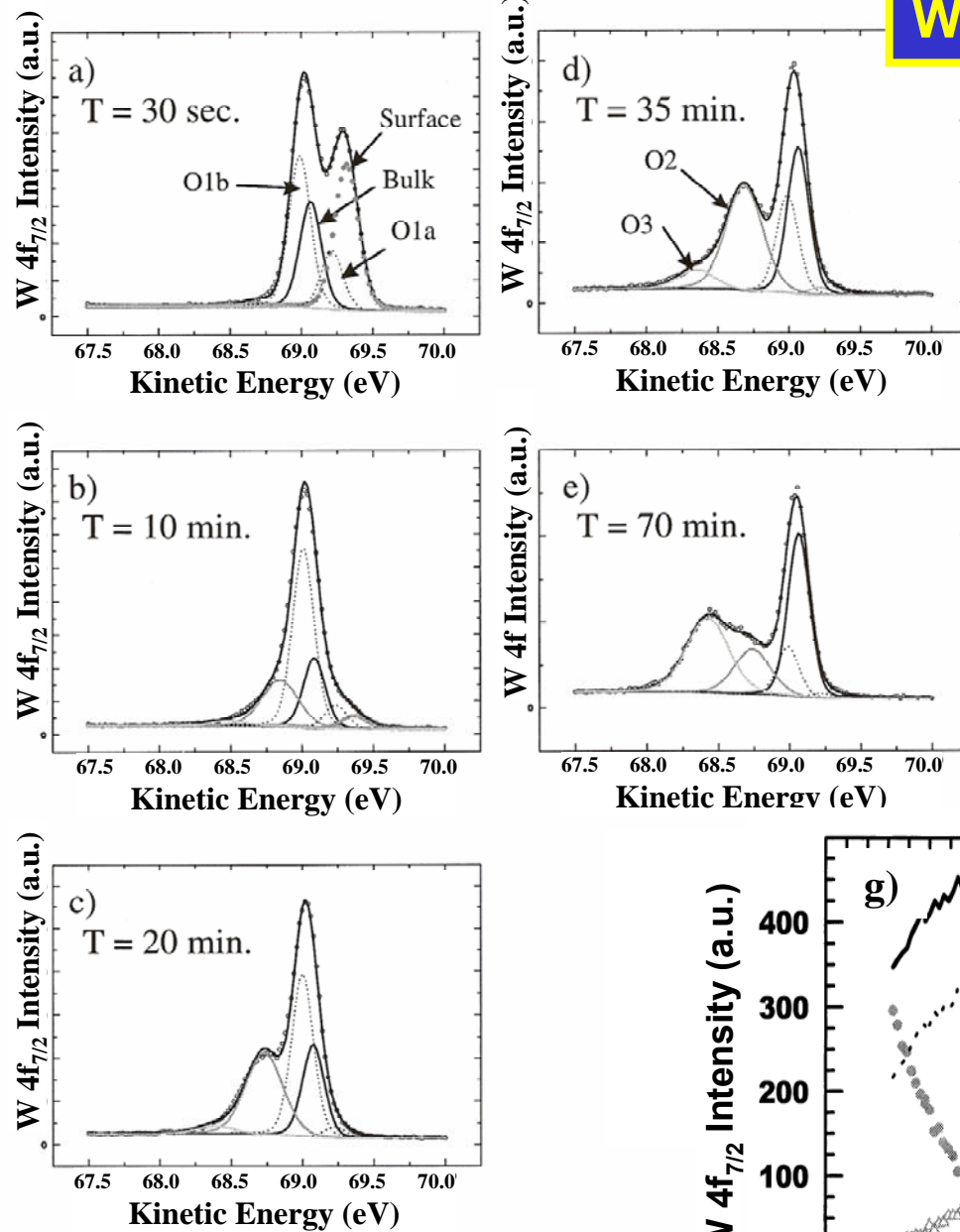
A thermochemical energy

DERIVATION OF HEAT OF SURFACE SEGREGATION FROM SURFACE CORE-LEVEL CHEMICAL SHIFTS

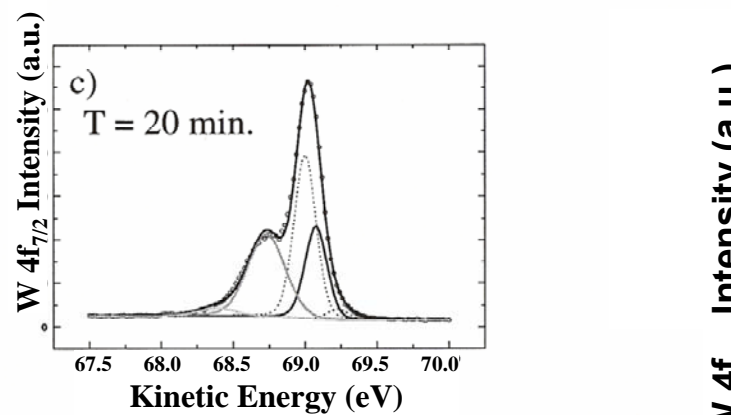
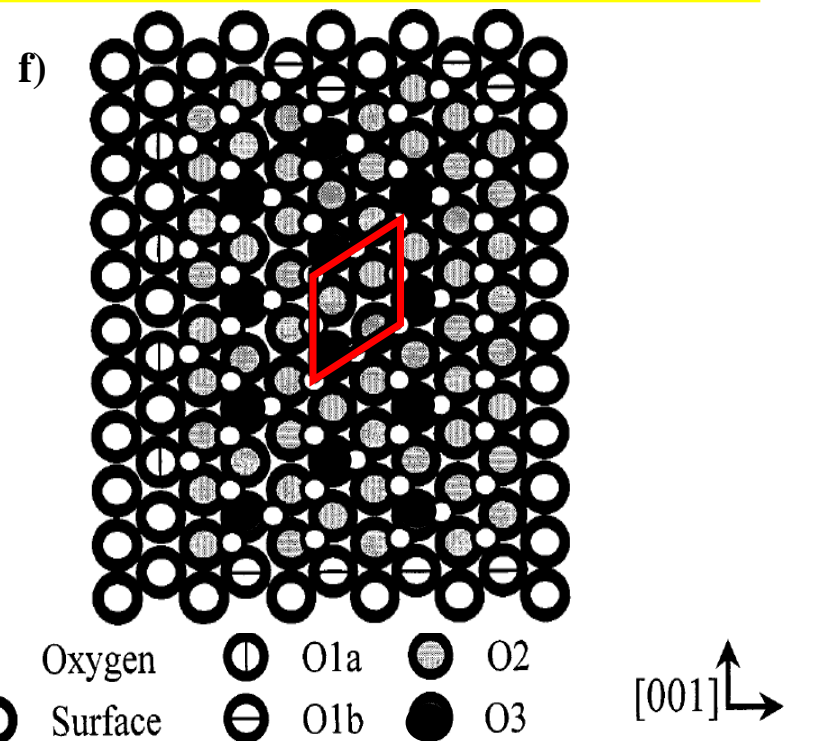
Fig. 4.30. The XPS surface core level shift approach to the heat of segregation of a binary alloy (Egelhoff, 1983). (Zangwill, p. 87)



Spanjaard et al., Surf. Sci.
Repts. 5, 1 (1985)



W(110)/O—W 4f_{7/2} Chemical Shifts

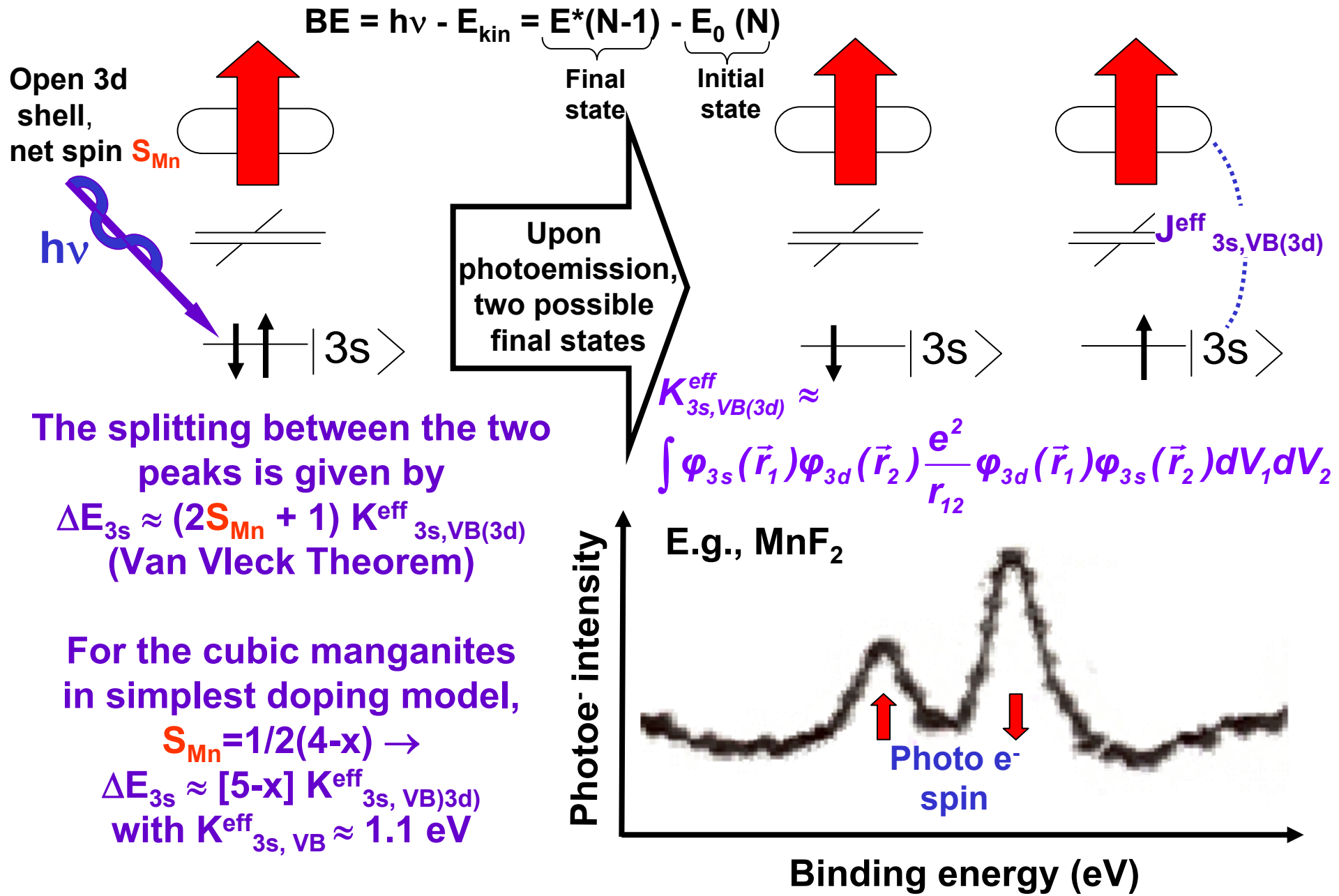


An early time-resolved reaction study (more later)

Outline

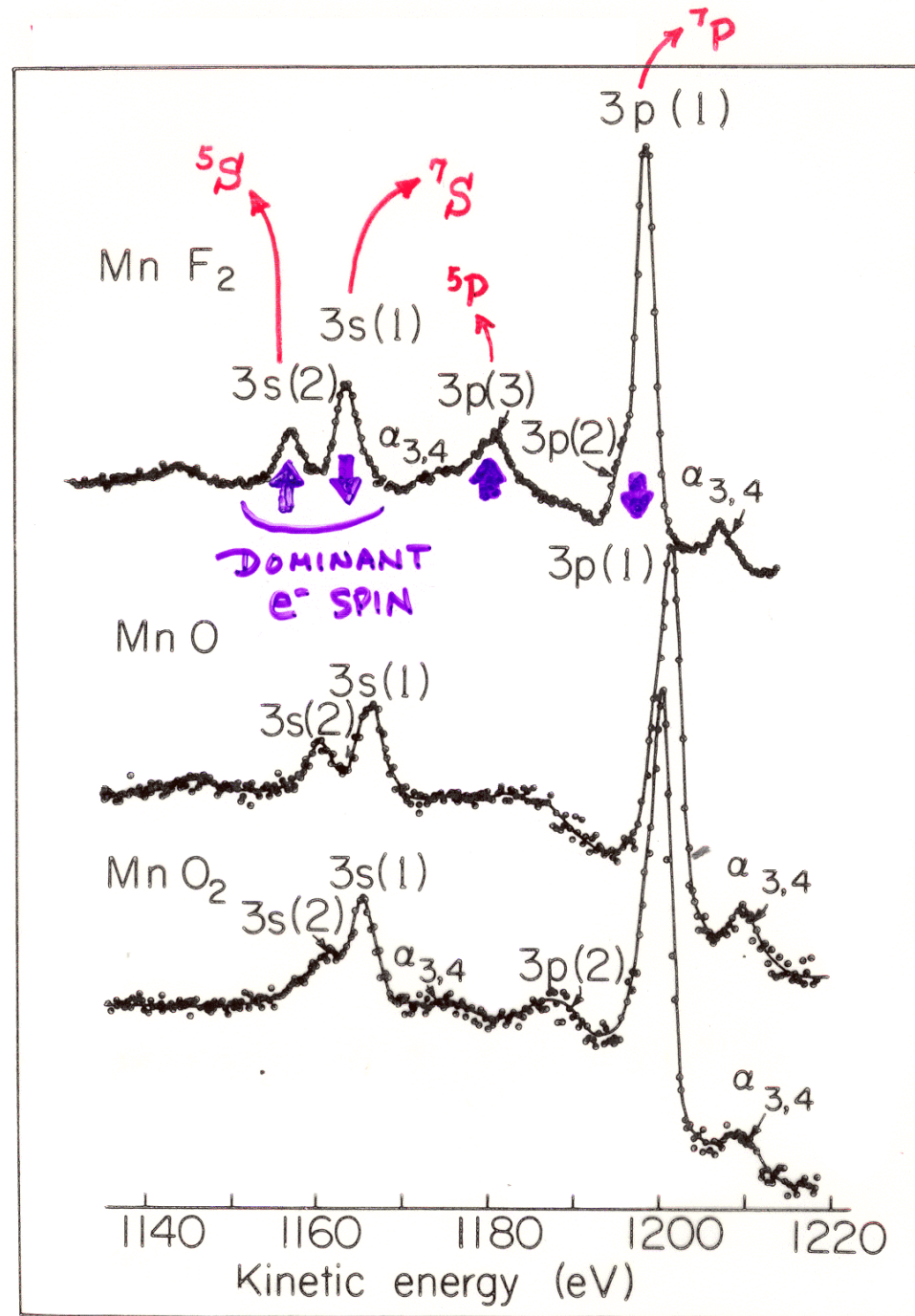
- Valence-band spectra: low-energy UPS limit and high-energy XPS limit
- Core-level chemical shifts: the potential model
- Core-level chemical shifts: equivalent-core ($Z+1$) and thermochemical energies
- Multiplet splittings and magnetism
- Spin-orbit splitting, the Fano effect, and spin-polarized outgoing electrons
- Magnetic circular dichroism (MCD) in core-level emission
- Non-magnetic circular dichroism in core-level emission: a.k.a. circular dichroism in angular distributions (CDAD)
- Various other final state effects providing information in core-level spectra

Multiplet splitting in core levels of transition metal oxides

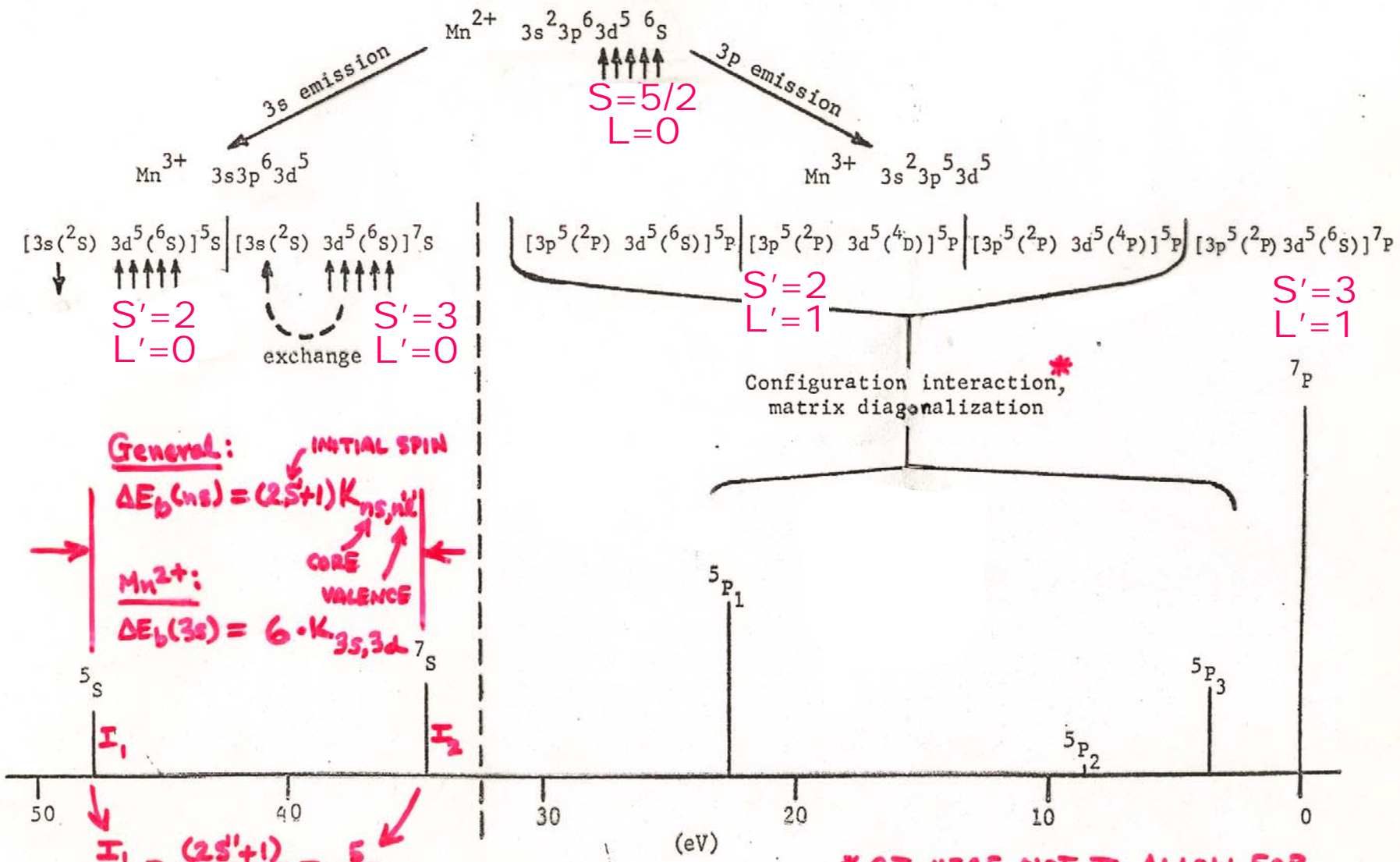


CORE-LEVEL MULTIPLET SPLITTINGS IN Mn COMPOUNDS

"Basic Concepts of XPS"
Figure 31



ORIGIN OF MULTIPLET SPLITTINGS IN Mn^{2+} : "ONE-ELECTRON" THEORY



$$\frac{I_1}{I_2} = \frac{(2S'+1)}{(2S'+1)} = \frac{5}{7}$$

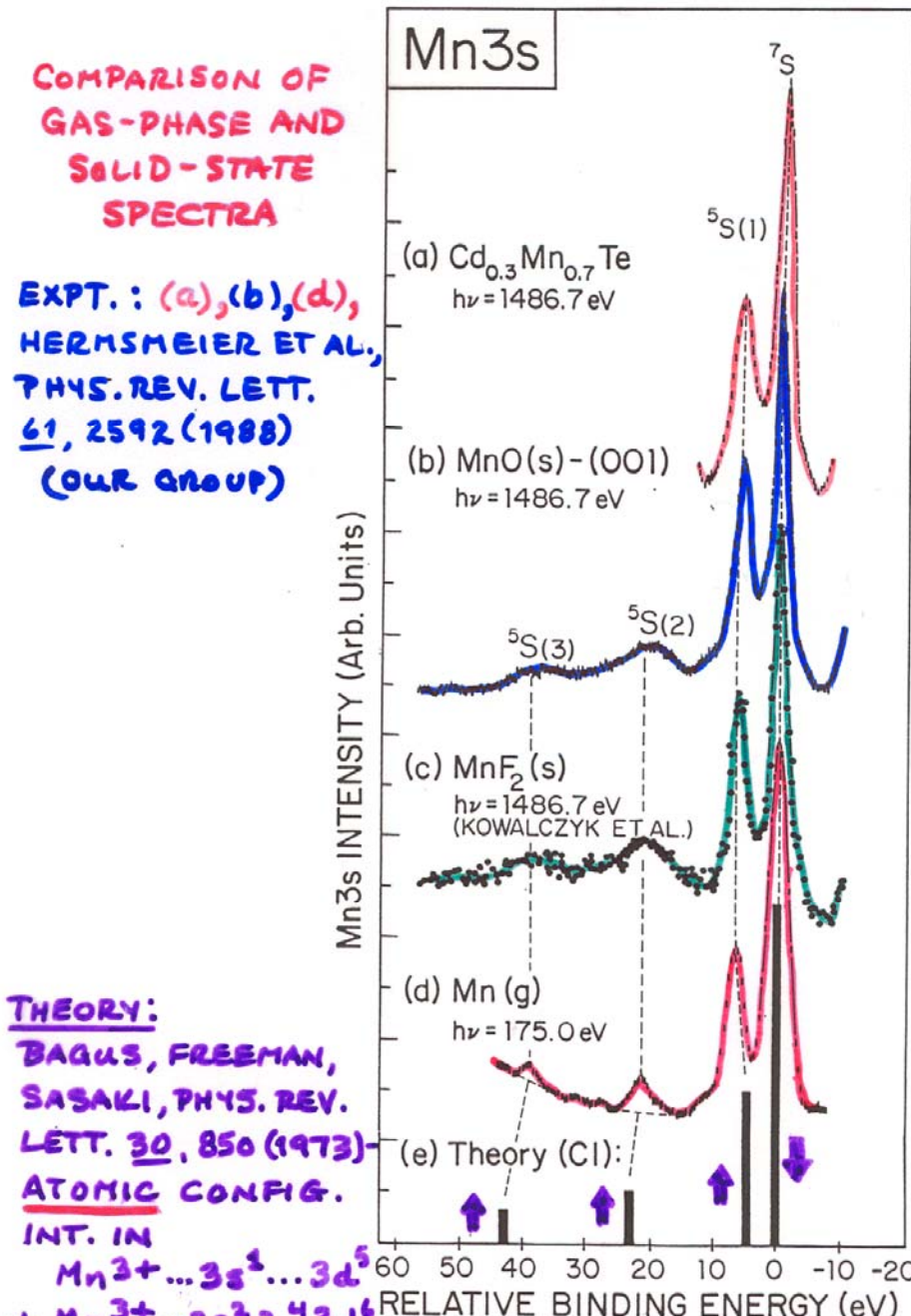
General Mn^{2+}

"Basic Concepts of XPS"
Figure 30

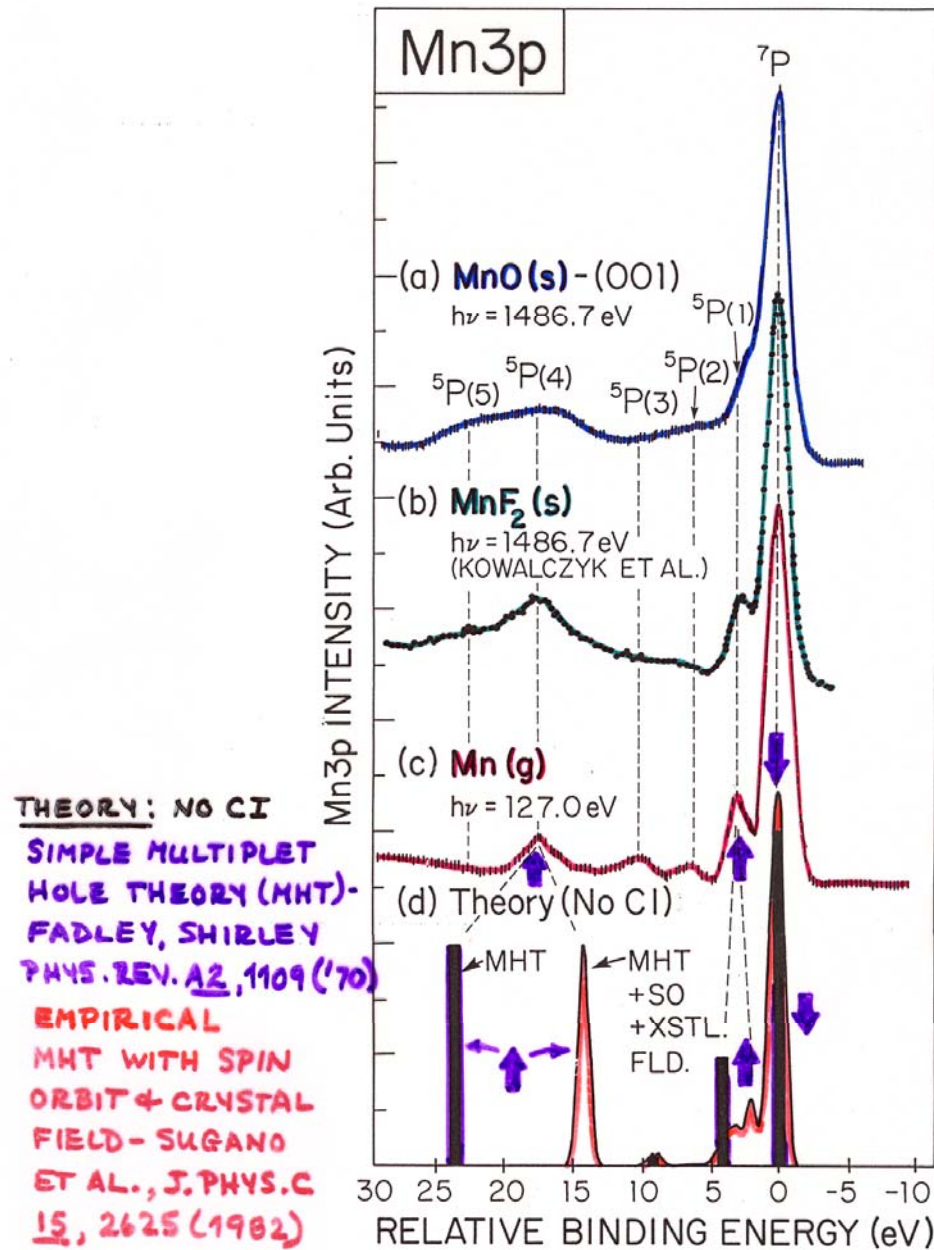
* CI HERE NOT TO ALLOW FOR e^-e^- CORRELATION, BUT JUST DIFFERENT COUPLING IN $3p^5 3d^5$

Correlation
CI effects:
anti-parallel
electrons

THEORY:
BAGUS, FREEMAN,
SASAKI, PHYS. REV.
LETT. 30, 850 (1973)
ATOMIC CONFIG.
INT. IN
 $Mn^{3+} \dots 3s^1 \dots 3d^5$
 $+ Mn^{3+} \dots 3s^2 3p^4 3d^6$

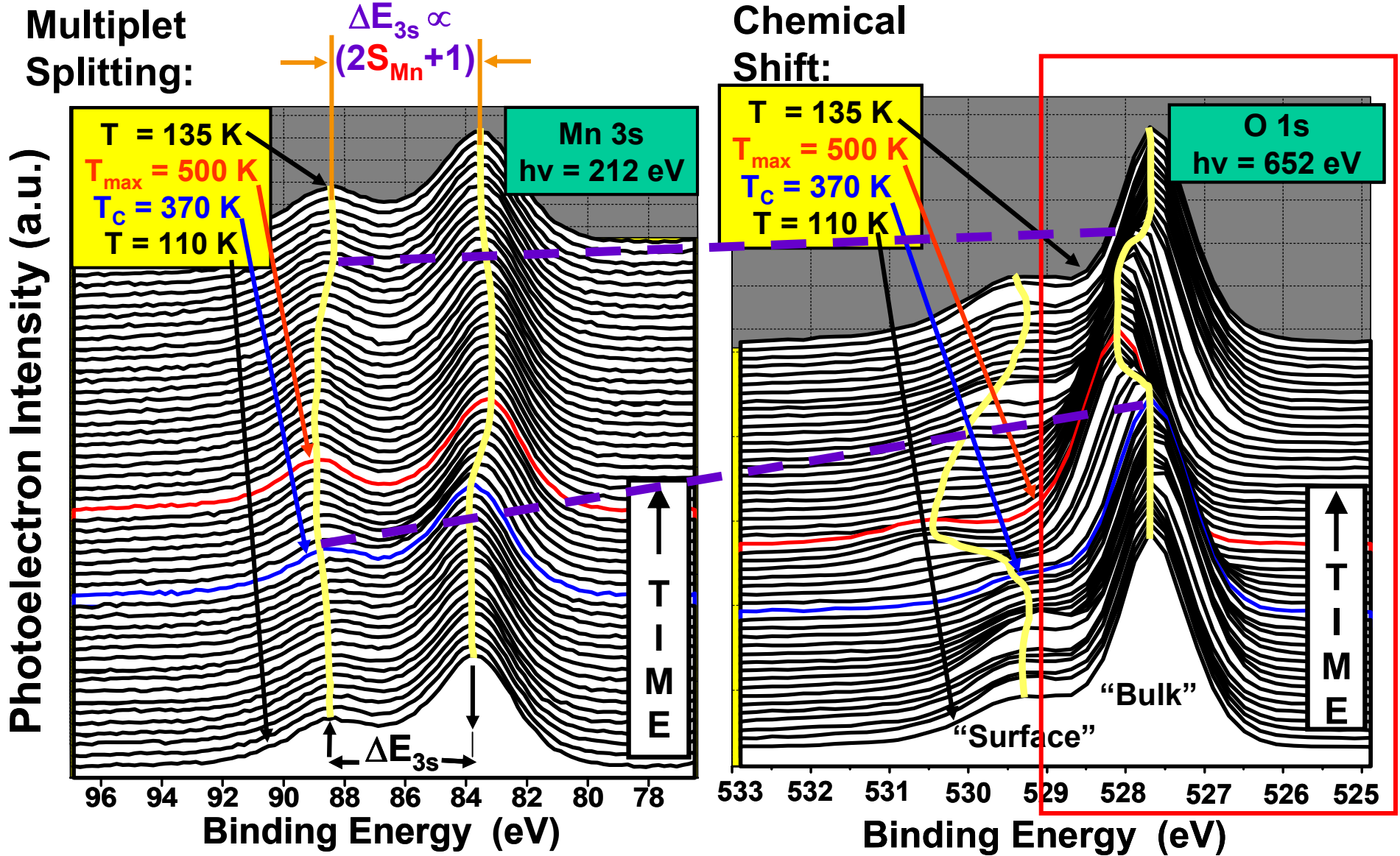


"Basic Concepts of XPS"
Figure 33



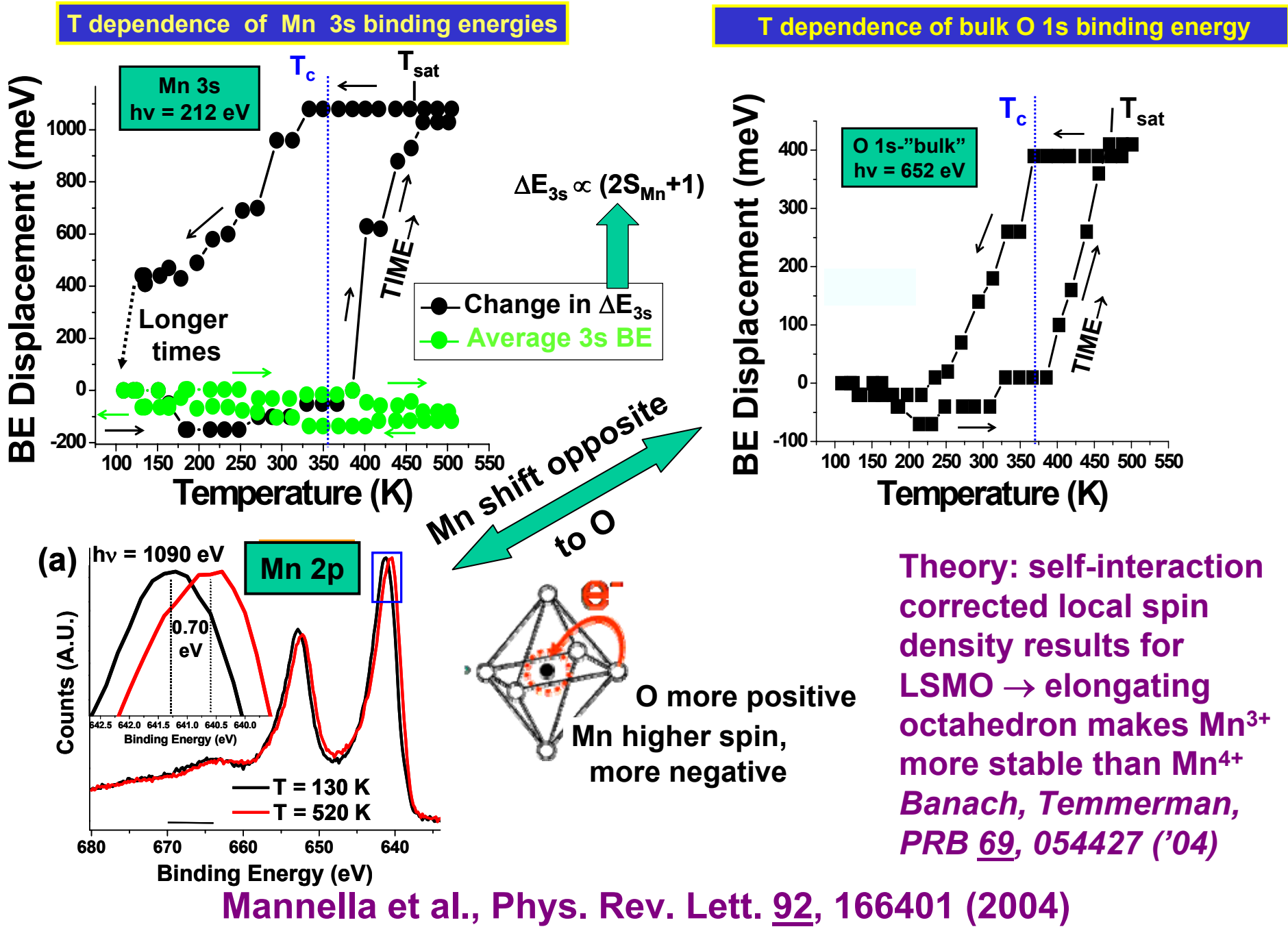
HERMSMEIER
 ET AL.,
 P.R.L. 61, 2592 ('88)

Temperature dependence of Mn3s and O1s spectra in a colossal magnetoresistive (CMR) oxide: $\text{La}_{0.7}\text{Sr}_{0.3}\text{MnO}_3$

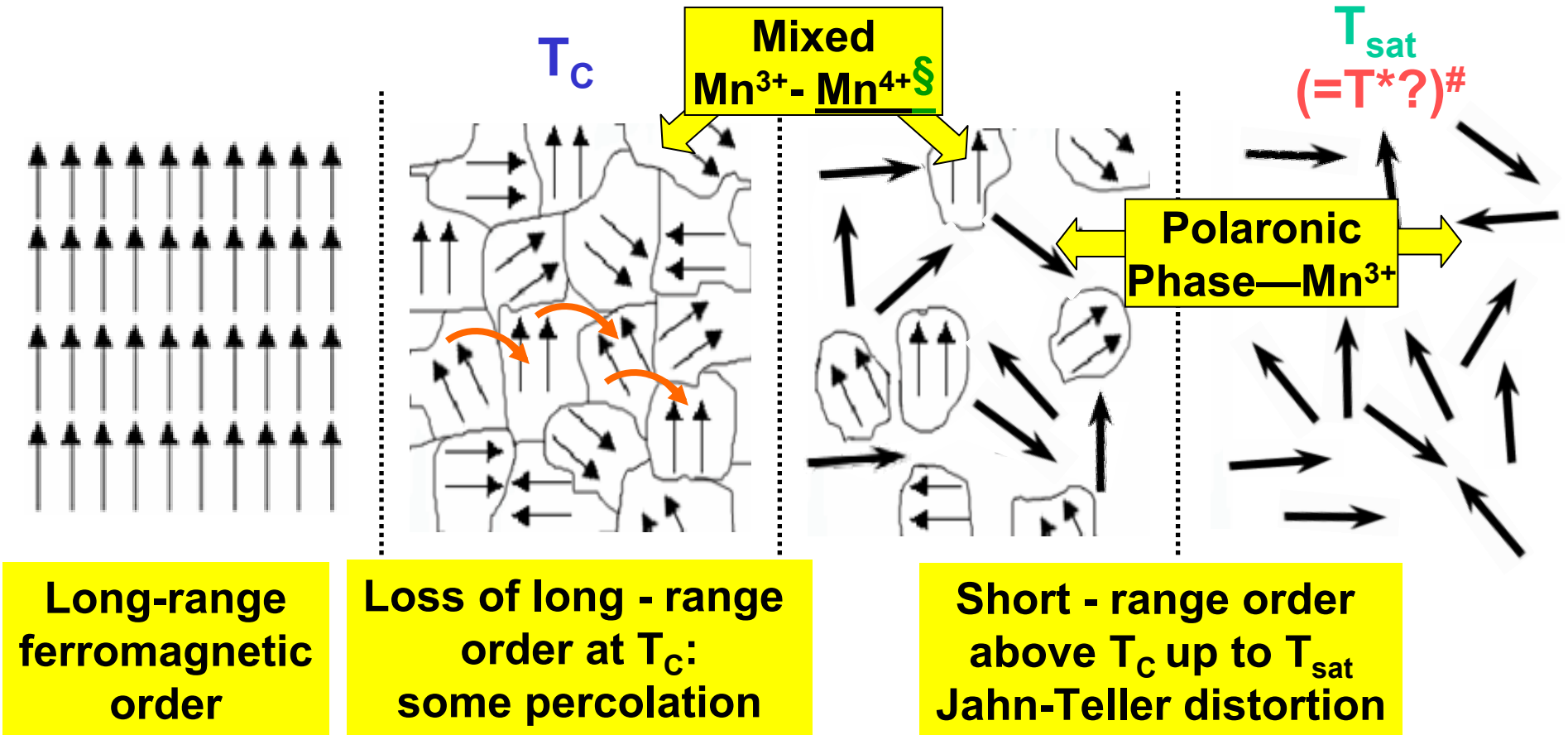


Increase of the Mn3s splitting-reversible

Increase of O1s BE-reversible



Suggested scenario—LSMO, $x = 0.3, 0.4$



Long-range
ferromagnetic
order

Loss of long - range
order at T_c :
some percolation

Short - range order
above T_c up to T_{sat}
Jahn-Teller distortion

§ Self-interaction corrected local spin density calcs. suggest Mn⁴⁺ dominant, but conversion to Mn³⁺ with JT distortion
Banach, Temmerman, PRB 69, 054427 ('04)

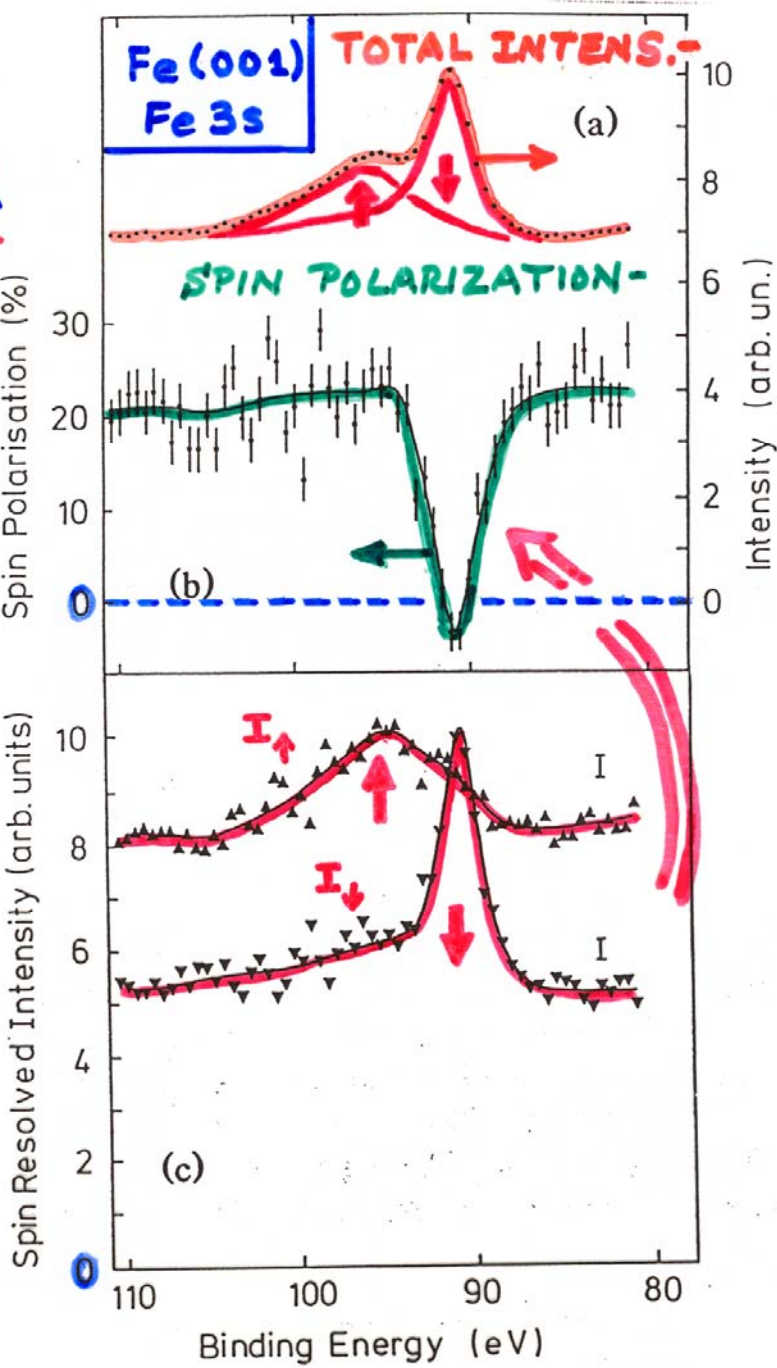
T^* = new T scale suggested
from theory
Dagotto et al.
PRL 87, 277202 (2001)

Mannella et al., PRL 92, 166401 ('04); PRB 70, 224433 ('04), and to be publ.

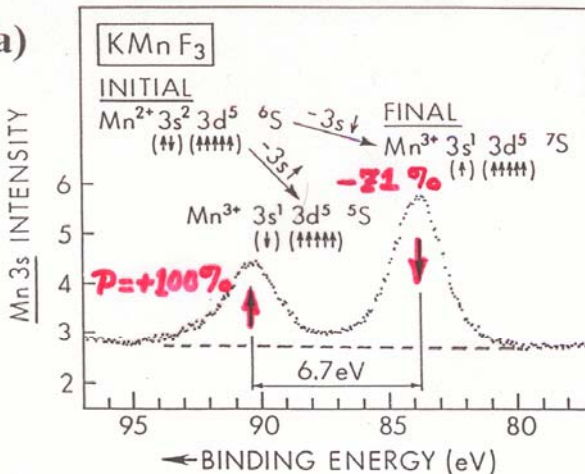
DIRECT
OBSERVATION
OF SPIN-SPLIT
CORE LEVELS
IN A
FERROMAGNET

$$\frac{I_{\uparrow} - I_{\downarrow}}{I_{\uparrow} + I_{\downarrow}}$$

HILLEBRECHT
ET AL.,
PHYS. REV. LETT.
65, 2450 (1990)



1
**MULTIPLET
IN A
MAGNETIC
ATOM**

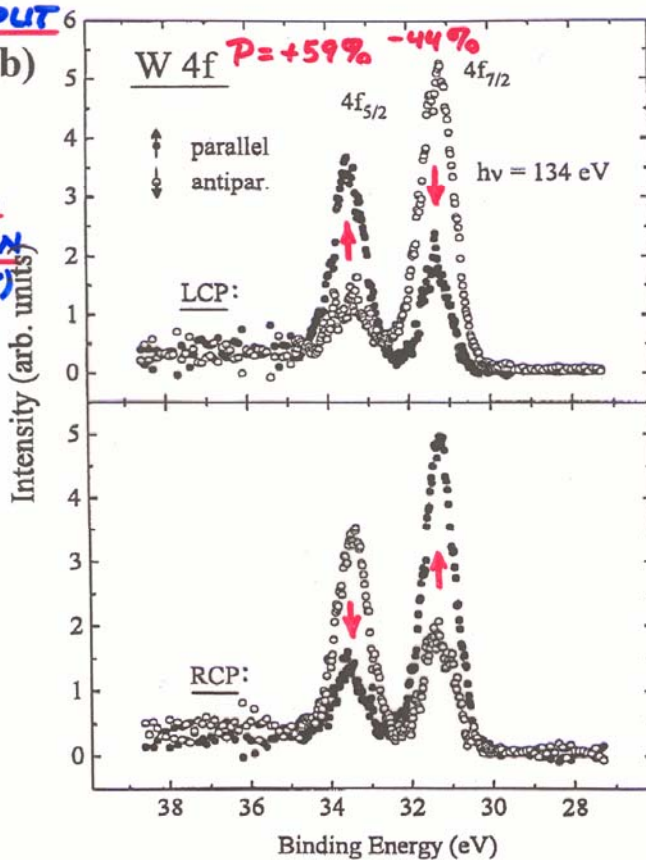


**SPIN POLARIZATION
IN CORE SPECTRA**

$$P = \frac{I_{\uparrow} - I_{\downarrow}}{I_{\uparrow} + I_{\downarrow}}$$

EXPT. - FINKOVIC
ET AL.
P.R.L. 55,
1227 (1985)

2
**SPIN-ORBIT SPLIT
LEVEL (b)
EXCITED
WITH
CIRCULAR
POLARIZATION
(FANO EFFECT)**



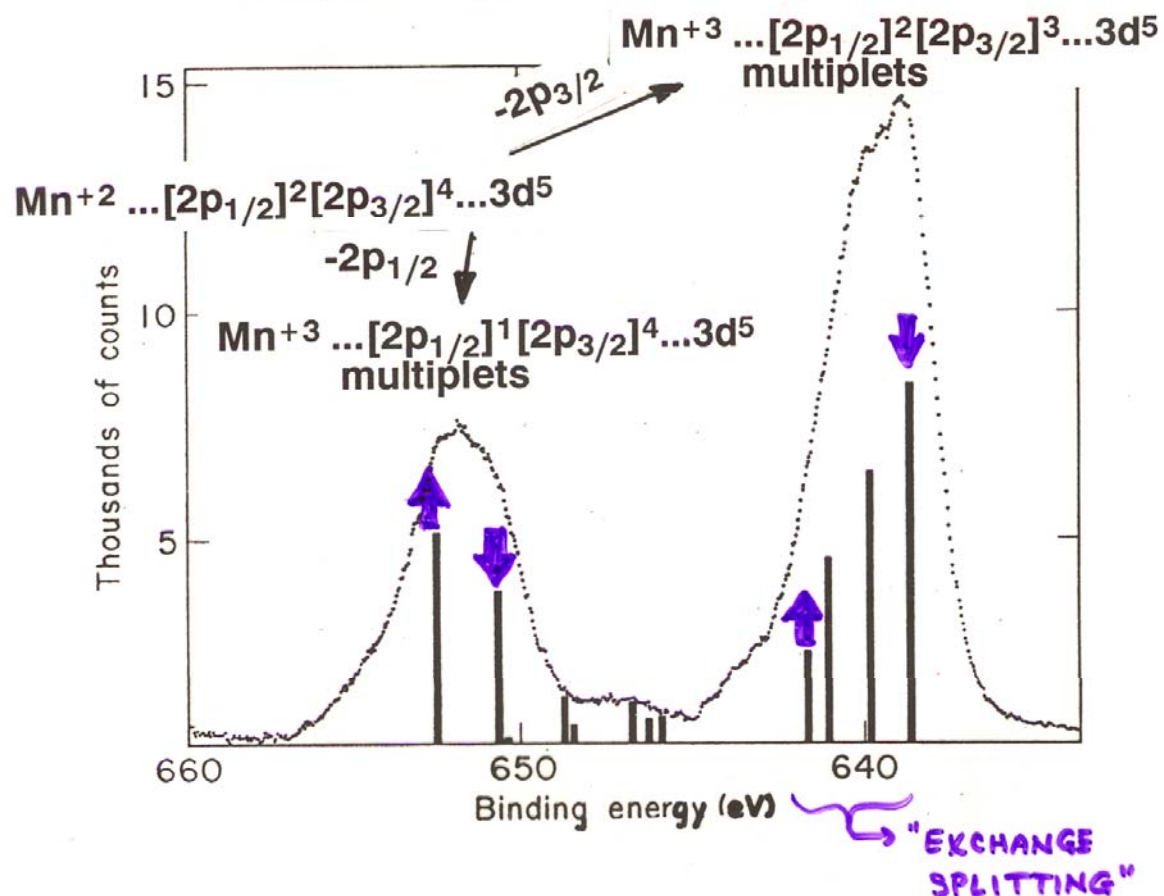
EXPT. - STARKE ET
AL.
PRB 53, R10544
(1996)

**Spin
internally
referenced
to spin of
each ion**

**Spin
externally
referenced
to \vec{k}_{hv} and \vec{M}
of sample**

MORE COMPLEX MULTIPLETS FOR $L > 0$
WITH SPIN-ORBIT COUPLING:

Mn 2p emission from MnF_2 :

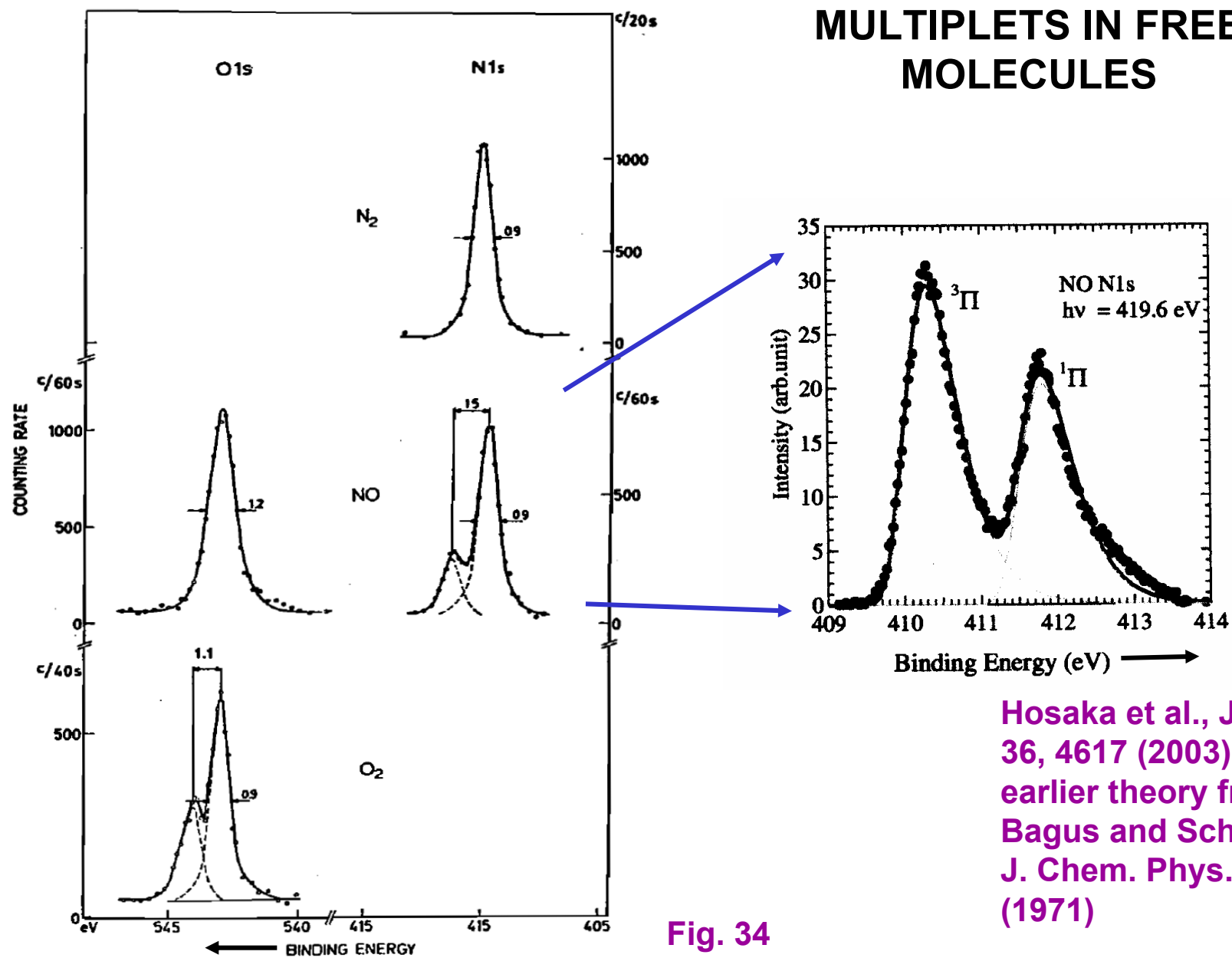


Expt.--Kowalczyk et al., Phys. Rev. B11, 1721 (1975)

Theory--Gupta and Sen, Phys. Rev. B10, 71 (1974)

Park et al., Phys. Rev. B37, 10867 (1988)

MULTIPLETS IN FREE MOLECULES



Hosaka et al., J. Phys. B 36, 4617 (2003), and earlier theory from Bagus and Schaefer, J. Chem. Phys. 55, 1474 (1971)

Fig. 34
Basic Concepts of XPS

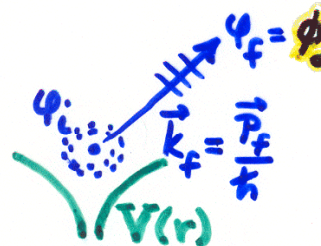
Outline

- Valence-band spectra: low-energy UPS limit and high-energy XPS limit
- Core-level chemical shifts: the potential model
- Core-level chemical shifts: equivalent-core ($Z+1$) and thermochemical energies
- Multiplet splittings
- Spin-orbit splitting, the Fano effect, and spin-polarized outgoing electrons
- Magnetic circular dichroism (MCD) in core-level emission
- Non-magnetic circular dichroism in core-level emission: a.k.a. circular dichroism in angular distributions (CDAD)
- Various other final state effects providing information in core-level spectra

PHOTOELECTRON EMISSION - BASIC MATRIX ELEMENTS & SELECTION RULES:

● ATOMIC-LIKE (LOCALIZED) STATES \Rightarrow CORE:

$$\Psi_i(\vec{r}) = \Psi_{n_i l_i m_i}(r, \theta, \phi) = R_{n_i l_i}(r) Y_{l_i m_i}(\theta, \phi) \quad \left\{ \begin{array}{l} \alpha(\sigma) = m_{si} = +\frac{1}{2} = \uparrow \\ \beta(\sigma) = m_{si} = -\frac{1}{2} = \downarrow \end{array} \right.$$



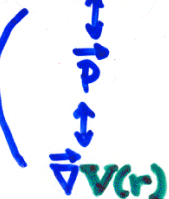
$$\Psi_f(\vec{r}, \vec{k}_f) = \Psi_{E_f}(\vec{r}, \vec{k}_f) \quad \left\{ \begin{array}{l} \alpha(\sigma) \\ \beta(\sigma) \end{array} \right.$$

$$= 4\pi \sum_{l_f, m_f} i^{l_f} e^{-i\delta_{l_f}} Y^*_{l_f m_f}(\theta_{k_f}, \phi_{k_f}) Y_{l_f m_f}(\theta, \phi) R_{E_f l_f}(r) \quad \left\{ \begin{array}{l} \alpha(\sigma) \\ \beta(\sigma) \end{array} \right.$$

PHASE SHIFT OF l_f WAVE IN $V(r)$

DIPOLE APPROX.: INT. $\propto |\langle \Psi_f | \hat{\epsilon} \cdot \vec{r} | \Psi_i \rangle|^2 = |\hat{\epsilon} \langle \Psi_f | \vec{r} | \Psi_i \rangle|^2 \Rightarrow \Delta l = l_f - l_i = \pm 1$

EQUIVALENT
WITHIN CONSTANT
FACTOR



- < $\Delta m = m_f - m_i = 0, \pm 1$
- < LINEAR POLARIZ.
- < $\Delta m = \pm 1$, CIRCULAR POLARIZATION

$$\Delta m_s = m_{sf} - m_{si} = 0 !$$

$E_f p^-$

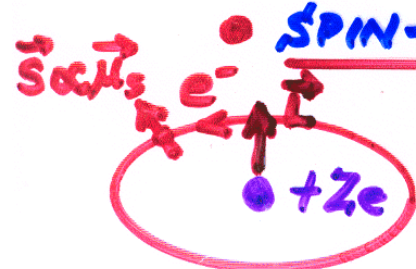
$m_f:$	+1	0	-1	+1	0	-1
$m_{sf}:$	+1/2	+1/2	+1/2	-1/2	-1/2	-1/2
$n_i S$						
$m_i:$	0	0				

spin up spin down

FOR A GIVEN $n_i / m_i m_{si}$: SUM OVER DEGENERATE INITIAL STATES $m_i m_{si}$ AND AVERAGE OVER FINAL STATES $E_f l_f m_f m_{sf}$ ACCESSED FROM EACH m_i TO YIELD DIFFERENTIAL SUBSHELL PHOTOELECTRIC CROSS SECTION :

$$d\sigma_{n_i l_i} / d\Omega$$

\propto PROBABILITY PER UNIT SOLID ANGLE OF EXCITING ONE ELECTRON FROM SUBSHELL n_i / i INTO THE DIRECTION k_f



SPIN-ORBIT SPLITTING OF LEVELS:

⇒ EFFECTIVE \vec{B} (NUCLEUS AROUND e^-) $\propto \vec{L}$

$$\hat{H}_{S-O} = \xi(r) \vec{L} \cdot \vec{S}$$

• SPLITS ALL nl LEVELS $\xrightarrow{2(2l+1)}$

$$nlj = l + \frac{1}{2} - 2l + 2$$

$$nlj = l - \frac{1}{2} - 2l$$

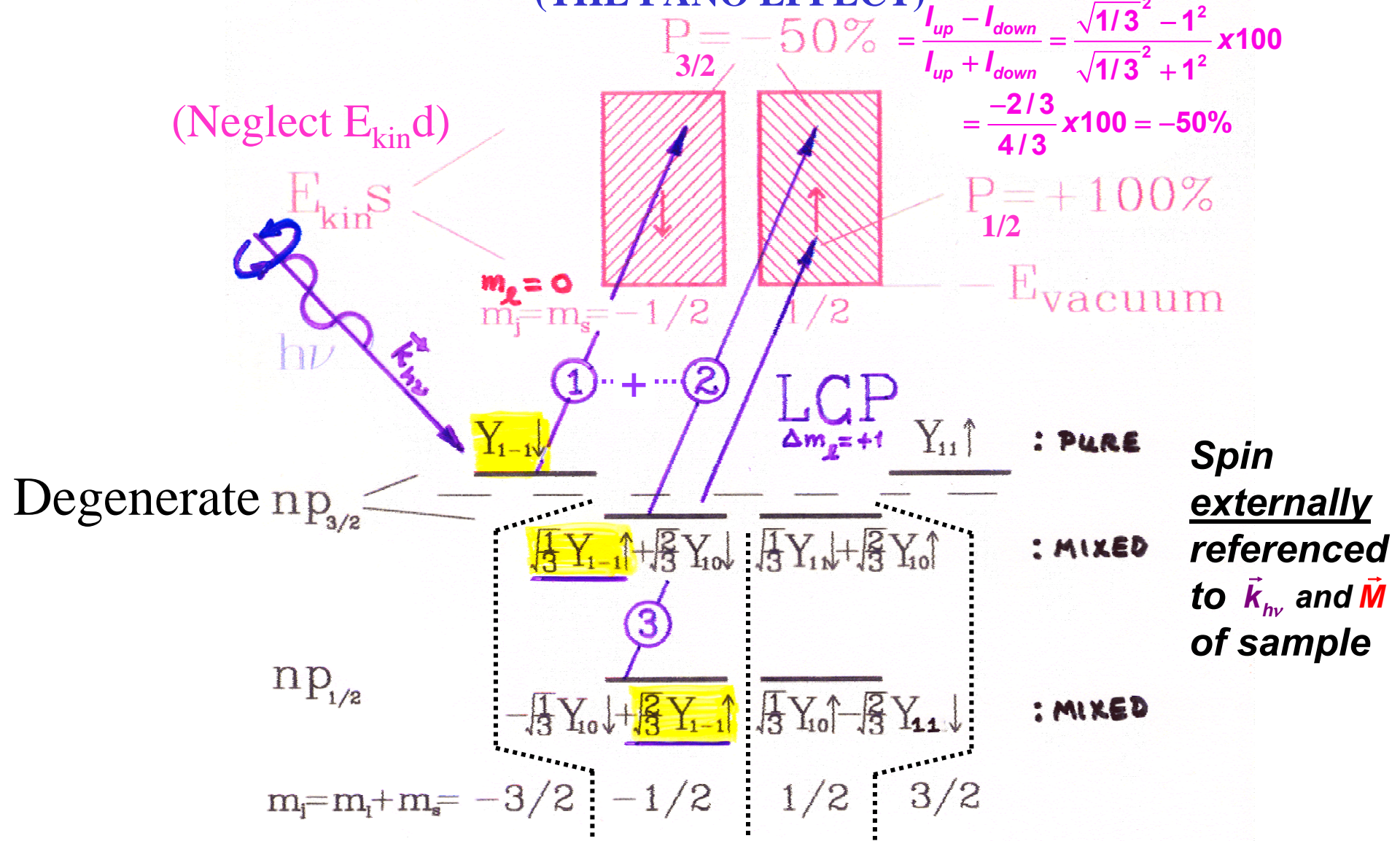
• MIXES SPIN + ORBITAL ANGULAR MOM.:

$$\Psi_{nljm_j} = C_1 \Psi_{nl,m_j - \frac{1}{2}} \begin{pmatrix} 1 \\ 0 \end{pmatrix} + C_2 \Psi_{nl,m_j + \frac{1}{2}} \begin{pmatrix} 0 \\ 1 \end{pmatrix}$$

$m_s = +\frac{1}{2}$ $m_s = -\frac{1}{2}$

WITH C1 AND C2 TABULATED CLEBSCH-GORDAN
OR WIGNER 3J SYMBOLS

PHOTOELECTRON SPIN POLARIZATION FROM CIRCULAR POLARIZATION AND SPIN-ORBIT SPLITTING (THE FANO EFFECT)



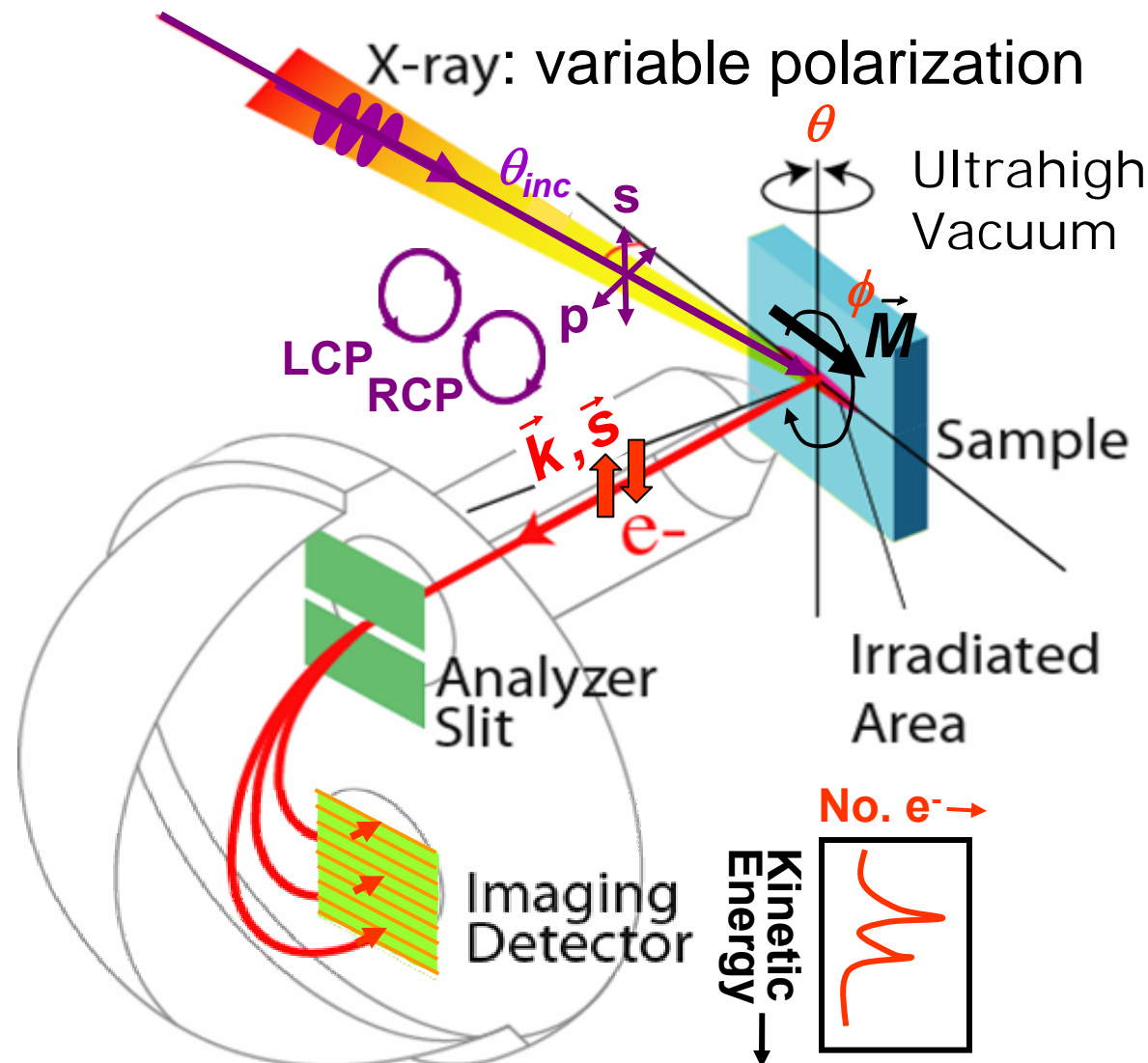
Spin polarization in core photoelectron spectra—expt.



Outline

- Valence-band spectra: low-energy UPS limit and high-energy XPS limit
- Core-level chemical shifts: the potential model
- Core-level chemical shifts: equivalent-core ($Z+1$) and thermochemical energies
 - Spin-orbit splitting, the Fano effect, and spin-polarized outgoing electrons
- • Magnetic circular dichroism (MCD) in core-level emission
 - Non-magnetic circular dichroism in core-level emission: a.k.a. circular dichroism in angular distributions (CDAD)
 - Various other final state effects providing information in core-level spectra

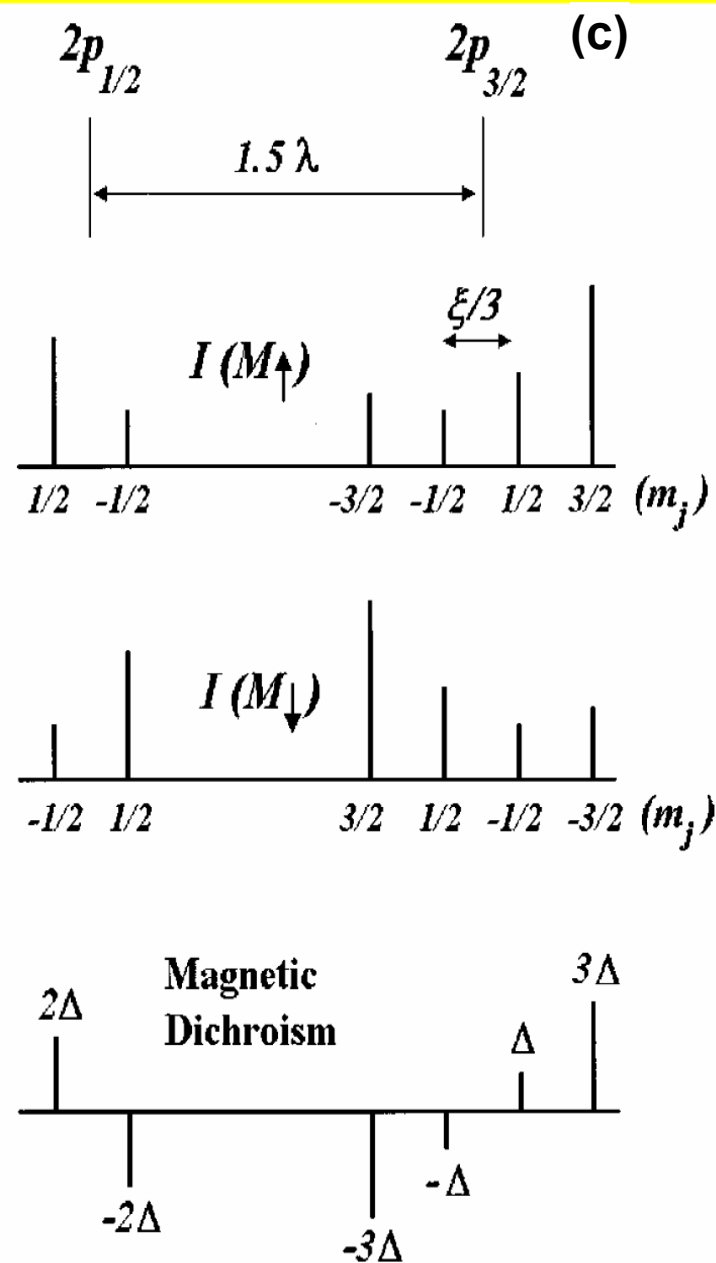
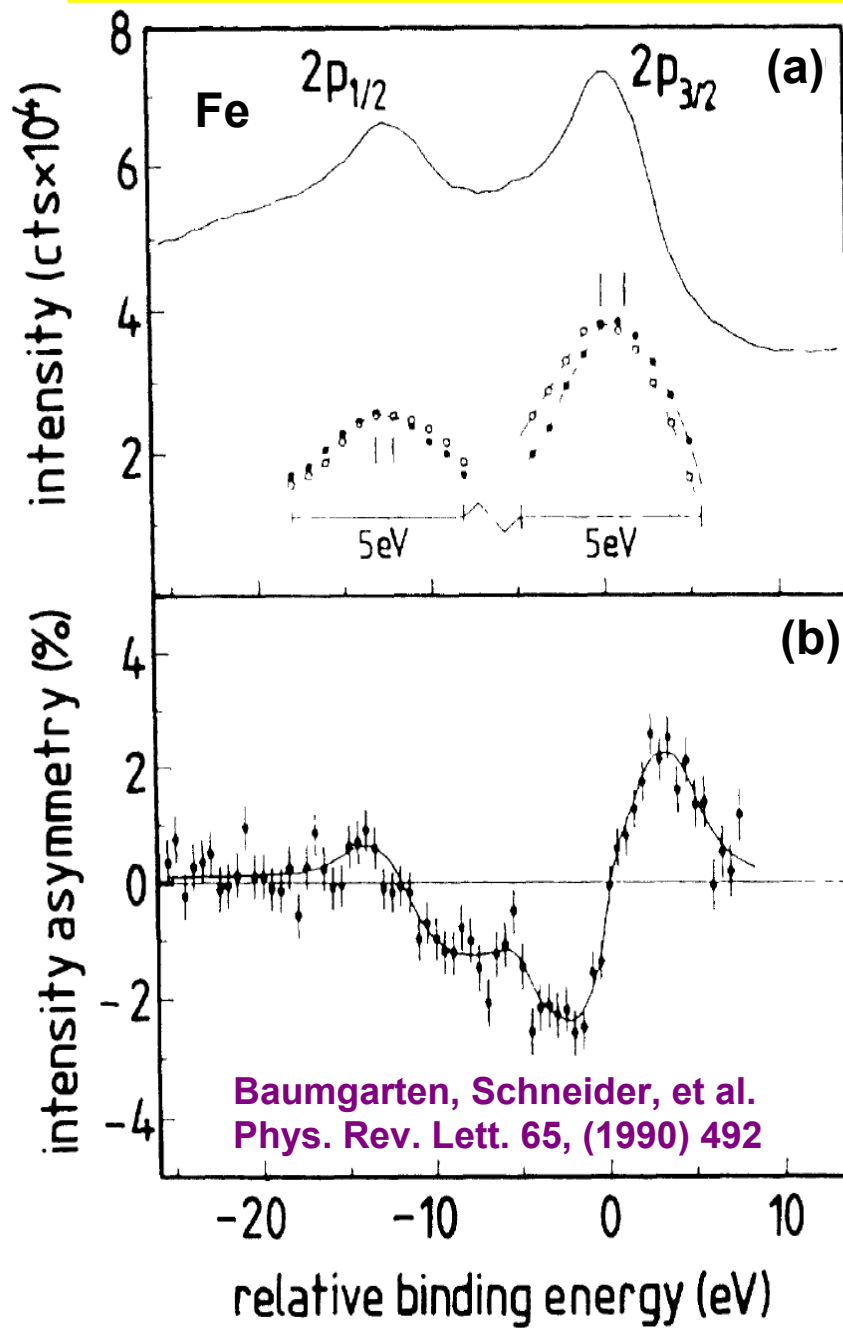
Typical experimental geometry for energy- and angle-resolved photoemission measurements



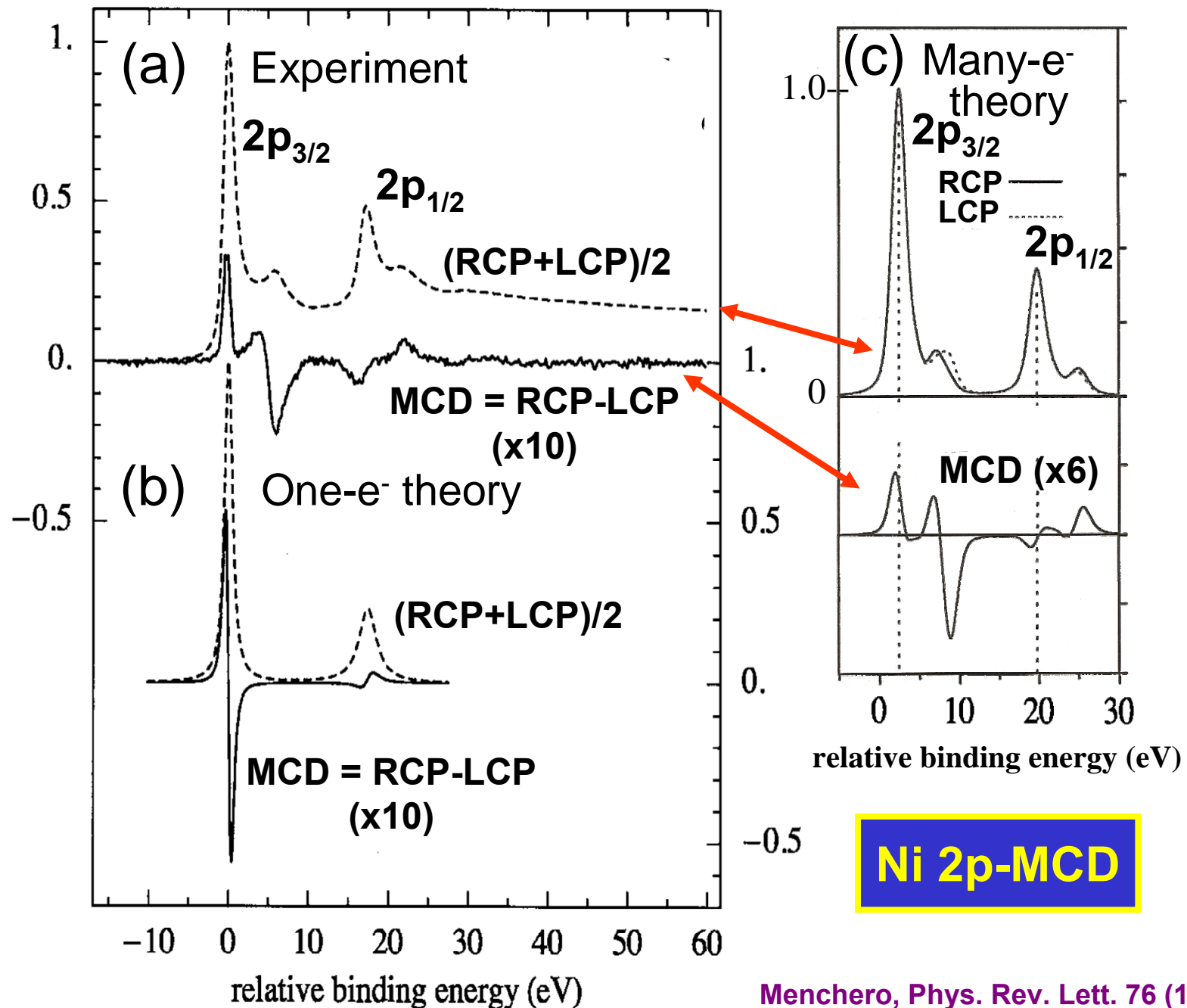
1st Expt.

Magnetic Circular Dichroism

1-e⁻ Theo.

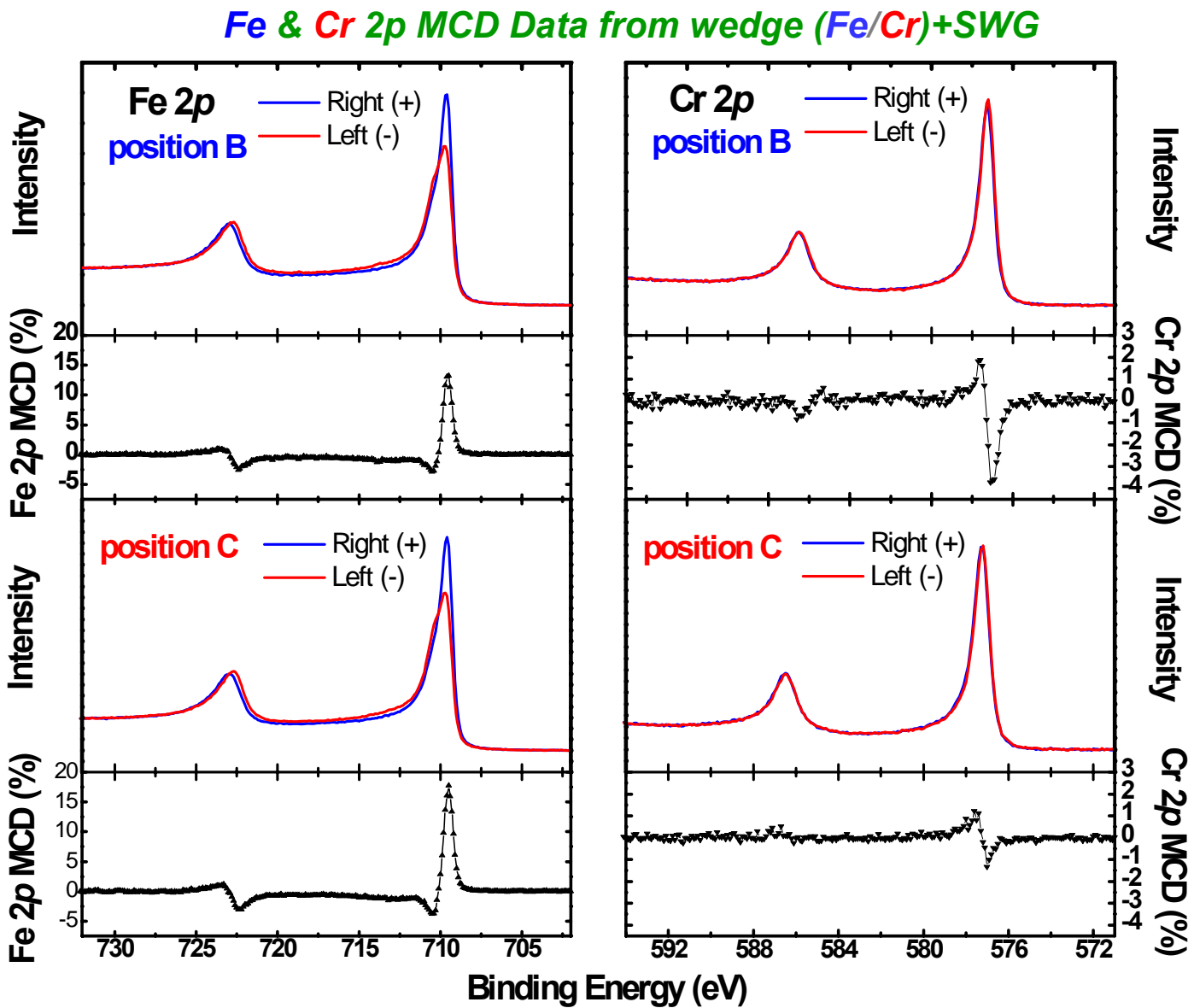
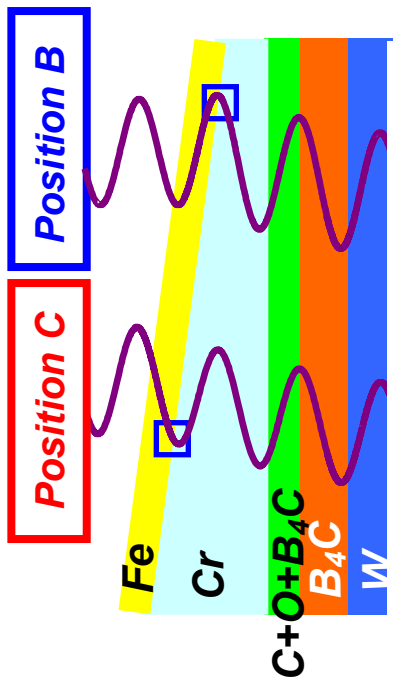


Menchero, Phys. Rev. B 57 (1998) 993



Application to a buried interface: with standing wave excitation

**Cr magnetization
Is antiparallel to
Fe; systematic
variation of MCD
strengths vs d_{cr}**

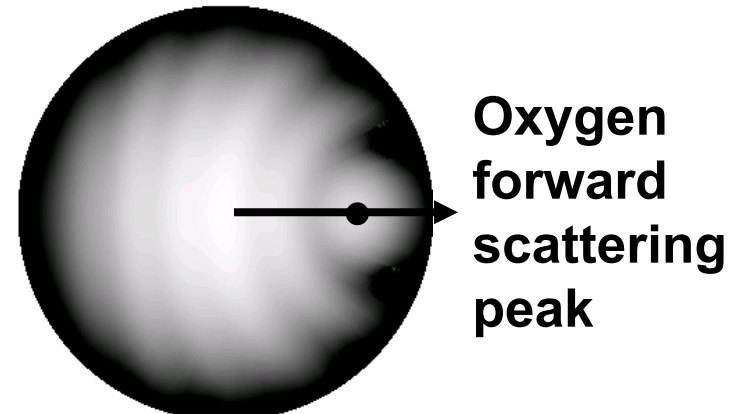
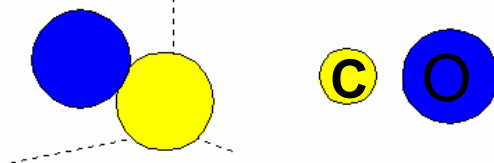


Outline

- Valence-band spectra: low-energy UPS limit and high-energy XPS limit
- Core-level chemical shifts: the potential model
- Core-level chemical shifts: equivalent-core ($Z+1$) and thermochemical energies
- Multiplet splittings
- Spin-orbit splitting, the Fano effect, and spin-polarized outgoing electrons
- Magnetic circular dichroism (MCD) in core-level emission
- Non-magnetic circular dichroism in core-level emission: a.k.a. circular dichroism in angular distributions (CDAD)
- Various other final state effects providing information in core-level spectra

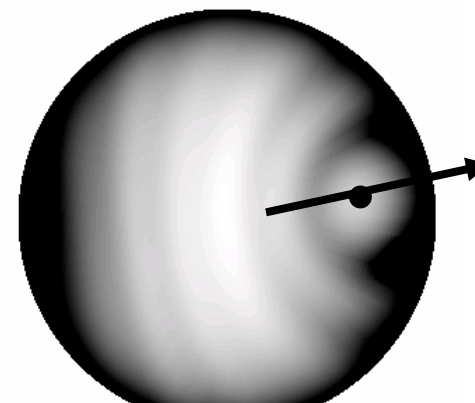
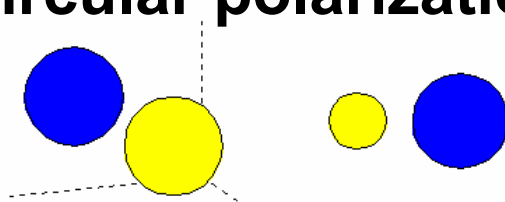
Circular dichroism in angular distributions: C 1s emission from CO, $E_{\text{kin}} = 200 \text{ eV}$

Linear p polarization:



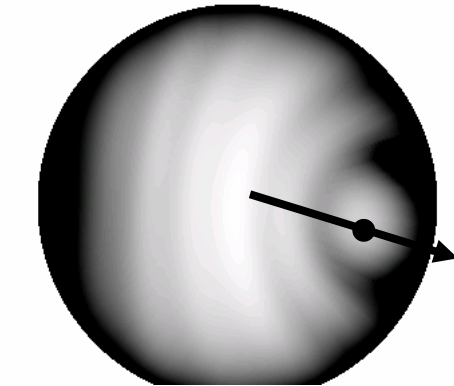
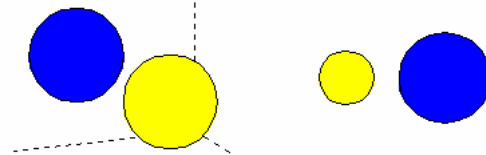
Oxygen
forward
scattering
peak

Right circular polarization:



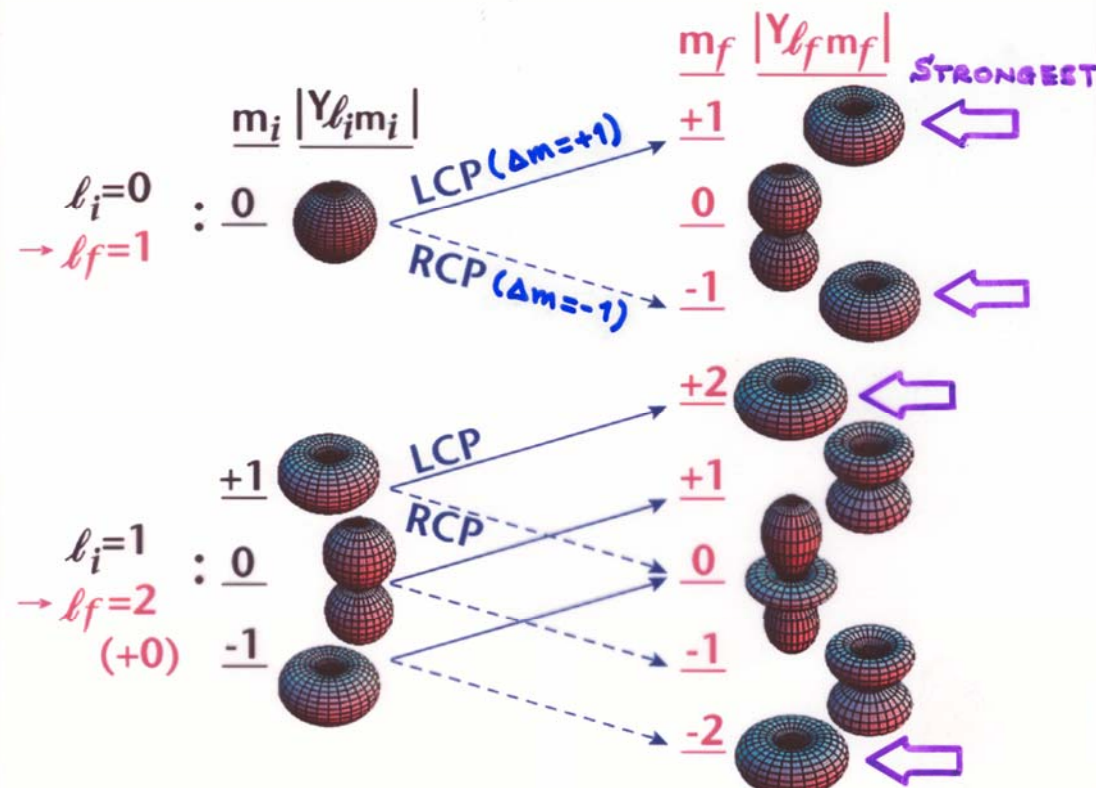
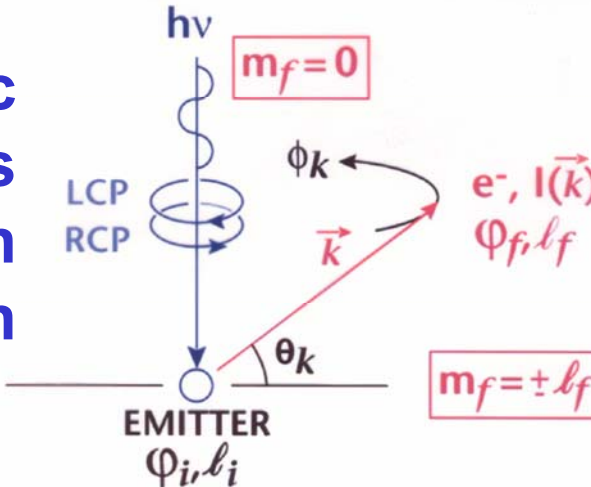
Circular
dichroism!
Why?

Left circular polarization:



CIRCULAR DICHROISM IN PHOTOELECTRON ANGULAR DISTRIBUTIONS (CDAD)

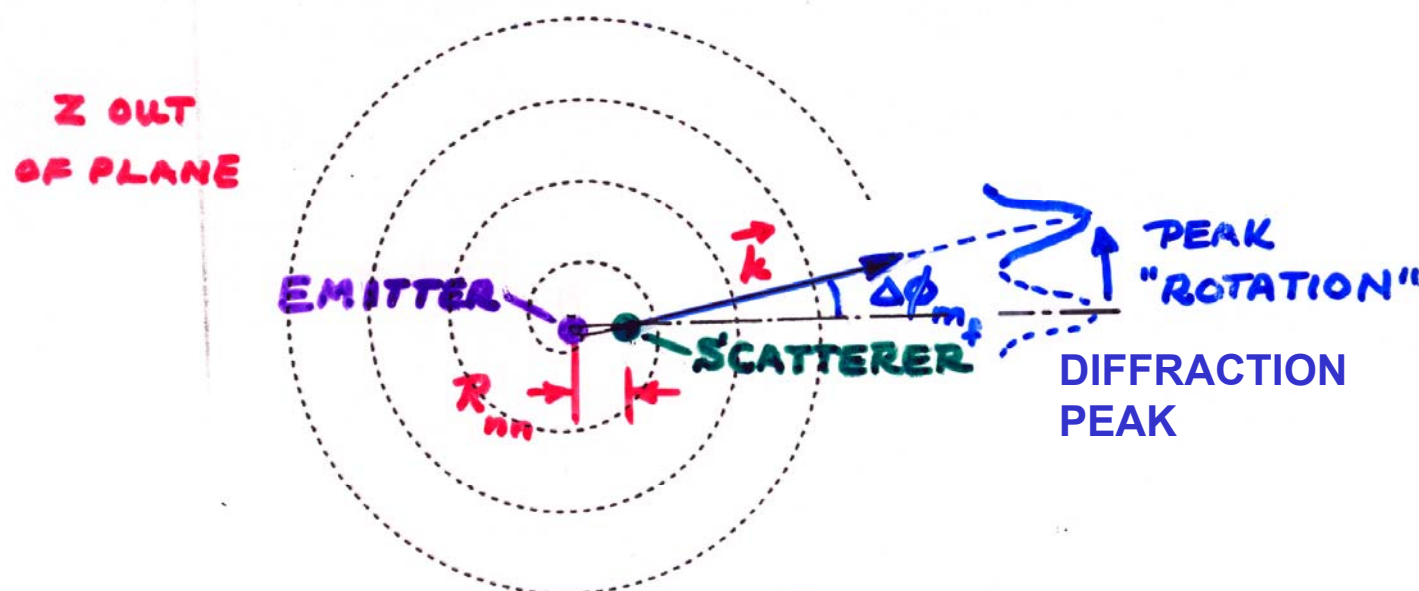
→ Non-magnetic
dichroism effects
due to photoelectron
diffraction



CIRCULAR DICHROISM IN PHOTOELECTRON DIFFRACTION

CONSTANT-PHASE SURFACE OF :

$$\psi_{\text{photo-e}^-}(r, \theta, \phi) \propto \frac{e^{ikr}}{r} H_{lm} e^{im_f \phi}$$



$$\left| \Delta\phi_{m_f} = \frac{m_f}{R_{nn,11} k_{11}} \right|$$

$$\overline{m_f} \approx m_{f,\max}$$

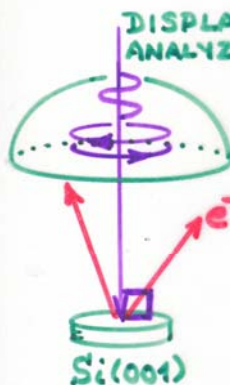
DAIMON ET AL.
JPN. J. APPL. PHYS.
32, L1480 ('93)

CIRCULAR DICHROISM - NON-MAGNETIC SYSTEMS

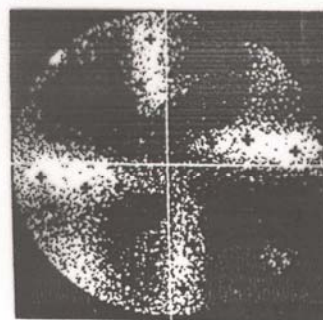
Si2p -- 250eV = E_{kin}

EXPERIMENT

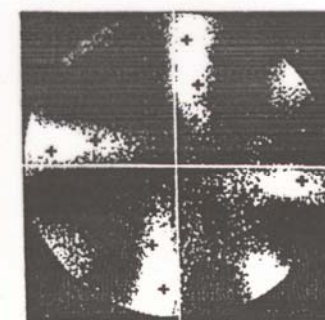
DISPLAY
ANALYZER



(a) LCP



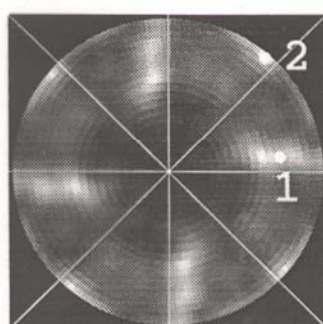
(b) RCP



DAIMON ET AL.
JPN. J. APPL. PHYS.
32, L1480 ('93)

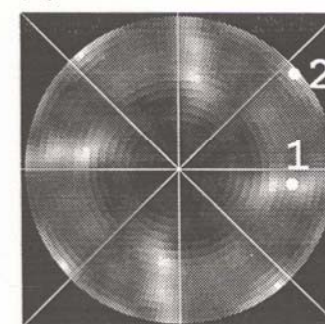
THEORY

(c) LCP

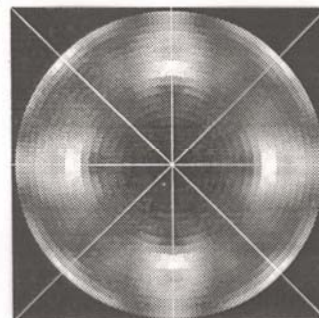


(d) RCP

KADUWELA ET AL.
P.R.B 50, 6203 ('94)

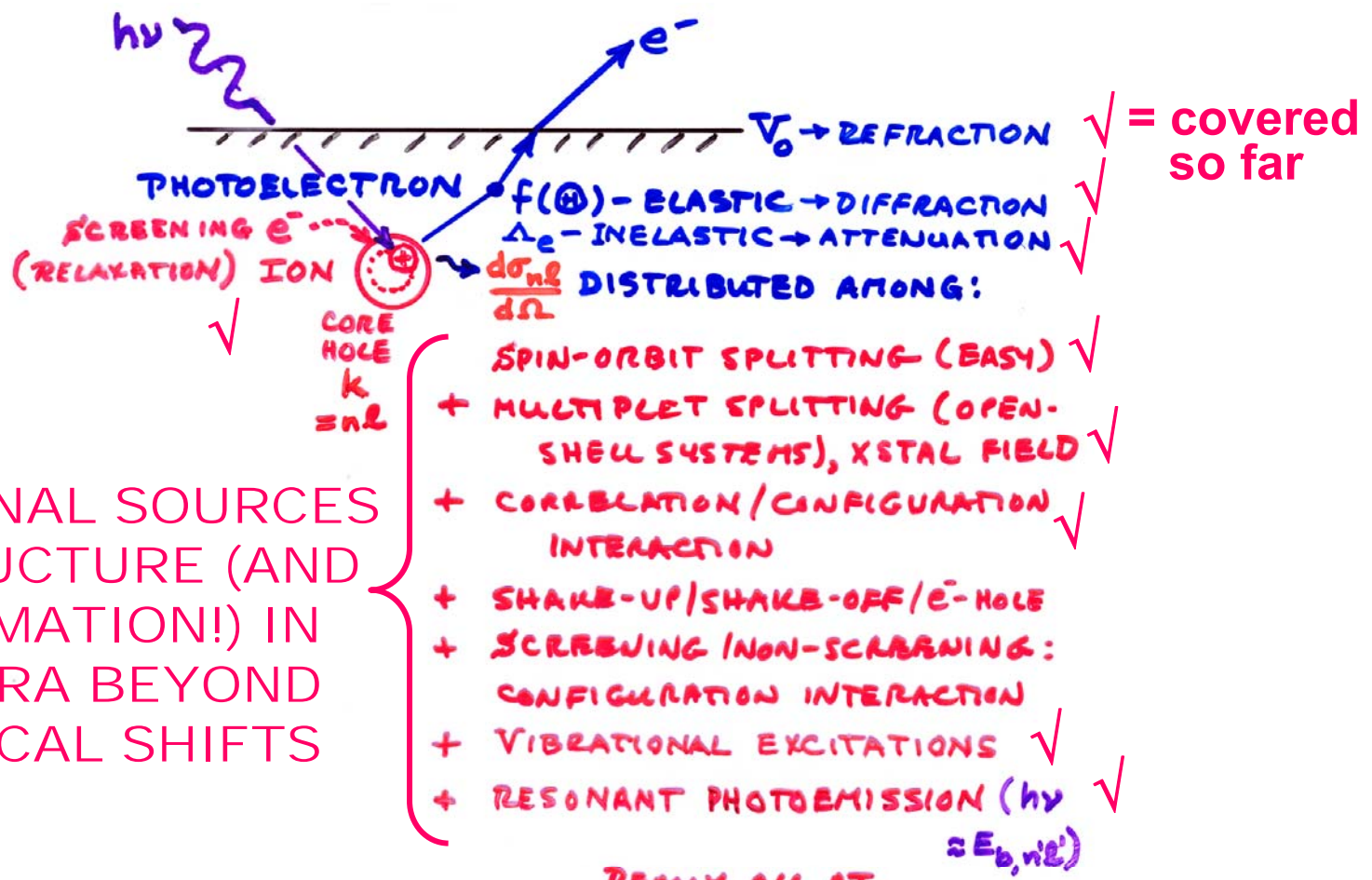


(e) UNPOLARIZED



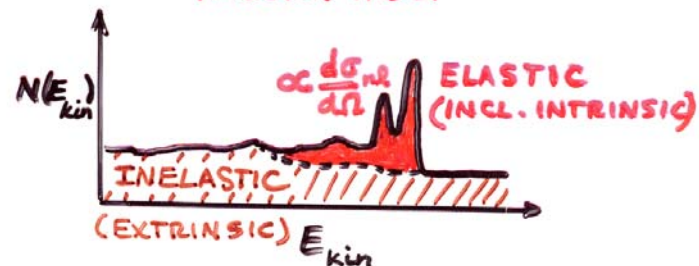
Outline

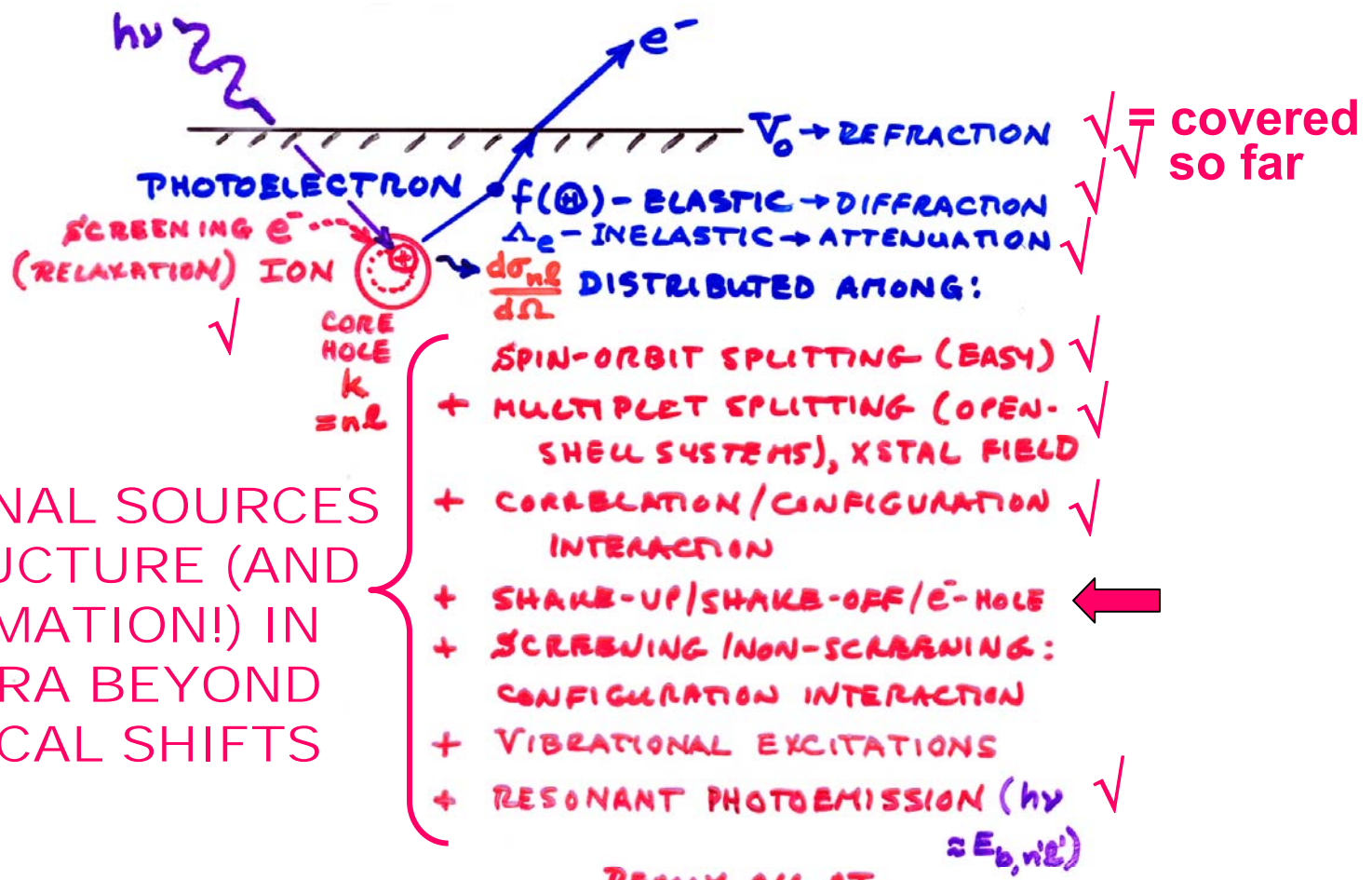
- Valence-band spectra: low-energy UPS limit and high-energy XPS limit
- Core-level chemical shifts: the potential model
- Core-level chemical shifts: equivalent-core ($Z+1$) and thermochemical energies
- Multiplet splittings
- Spin-orbit splitting, the Fano effect, and spin-polarized outgoing electrons
- Magnetic circular dichroism (MCD) in core-level emission
- Non-magnetic circular dichroism in core-level emission: a.k.a. circular dichroism in angular distributions (CDAD)
- Various other final state effects providing information in core-level spectra



ADDITIONAL SOURCES OF STRUCTURE (AND INFORMATION!) IN SPECTRA BEYOND CHEMICAL SHIFTS

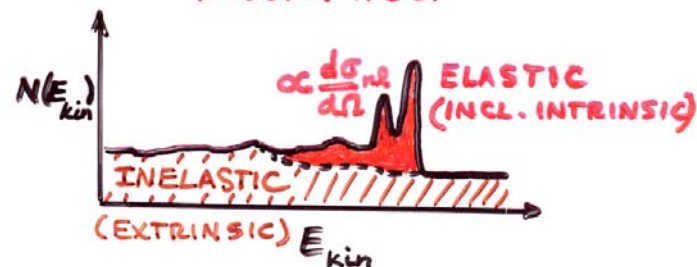
REALLY ALL AT ONCE, BUT SUM RULES + THEORY HELP



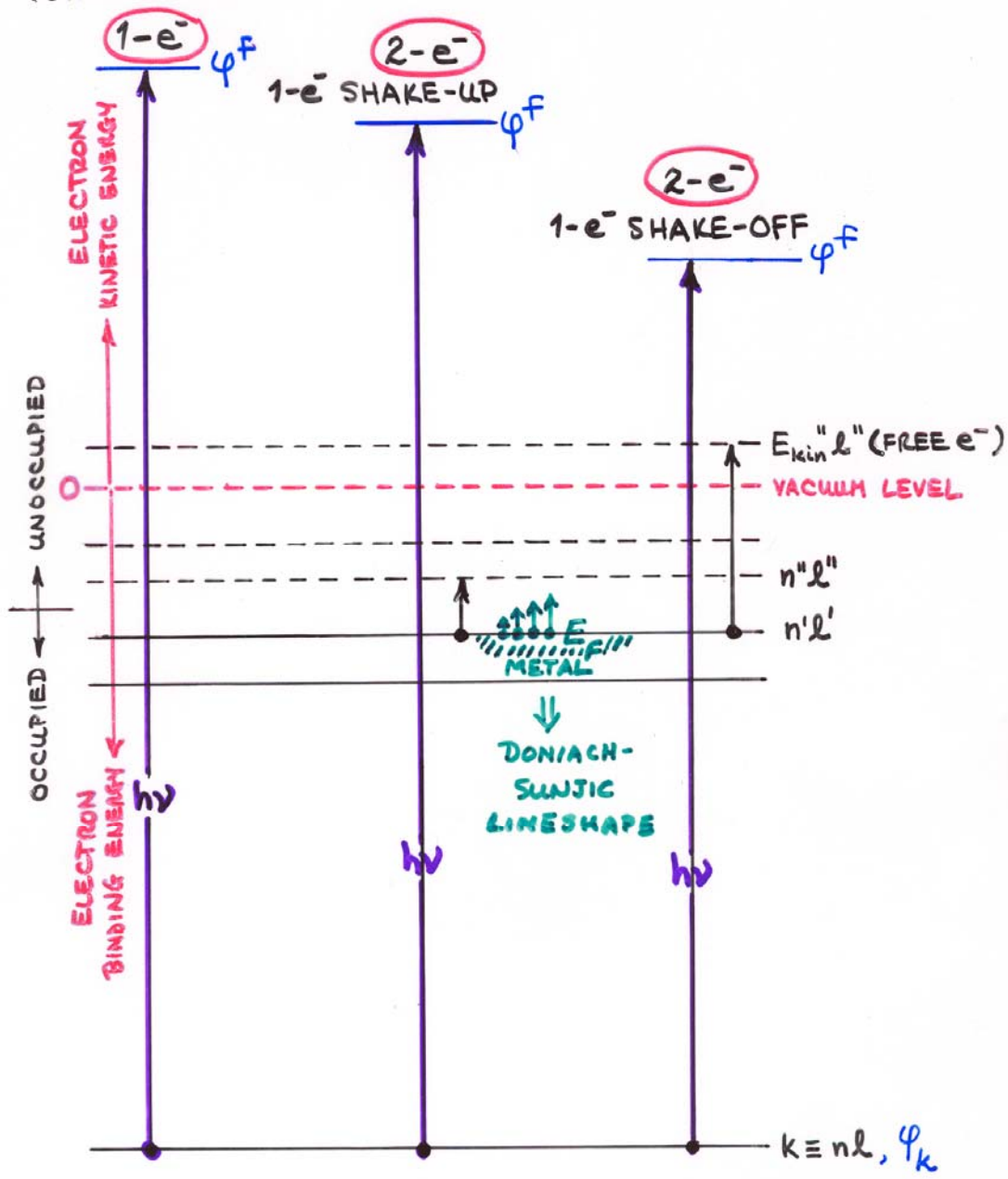


ADDITIONAL SOURCES OF STRUCTURE (AND INFORMATION!) IN SPECTRA BEYOND CHEMICAL SHIFTS

REALLY ALL AT ONCE, BUT SUM RULES + THEORY HELP



TOTAL NO. e^- :



MULITIELECTRON EFFECTS IN CORE EMISSION

INTENSITIES IN PHOTOLECTRON SPECTRA:

- GENERAL: FINAL STATE K (K-SUBSHELL + ALL OTHER DESIGN.)

$$\text{INT}_K \propto |\hat{e} \cdot \langle \Psi_{\text{tot}}^f(N, K) | \sum_{i=1}^N \vec{r}_i | \Psi_e^i(N) \rangle|^2 \quad (\text{DIPOLE APPROX.})$$

- BORN-OPPENHEIMER: e⁻'S FAST, VIBRATIONS SLOW

$$\text{INT}_K \propto |\underbrace{\langle \Psi_{\text{VIB}, v}^f | \Psi_{\text{VIB}, v}^i \rangle|^2}_{\text{FRANCK-CONDON FACTOR}} |\hat{e} \cdot \langle \Psi_e^f(N, K) | \sum_{i=1}^N \vec{r}_i | \Psi_e^i(N) \rangle|^2$$

- SUDDEN APPROXIMATION: $\Psi_K \rightarrow \Psi_f = \text{PHOTOE}^-$ (FAST)

$\Psi_i \rightarrow \Psi'_i$
 $K \text{ HOLE} \rightarrow \begin{cases} \Psi'_{K-1} \rightarrow \Psi'_{K-1} \\ \vdots \\ \Psi_{K+1} \rightarrow \Psi'_{K+1} \\ \vdots \\ \Psi_N \rightarrow \Psi_N \end{cases}$ } (slow)

$$\text{INT}_K \propto |\langle \Psi_{\text{VIB}, v}^f | \Psi_{\text{VIB}, v}^i \rangle|^2 |\underbrace{\langle \Psi_e^f(N-1, K) | \Psi_e^{1-}(N-1, K) \rangle}_{\begin{array}{l} \text{SAME SUBSHELL COUPLING} \\ \hookrightarrow \text{NORMAL } \frac{dG_K}{d\Omega} \end{array}}|^2$$

- SLATER DETS. FOR $\Psi_e^f = \det(\Psi'_1, \Psi'_2, \dots, \Psi'_{K-1}, \Psi_{K+1}, \dots, \Psi_N)$

$$\Psi_R = \det(\Psi_1, \Psi_2, \dots, \Psi_{K-1}, \Psi_{K+1}, \dots, \Psi_N)$$

$$\text{INT}_K \propto |\langle \Psi_{\text{VIB}, v}^f | \Psi_{\text{VIB}, v}^i \rangle|^2 |\langle \Psi'_1 | \Psi_1 \rangle|^2 |\langle \Psi'_2 | \Psi_2 \rangle|^2 \dots |\langle \Psi'_{K-1} | \Psi_{K-1} \rangle|^2 / |\langle \Psi'_{K+1} | \Psi_{K+1} \rangle|^2 \dots |\langle \Psi_N' | \Psi_N \rangle|^2$$

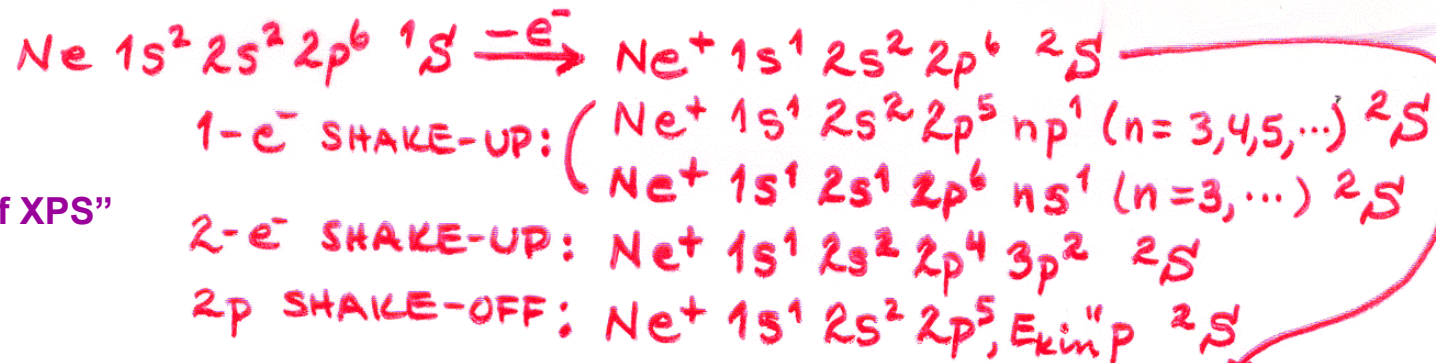
$$|\hat{e} \cdot \langle \Psi_f | \vec{r} | \Psi_K \rangle|^2$$

1e⁻ DIPOLE $\rightarrow d\sigma/d\Omega$

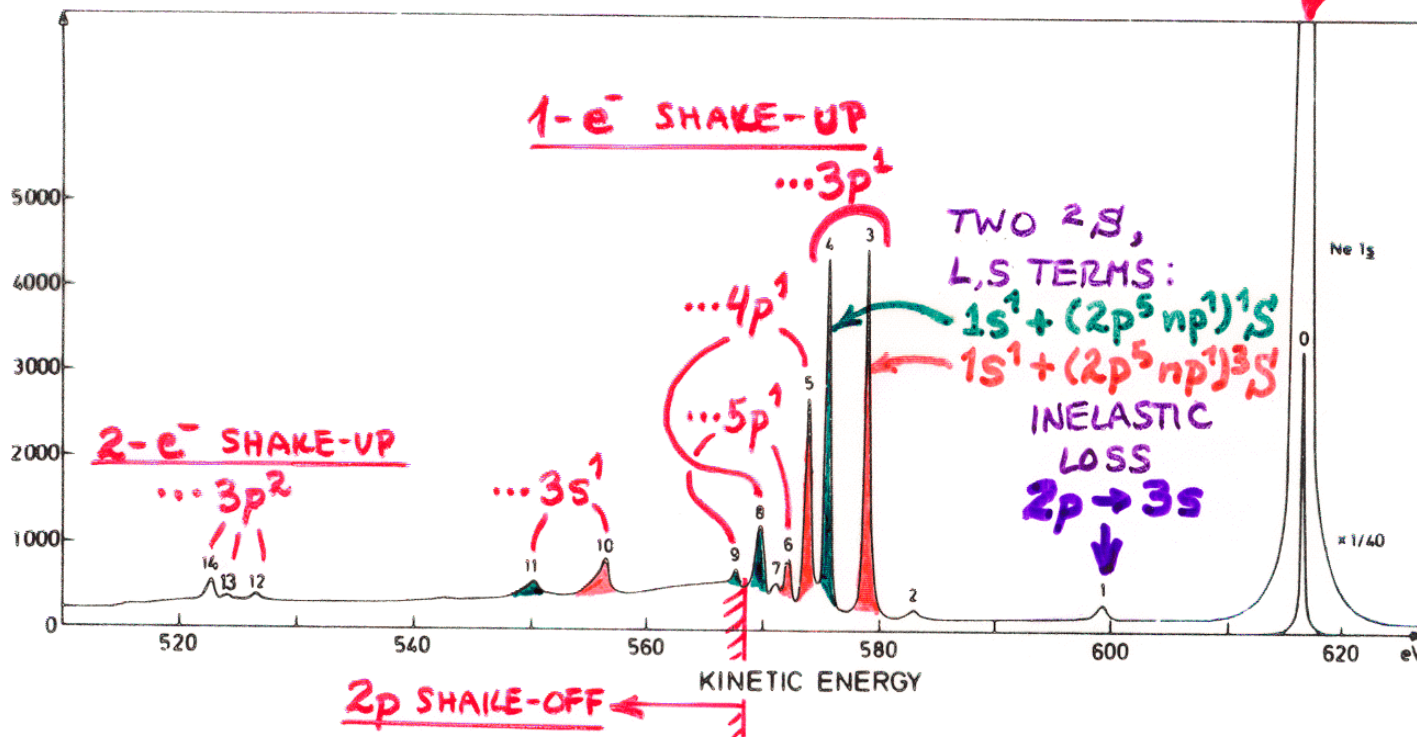
(N-1)e⁻ SHAKE-UP/
SHAKE-OFF \rightarrow
"MONOPOLE"

- PLUS DIFFRACTION EFFECTS IN Ψ_f ESCAPE

NEON 1s SHAKE-UP / SHAKE-OFF:

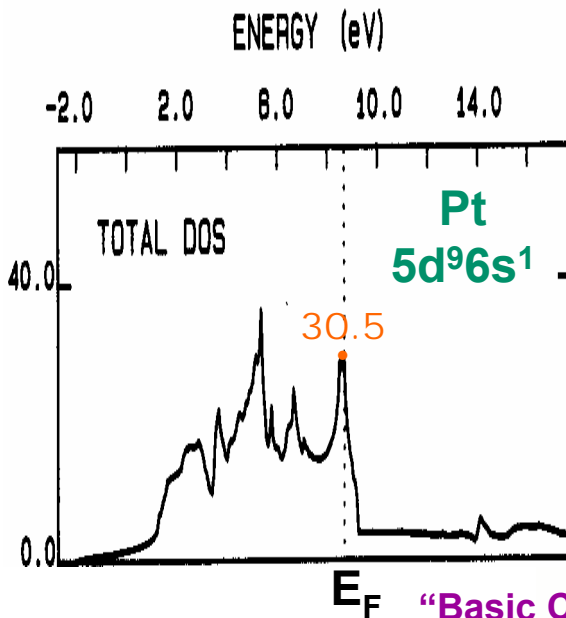
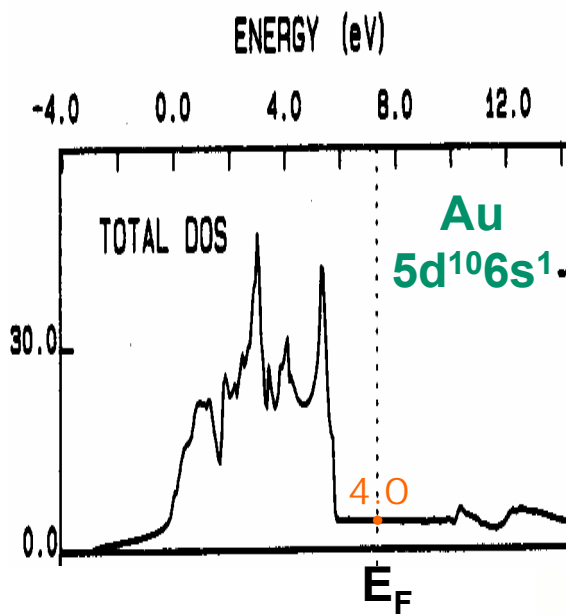


"Basic Concepts of XPS"
Figure 36

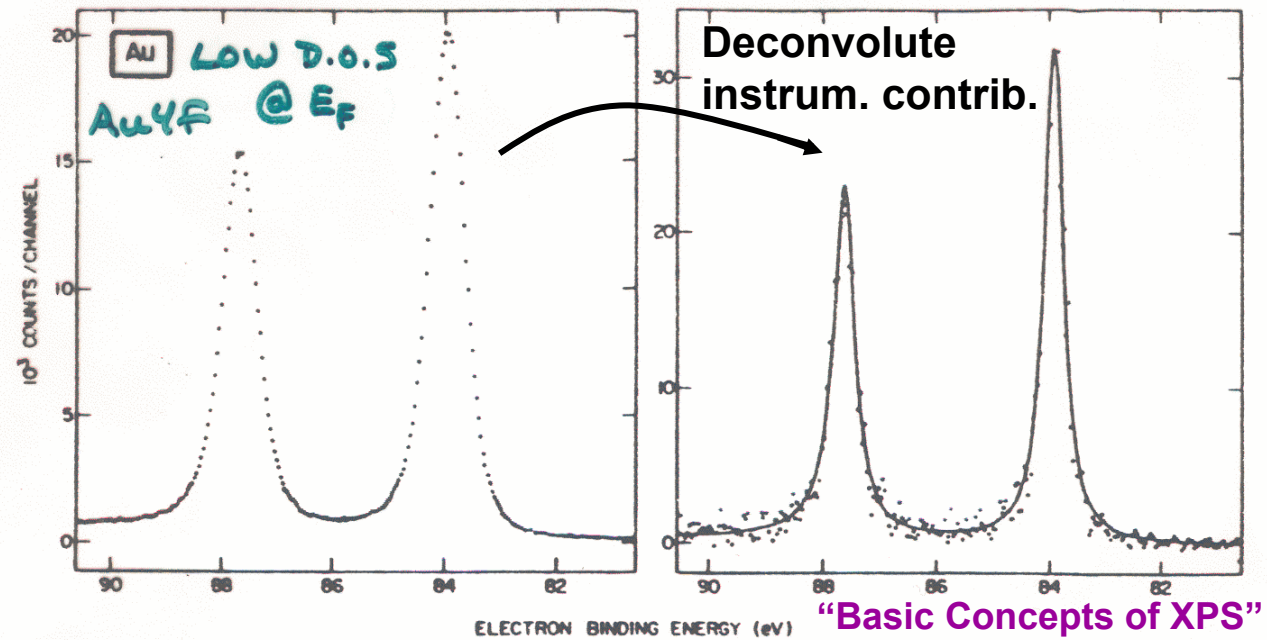


OVERALL: ~12% SHAKE-UP + 16% SHAKE-OFF ≈ 28% OF EVENTS

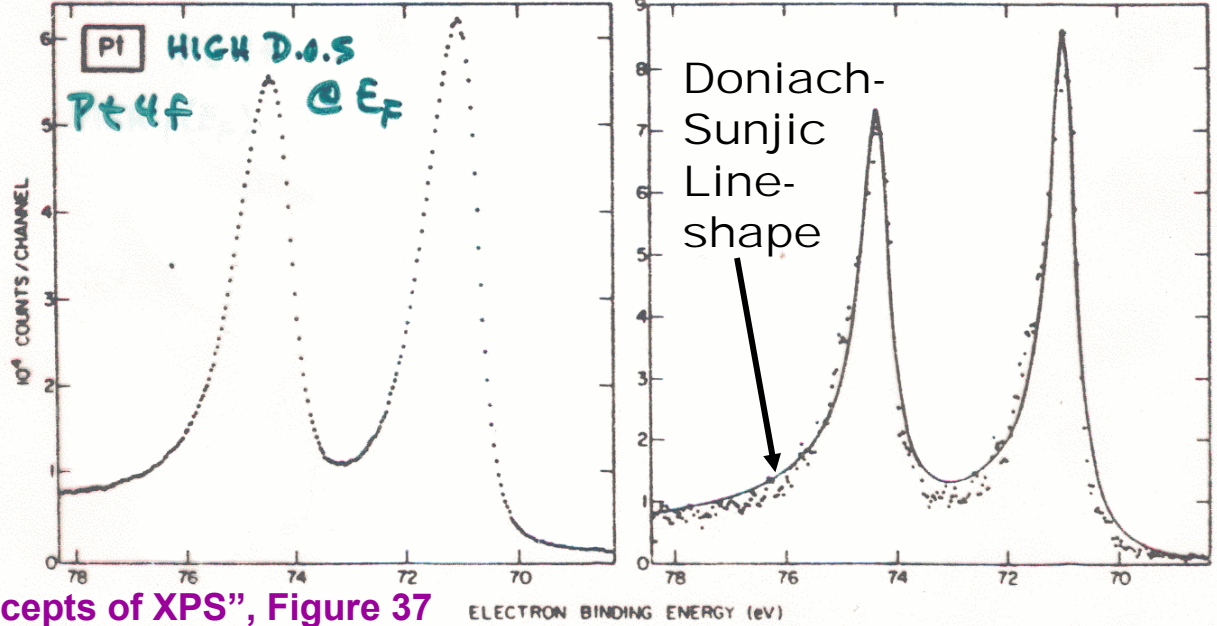
BAND THEORY—D.O.S:



ELECTRON-HOLE EXCITATIONS IN METALS:



"Basic Concepts of XPS"
Figure 10



"Basic Concepts of XPS", Figure 37

TWO SUDDEN-APPROXIMATION

SUM RULES:

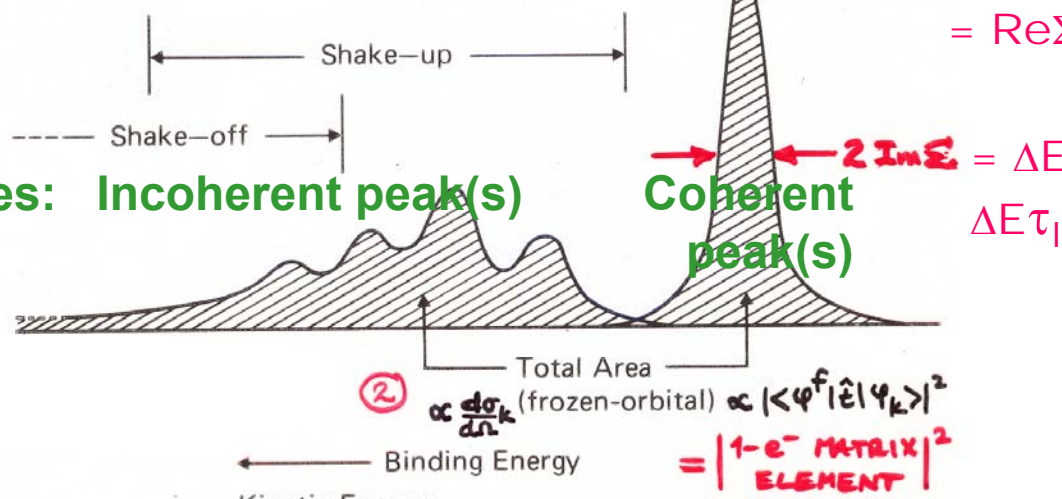
$$\textcircled{1} \quad \left\{ \begin{array}{l} \text{AVERAGE} \\ \text{BINDING} \\ \text{ENERGY} \end{array} \right\} = \frac{\sum_{j=1}^{\text{ALL}} I_j E_b^V(k_j)}{\sum_{j=1}^{\text{ALL}} I_j} = -\epsilon_k \quad \text{KOOPMANS'}$$

Ground-
State
of Ion =
Adiabatic
peak

$$E_b^V(k)_1$$

$$\approx \delta E_{\text{relax}}$$

$$= \text{Re}\Sigma$$



Σ = many-body
"self energy"
 $= \text{Re}\Sigma + i\text{Im}\Sigma$

$$\Delta E \tau_{\text{lifetime}} \approx \hbar/2$$

In valence-band studies: Incoherent peak(s)

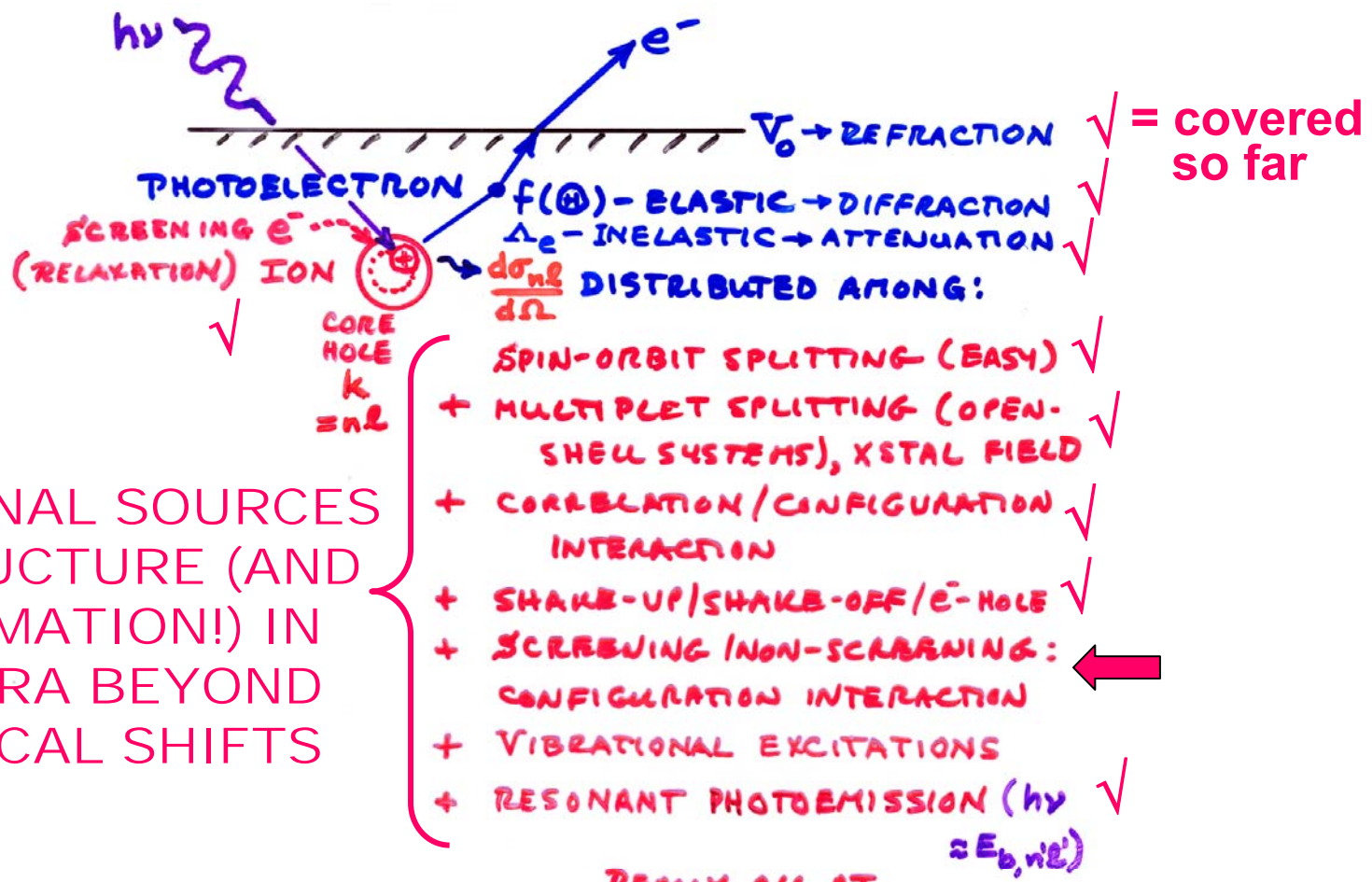
TWO GENERAL INTENSITY RESULTS:

$$\textcircled{1} \quad I_j \propto |\langle \varphi_{(1)}^f | \hat{t} | \psi_k(1) \rangle|^2 |\langle \Psi^f(N-1,j) | \bar{\Psi}_R(N-1) \rangle|^2$$

$k \in \text{MISSING}$

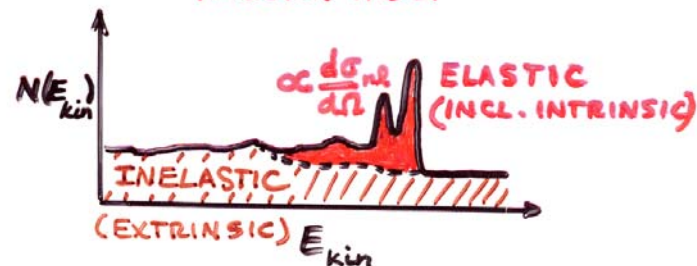
Figure 8 -- Schematic illustration of a photoelectron spectrum involving shake-up and shake-off satellites. The weighted average of all binding energies yields the Koopmans' Theorem binding energy $-\epsilon_k$ (sum rule (77)), and the sum of all intensities is proportional to a frozen-orbital cross section σ_k (sum rule (78)). The adiabatic peak corresponds to formation of the ground-state of the ion ($E_b(k)_1 \equiv E_b(K=1)$).

$$\textcircled{2} \quad \begin{aligned} (\text{TOTAL SHAKE-UP} + \text{SHAKE-OFF}) &= 1 - |\langle \Psi^f(N-1,1) | \bar{\Psi}_R(N-1) \rangle|^2 \\ &\approx 15-25\% \text{ FOR ATOMS/MOLEC.} \end{aligned}$$



ADDITIONAL SOURCES OF STRUCTURE (AND INFORMATION!) IN SPECTRA BEYOND CHEMICAL SHIFTS

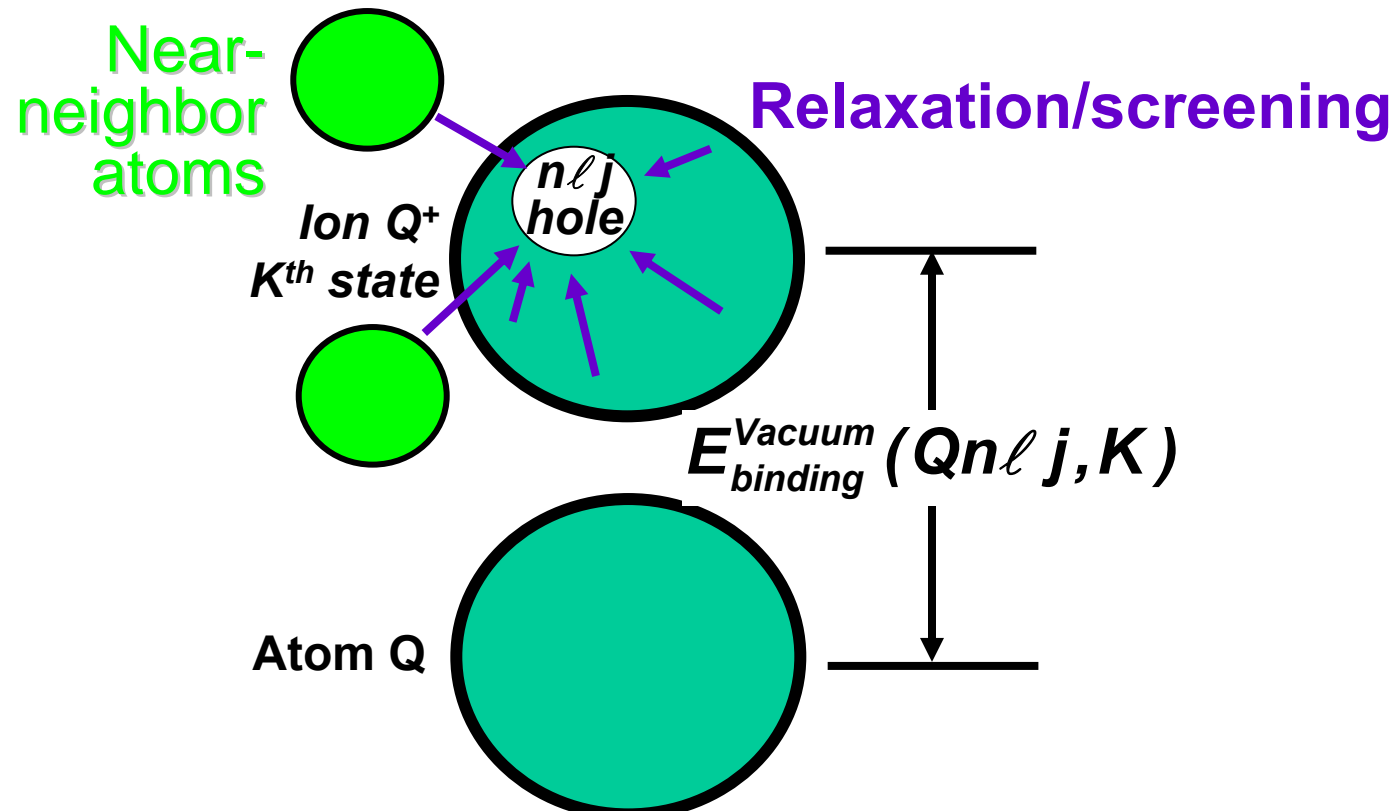
REALLY ALL AT ONCE, BUT SUM RULES + THEORY HELP

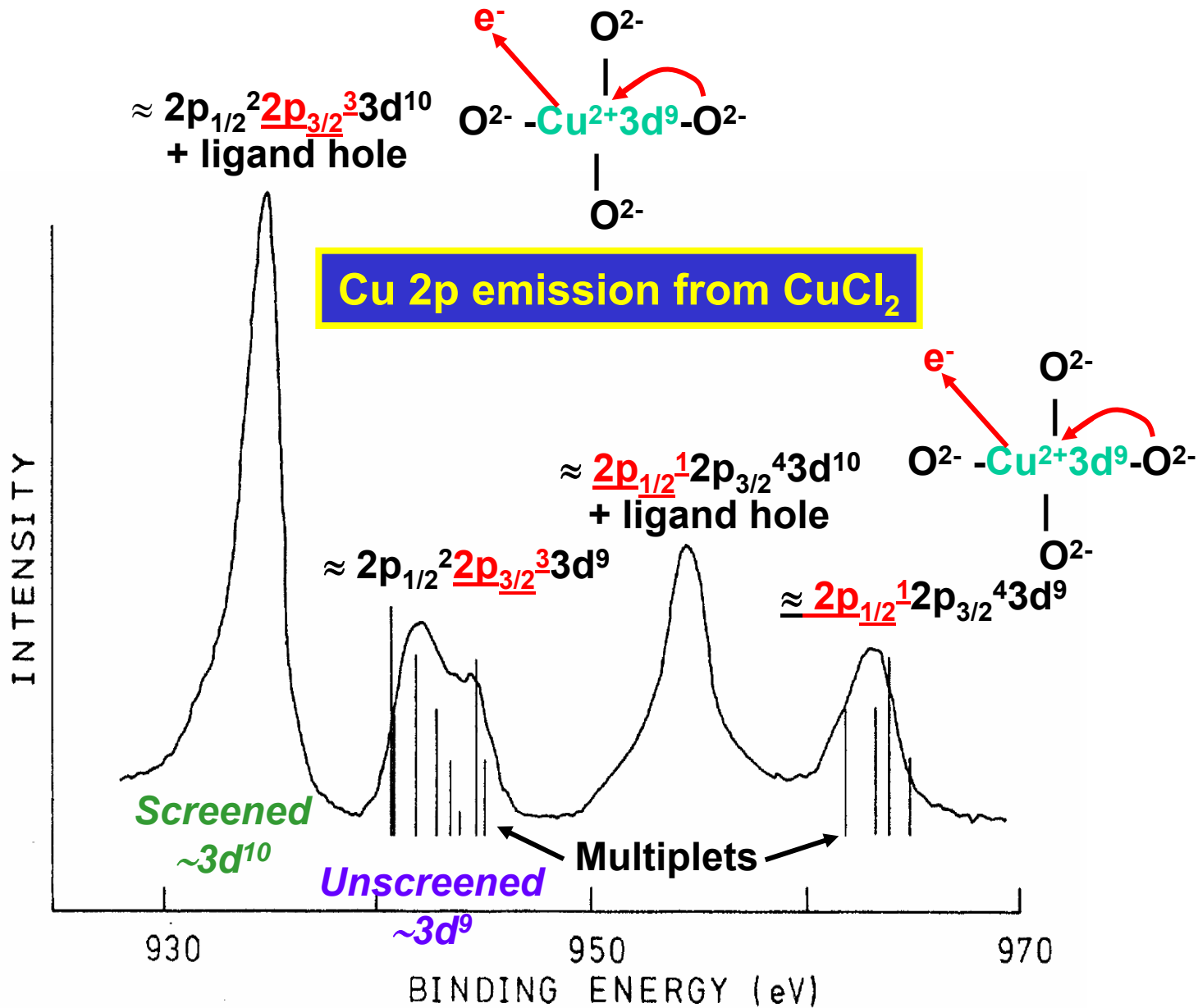


Basic energetics—Many e⁻ & many atom picture

$$h\nu = E_{binding}^{Vacuum} + E_{kinetic} = E_{binding}^{Fermi} + \varphi_{spectrometer} + E_{kinetic}$$

$$E_{binding}^{Vacuum}(Qn\ell j, K) = E_{final}(N - 1, Qn\ell j \text{ hole}, K) - E_{initial}(N)$$

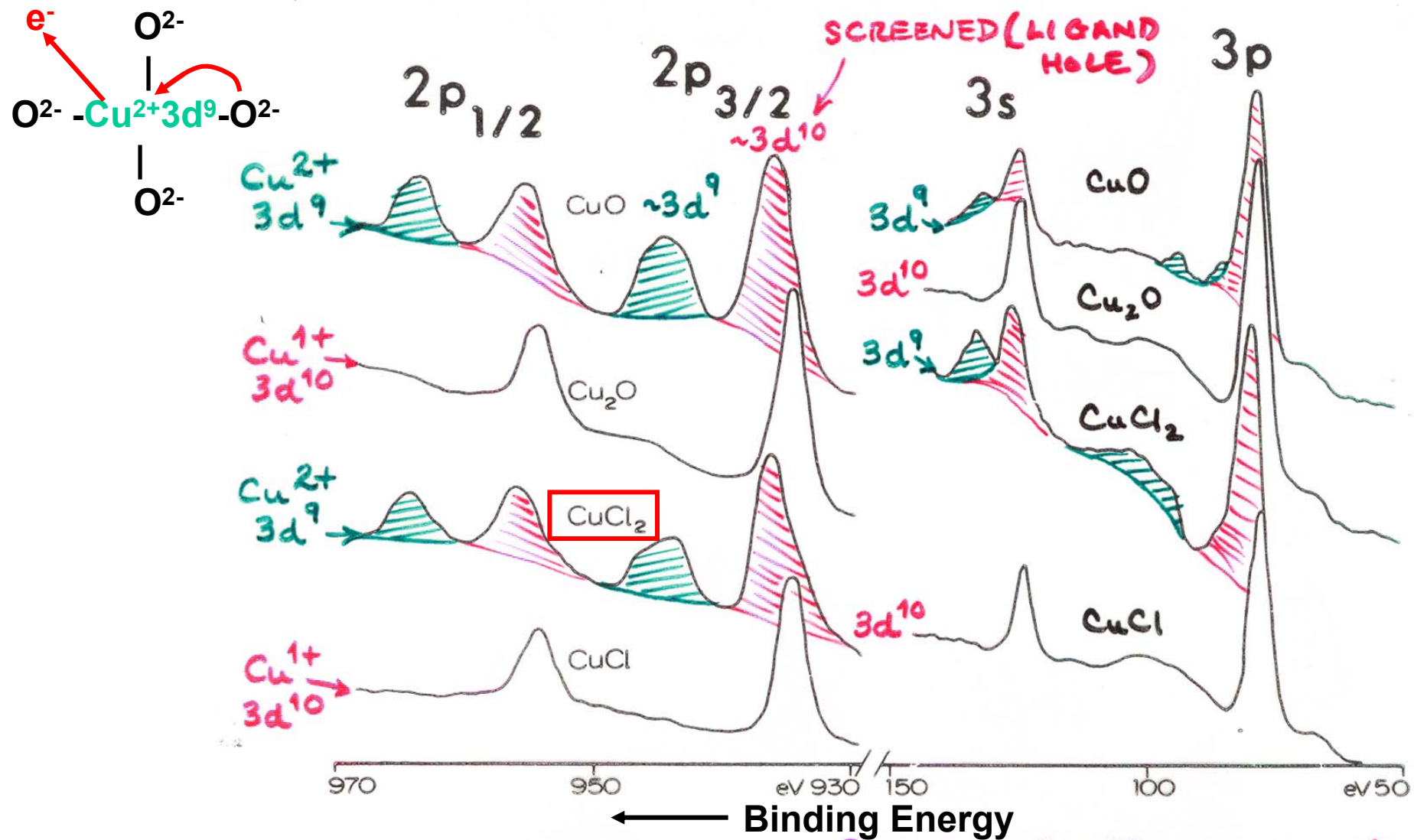




$$\Psi_{final,K}(N-1) = C_{1,K}(2p_{1/2}^2 2p_{3/2}^3 3d^{10} + \text{Cl hole}) + C_{2,K}(2p_{1/2}^2 2p_{3/2}^3 3d^9)$$

Van der Laan et al., Phys. Rev. B 23 (1981) 4369

SATELLITES & CHARGE-TRANSFER SCREENING



"Basic Concepts of XPS" ACTUAL FINAL STATE $\Psi \approx C_1 \phi_1(3d^{10} - \text{SCREENED}) + C_2 \phi_2(3d^9 - \text{UNSCREENED})$

Figure 38

Screening
depends on
Ionicity/covalency →
satellite intensities
can be used to
measure interaction
parameters

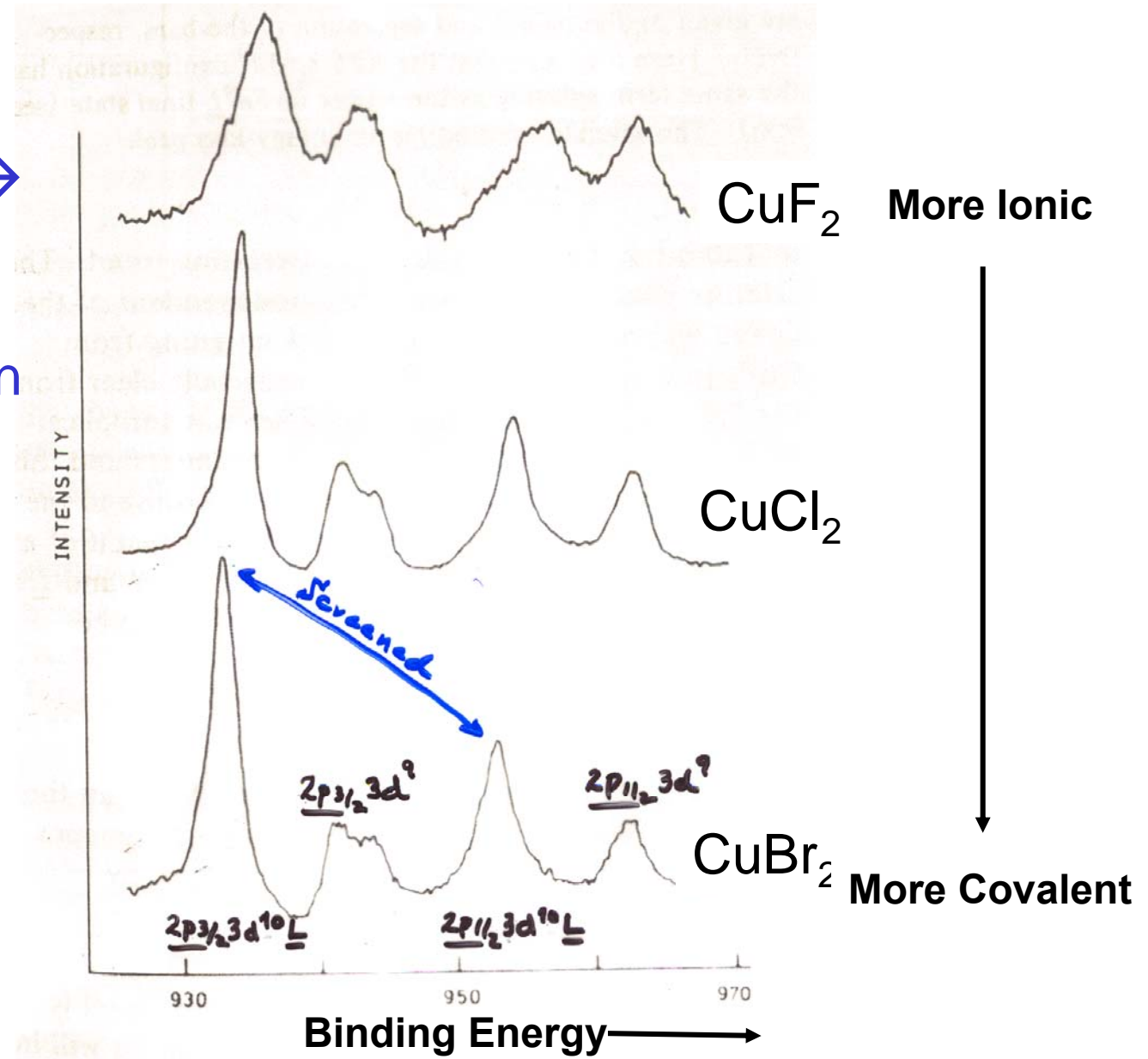


FIG. 1. Cu 2p photoelectron spectra of Cu dihalides. The lines leading to a final state with a ligand hole (L) show a chemical shift.

Screening
depends on
Ionicity/covalency →
satellite intensities
can be used to
measure interaction
parameters

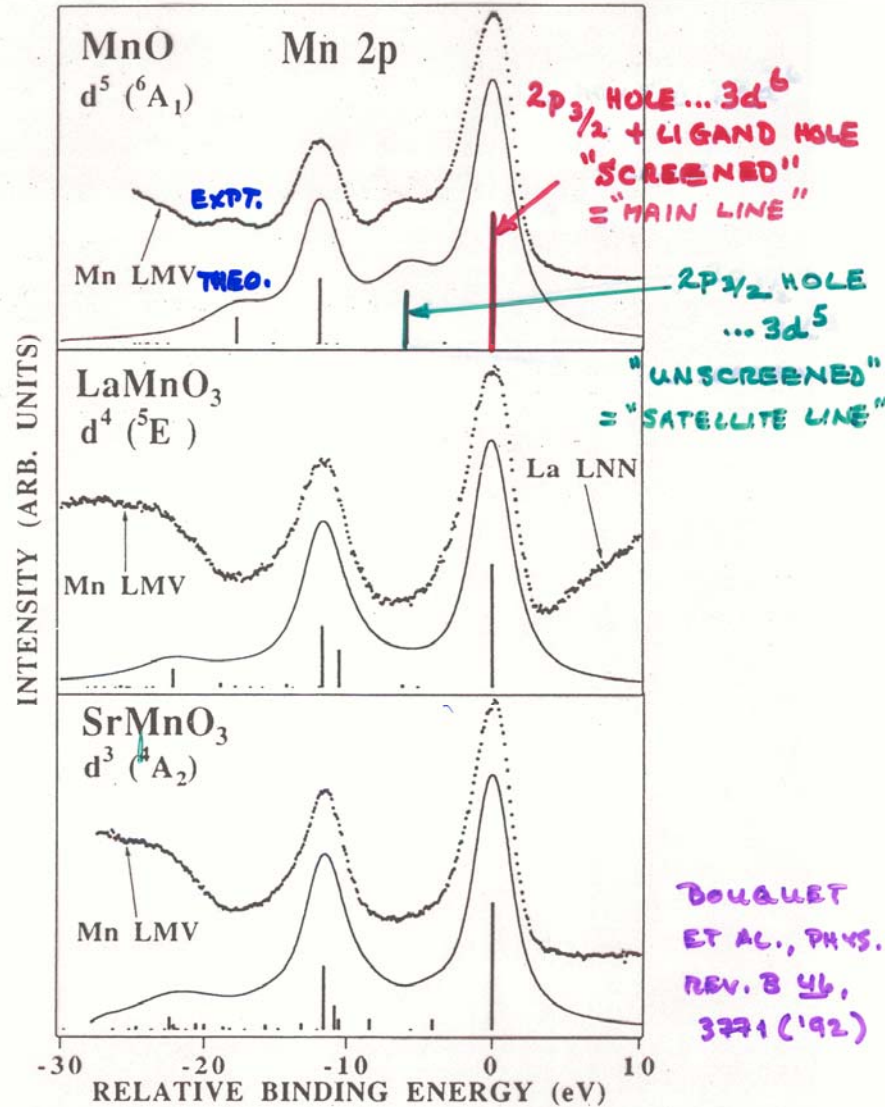
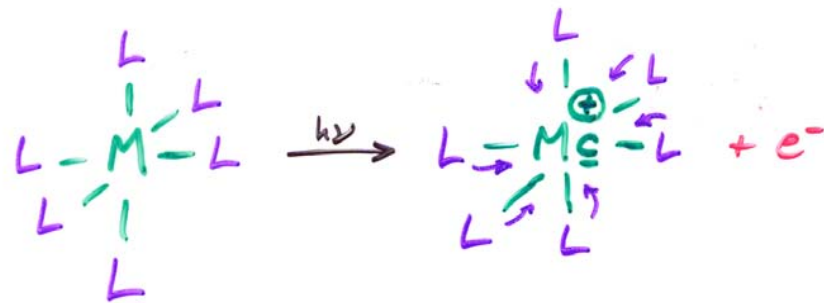


FIG. 1. Theoretical $2p$ core-level XPS spectra (solid line) compared with experimental data (dots) after background subtraction for Mn cations with varying valence. Emission due to the Mn LMV Auger peak is observed on the high-binding-energy side of the $2p_{1/2}$ spin-orbit peak, partially obscuring the $2p_{1/2}$ satellite structure.

CONFIGURATION INTERACTION APPROACH TO SCREENING IN TRANSITION-METAL (RARE-EARTH) COMPOUNDS:

(SUGANO, LARSEN ~ SAWATEKI, VANDERLAAN, FUJIMORI, OH, ET AL.)



\underline{c} = CORE HOLE ON METAL

\underline{L} = VALENCE (γ) HOLE ON LIGAND

$$\Psi_i = a_0 |d^n\rangle + \sum_m a_m |d^{(n+m)} \underline{L}^m\rangle$$

$$\Psi_f = b_0 |\underline{c} d^n\rangle + \sum_m b_m |\underline{c} d^{(n+m)} \underline{L}^m\rangle$$

WITH INTERACTIONS OF :

ΔD_g = CRYSTAL FIELD (OFTEN NEGLECTED)

$$\begin{aligned}\Delta &= \text{LIGAND-TO-METAL CHARGE TRANSF. ENERGY} \\ &= E(d^{n+1} \underline{L}) - E(d^n)\end{aligned}$$

$$\begin{aligned}\Pi &= d-d \text{ COULOMB REPULSION ENERGY} \\ &= E(d^{n-1}) + E(d^{n+1}) - 2E(d^n)\end{aligned}$$

$$\begin{aligned}\Gamma &= \text{LIGAND P-TO-METAL d HYBRIDIZATION} \\ &= \langle d_\alpha | \hat{H} | p_\alpha \rangle \quad (\alpha = \text{SAME SYMMETRY})\end{aligned}$$

$$Q = \text{CORE-HOLE-TO-d INTERACTION: } \langle \underline{c} | \hat{H} | d \rangle \approx J_{cd}$$

WITH INTENSITIES FROM SUDDEN APPROX.

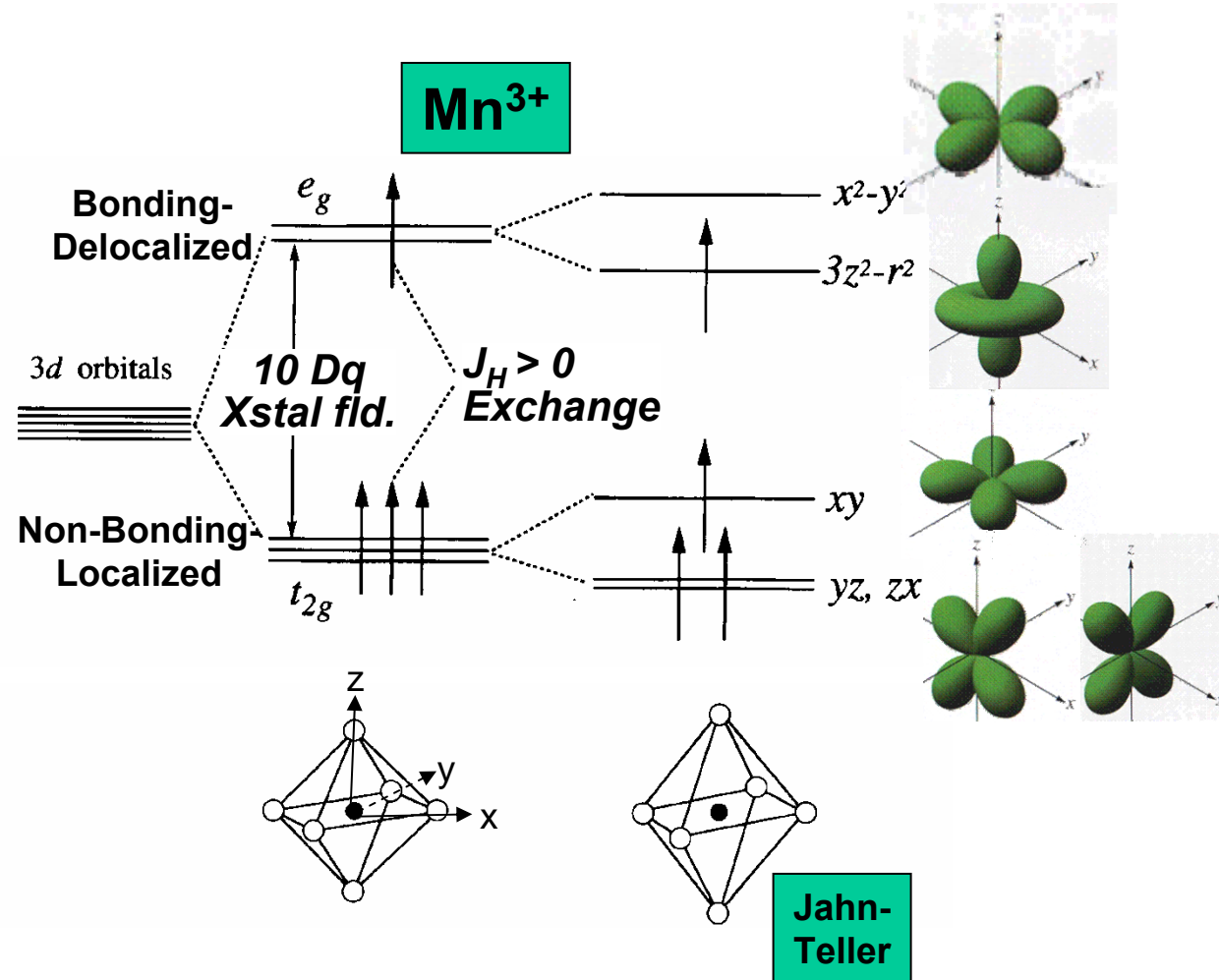
AS:

$$I(E_{kin}) \propto \sum_{f,k} | \langle \Psi_f(N-1, k) | \Psi_{R_e}(N-1, k) \rangle |^2 \cdot \delta(hv - E_f - E_{kin})$$

$\downarrow = \underline{c} = \text{CORE HOLE}$

WHERE: $\Psi_{R_e}(N-1, k) = \Psi_i (N \text{ WITH } k \text{ HOLE} = \underline{c})$

E.g.—Crystal field in Mn^{3+} with negative octahedral ligands



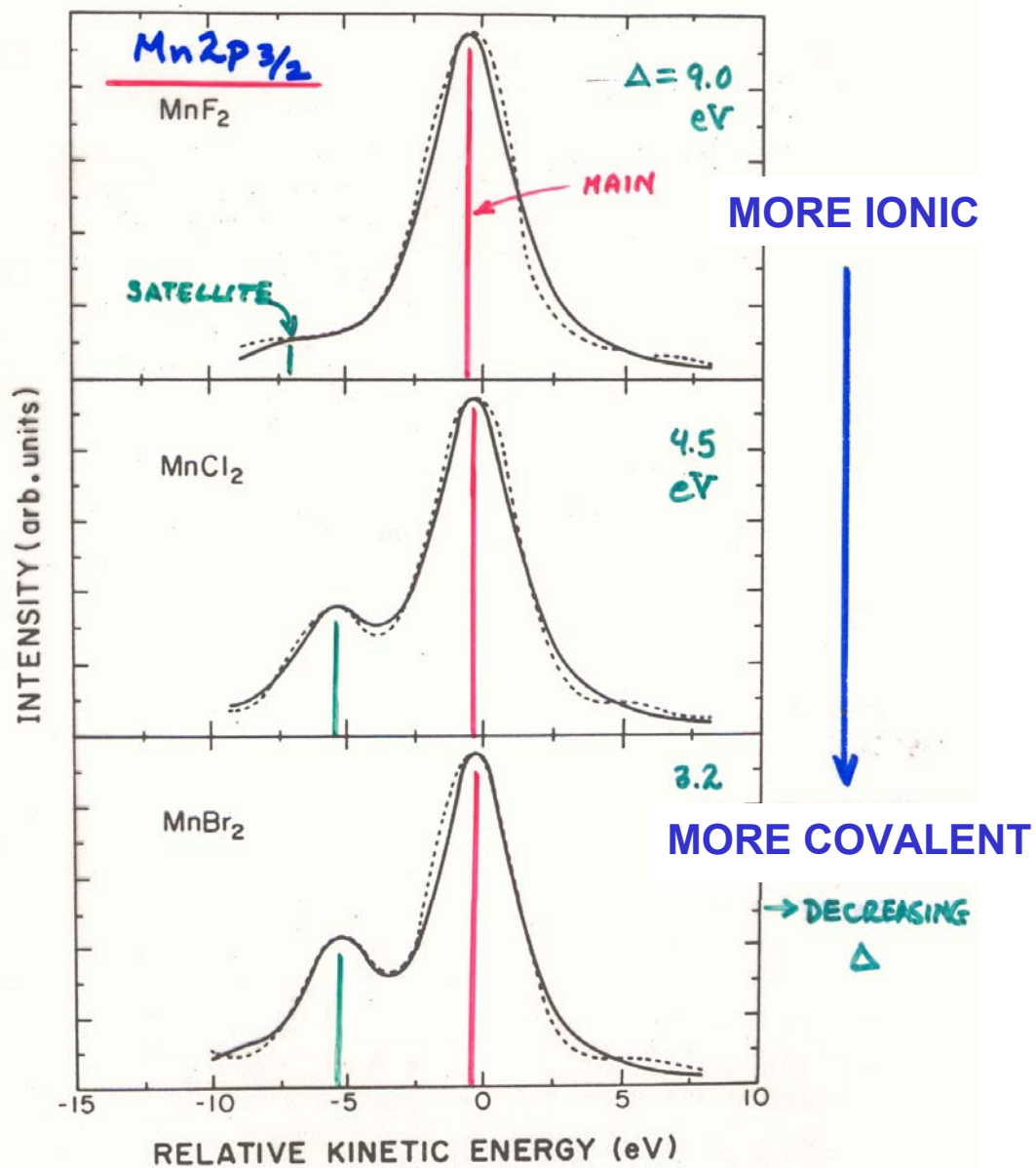
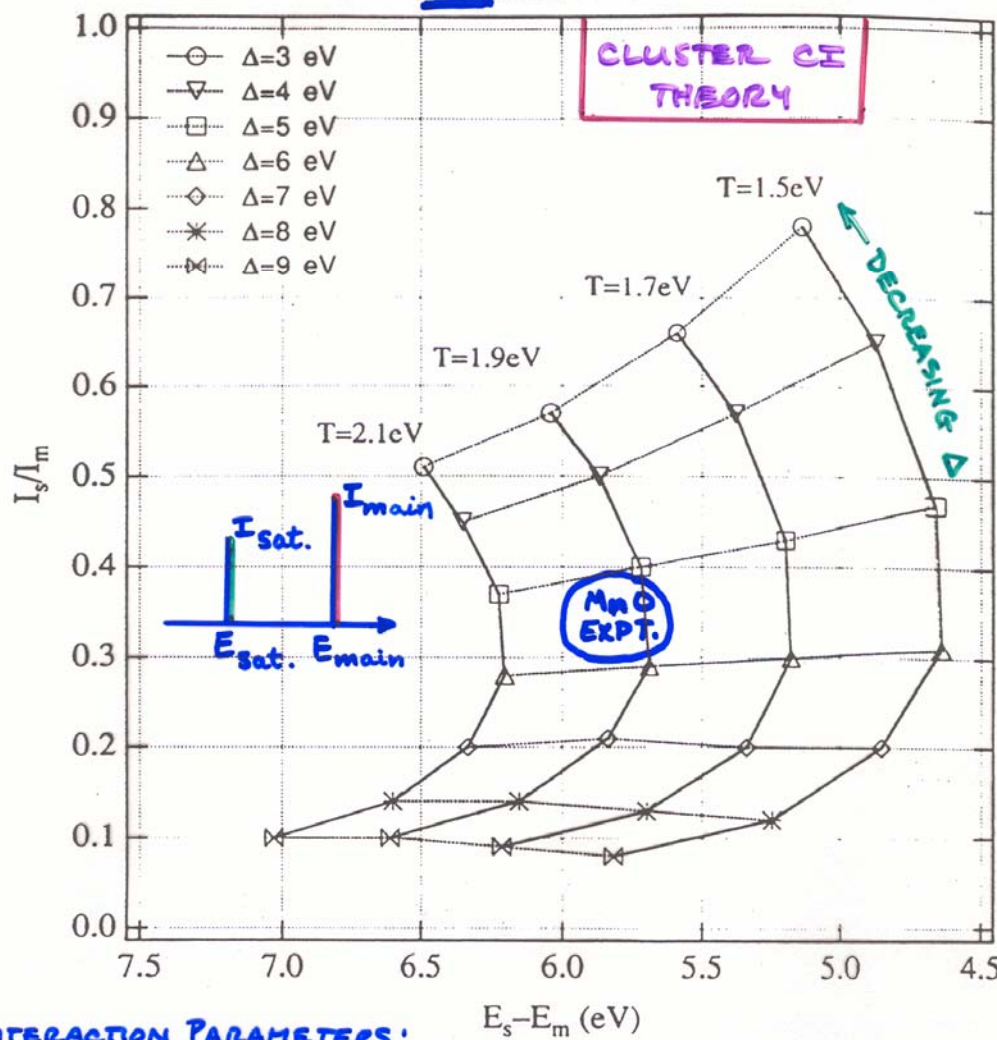


FIG. 6. Fits of the cluster model results with the experimental $2p_{3/2}$ spectra of the manganese dihalides. The parameters used are listed in Table II. A Lorentzian broadening is 2.6–3.0 eV, and a Gaussian broadening of 1.2 eV (FWHM) was used.

ANALYSIS VIA ANDERSON IMPURITY MODEL
 Mn^{2+} (HS) $U=6.0$ eV



INTERACTION PARAMETERS:

U = 3d-3d COULOMB REPULSION ENERGY

Δ = LIGAND-TO-METAL CHARGE TRANSFER ENERGY

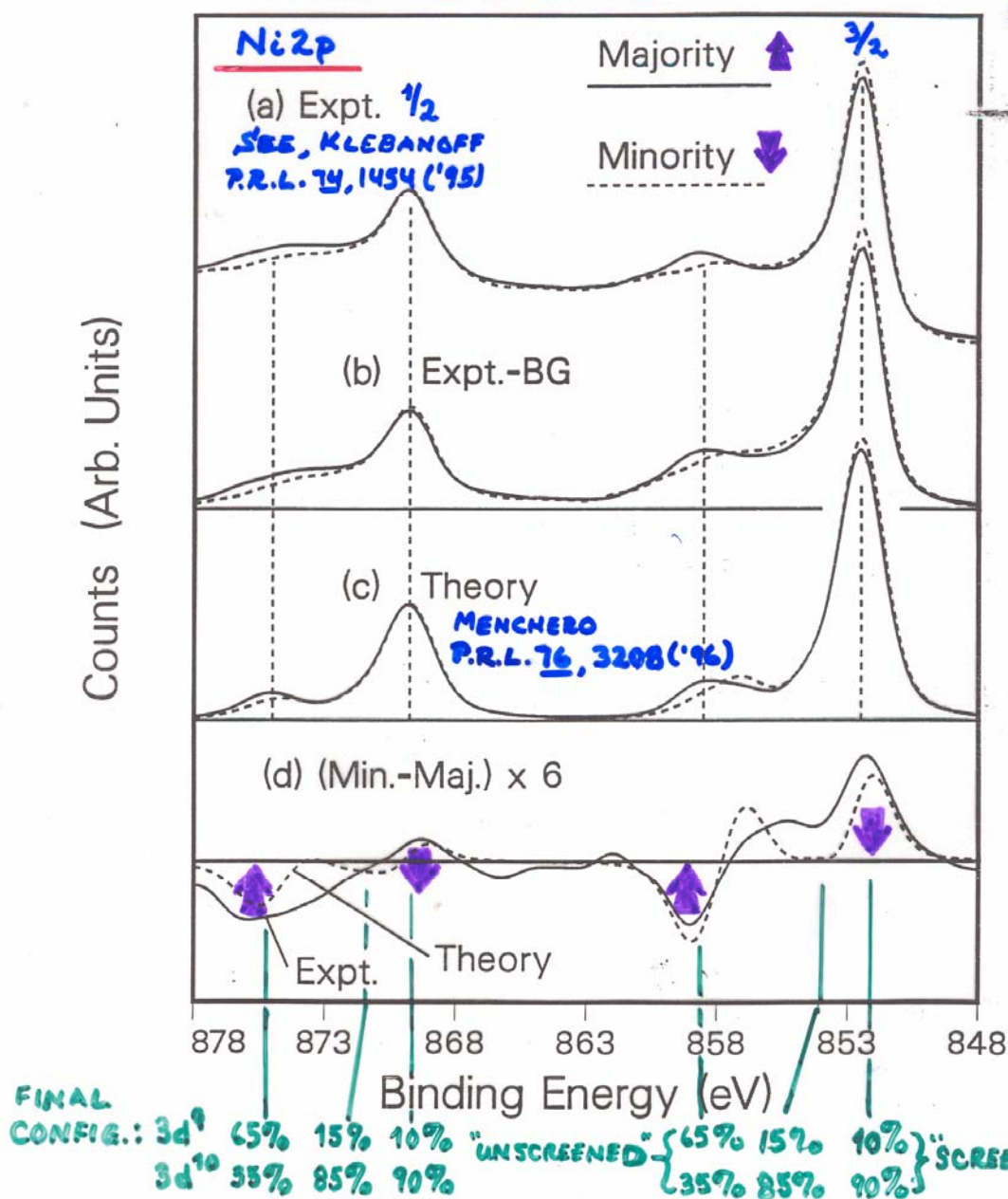
T = LIGAND P - METAL 3d HYBRIDIZATION ENERGY

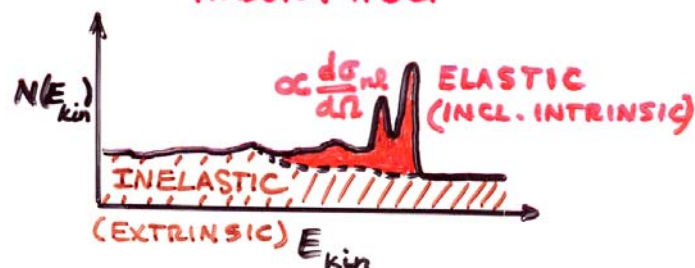
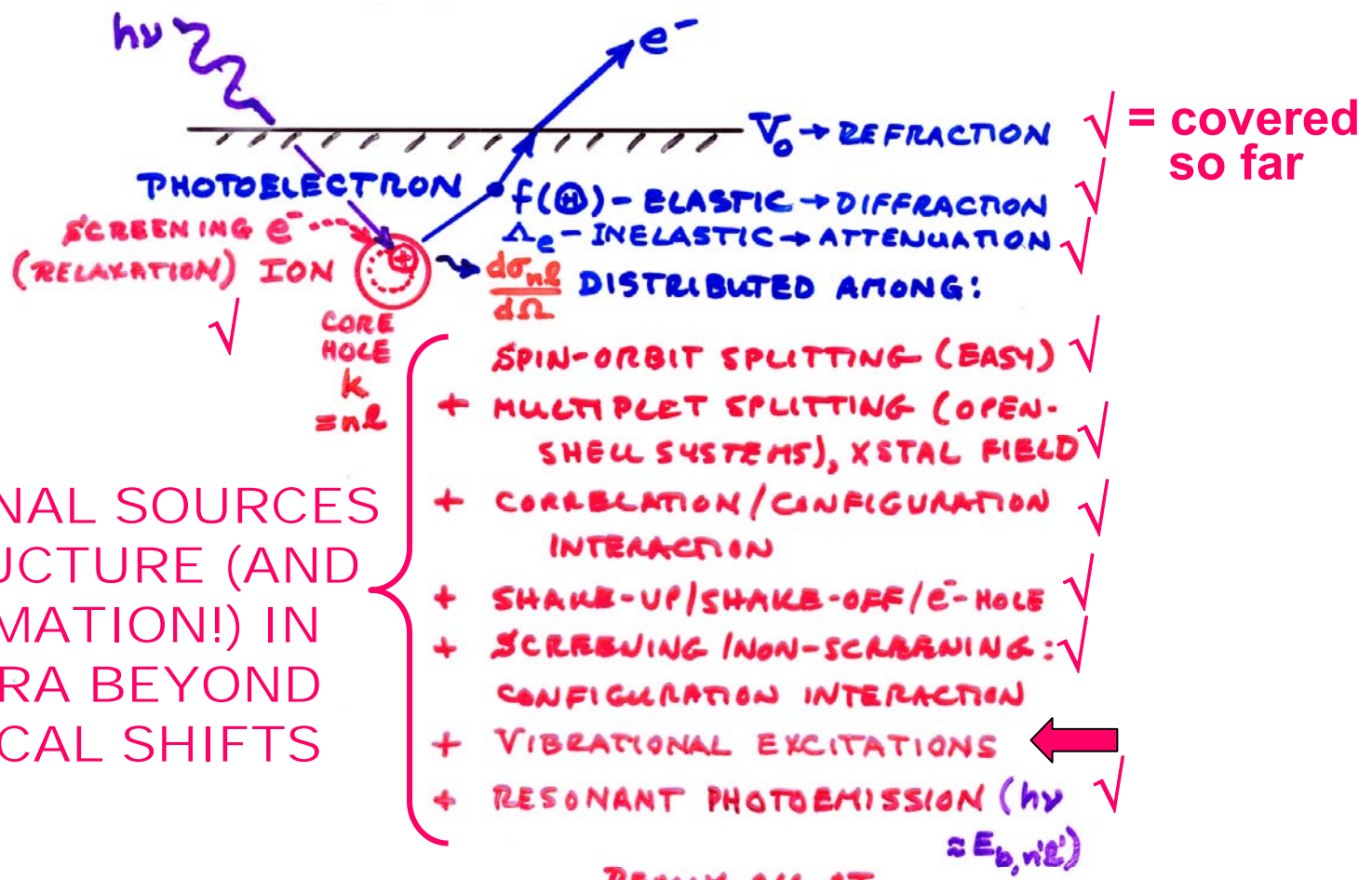
Q = CORE HOLE-3d COULOMB ENERGY BOUGUET ET AL.,
 J. EL. SP. 82, 87 (1996)

SPIN-ORBIT SPLITTING + MULTIPLETS + SCREENING IN A METAL : Ni - INITIAL CONFIG.: $43^9\text{,}3d^9$

$\sim 15\% 3d^8$

$42\% 3d^{10}$





ADDITIONAL SOURCES OF STRUCTURE (AND INFORMATION!) IN SPECTRA BEYOND CHEMICAL SHIFTS

INTENSITIES IN PHOTOELECTRON SPECTRA:

- GENERAL: FINAL STATE K (K-SUBSHELL + ALL OTHER DESIGN.)

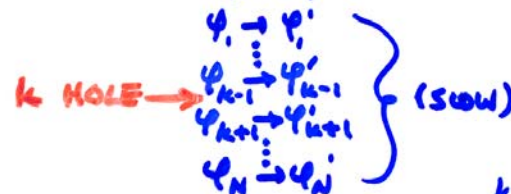
$$\text{INT}_K \propto |\hat{e} \cdot \langle \Psi_{\text{tot}}^f(N, K) | \sum_{i=1}^N \vec{r}_i | \Psi_e^i(N) \rangle|^2 \quad (\text{DIPOLE APPROX.})$$

- BORN-Oppenheimer: e-'s fast, vibrations slow

$$\text{INT}_K \propto |\langle \Psi_{\text{vib}, v}^f | \Psi_{\text{vib}, v}^i \rangle|^2 |\hat{e} \cdot \langle \Psi_e^f(N, K) | \sum_{i=1}^N \vec{r}_i | \Psi_e^i(N) \rangle|^2$$

FRANCK-CLOUDON FACTOR

- SUDDEN APPROXIMATION: $\Psi_K \rightarrow \Psi_f = \text{PHOTOE}^-$ (FAST)



$$\text{INT}_K \propto |\langle \Psi_{\text{vib}, v}^f | \Psi_{\text{vib}, v}^i \rangle|^2 |\langle \underbrace{\Psi_e^f(N-1, K)}_{\text{K MISSING}} | \Psi_e^{f, \dagger}(N-1, K) \rangle|^2$$

$|\hat{e} \cdot \langle \Psi_f | \vec{r} | \Psi_K \rangle|^2$ SAME SUBSHELL COUPLING +
TOTAL L,S \rightarrow "MONOPOLE"

$\hookrightarrow \text{NORMAL } \frac{dG_K}{d\Omega}$

- SLATER DETS. FOR $\Psi_e^f = \det(\Psi_1' \Psi_2' \dots \Psi_{K-1}' \Psi_{K+1}' \dots \Psi_N')$

$$\Psi_K = \det(\Psi_1 \Psi_2 \dots \Psi_{K-1} \Psi_{K+1} \dots \Psi_N)$$

$$\text{INT}_K \propto |\langle \Psi_{\text{vib}, v}^f | \Psi_{\text{vib}, v}^i \rangle|^2 |\langle \Psi_1' | \Psi_1 \rangle|^2 |\langle \Psi_2' | \Psi_2 \rangle|^2 \dots$$

$$|\langle \Psi_{K-1}' | \Psi_{K-1} \rangle|^2 |\langle \Psi_{K+1}' | \Psi_{K+1} \rangle|^2 \dots |\langle \Psi_N' | \Psi_N \rangle|^2 \dots$$

$$|\hat{e} \cdot \langle \Psi_f | \vec{r} | \Psi_K \rangle|^2$$

1e- DIPOLE $\rightarrow d\sigma/d\Omega$

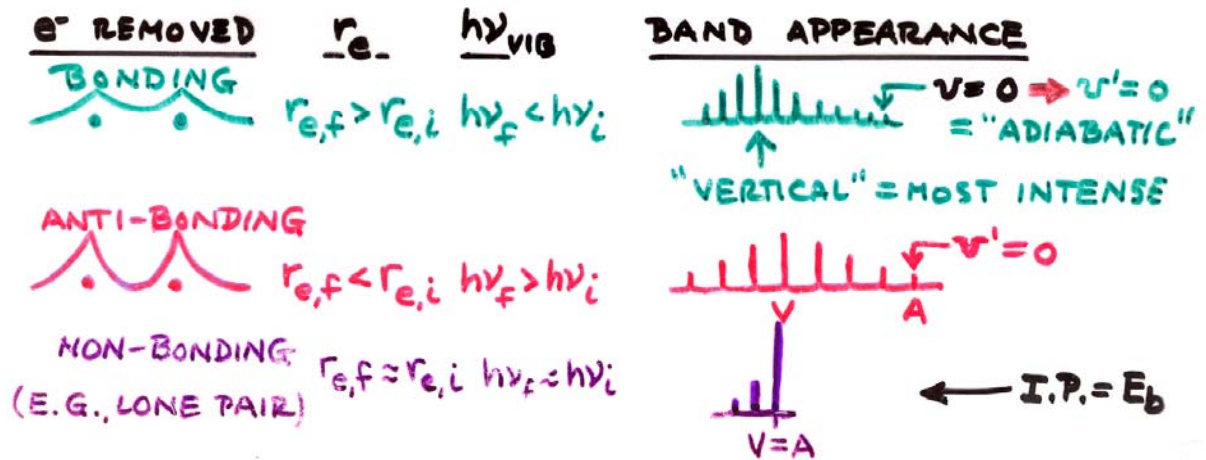
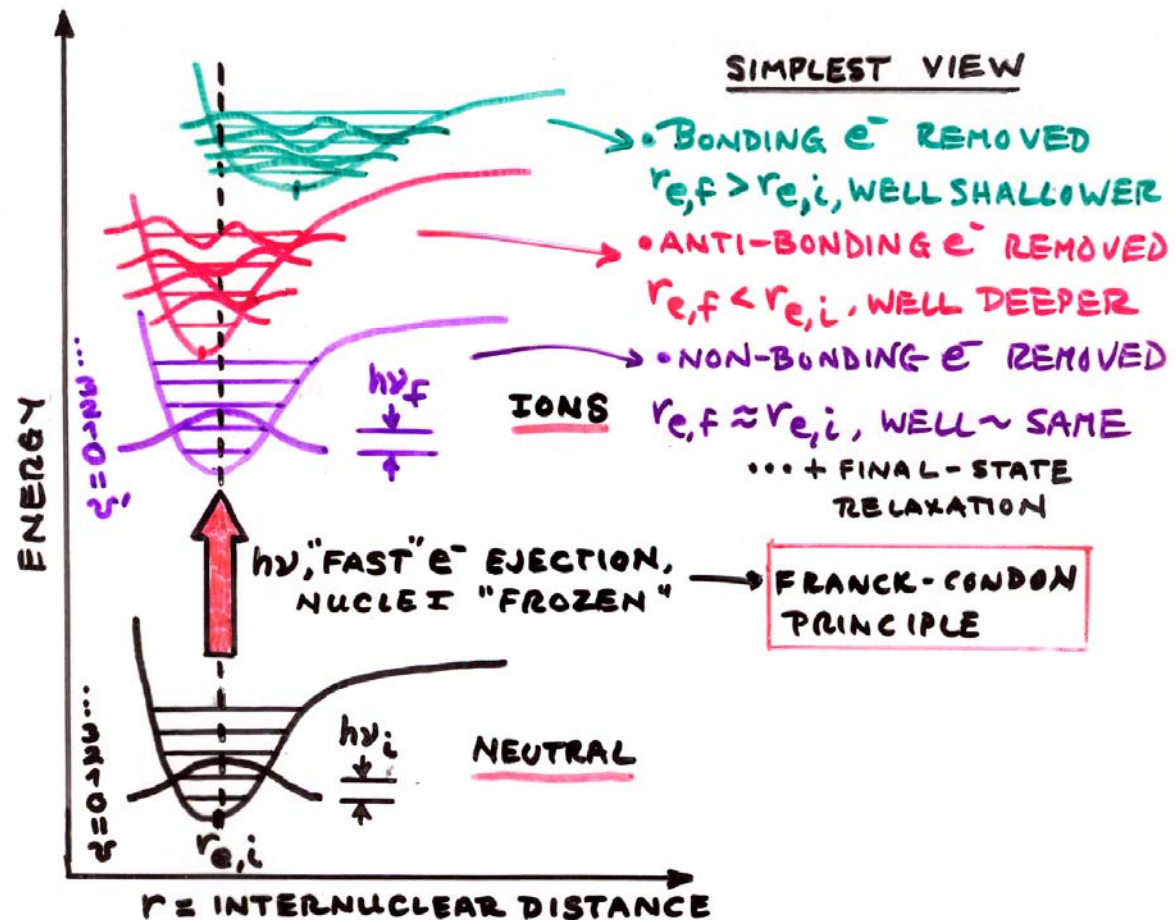
(N-1)e- SHAKE-UP/
SHAKE-OFF \rightarrow
"MONOPOLE"

- PLUS DIFFRACTION EFFECTS IN Ψ_f ESCAPE

VIBRATIONAL STRUCTURE IN VALENCE-LEVEL (MO) SPECTRA

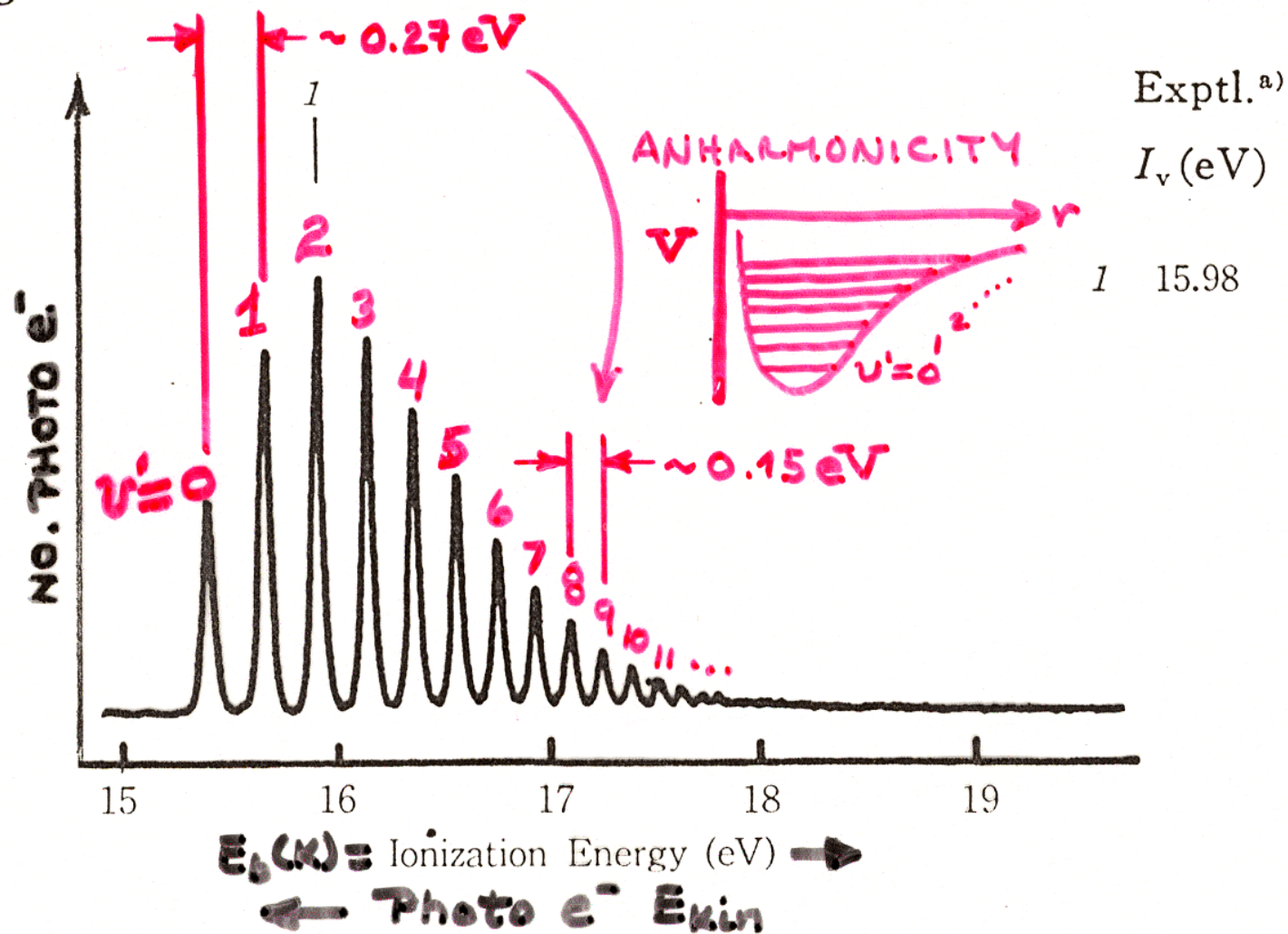
Diatom A-B example

(Also applies to core-level emission if equilibrium distance changes on forming core hole)



VIBRATIONAL STRUCTURE IN VALENCE-LEVEL (MO) SPECTRA

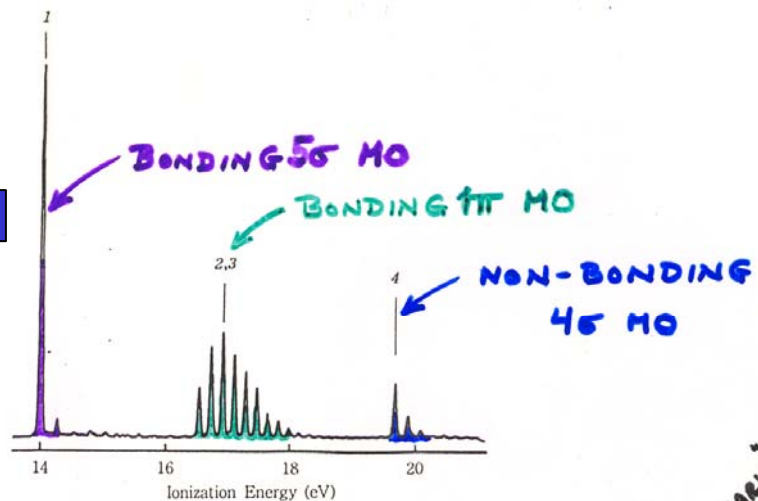
H_2 Hydrogen



(9) CO Carbon Monoxide

UV PHOTOELECTRON SPECTRUM OF CO

Vibrational fine structure ←



KOOPMANS'				CI FINAL STATE		
Exptl. ^{a)}	SCF MO [6-31 G] ^{b)}			CI (Ionic State) [6-31 G] ^{c)}		
I_v (eV)	$-\epsilon$ (eV)	MO	Character	E (eV)	State	Configuration
1 14.01	14.99	5σ (7)	σ_{CO}	13.11	$1^{\pm}\Sigma^+$	$0.93(7^{-1})$ $-0.15(6^{-1}, 7^{-1}, 9)_s$ $-0.15(5^{-1}, 7^{-1}, 8)_s$
2 16.91	17.48	1π (6, 5)	π_{bond}	16.69	$1^{\pm}\Pi$	$0.95(6^{-1})$; $0.95(5^{-1})$
3 16.91	17.48	4σ (4)	n_O	19.29	$2^{\pm}\Sigma^+$	$0.92(4^{-1})$ $+0.16(6^{-1}, 7^{-1}, 9)_s$ $+0.16(5^{-1}, 7^{-1}, 8)_s$
4 19.72	21.69					

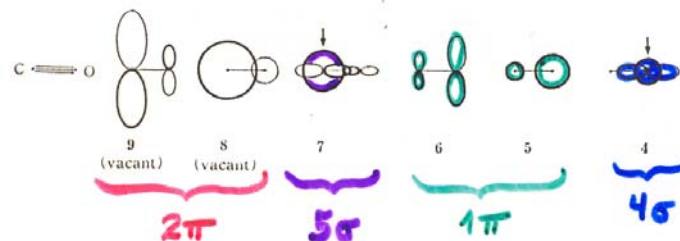
PRIMARY HOLES

RELAX + CORREL.

a) The spectrum : this work. The I_v 's : Turner *et al.* (215). See also other works : Turner and May (215a); Carlson and Jonas (54); Gardner and Samson (104); Edqvist *et al.* (90); Potts and Williams (182a); and Natalis *et al.* (165).

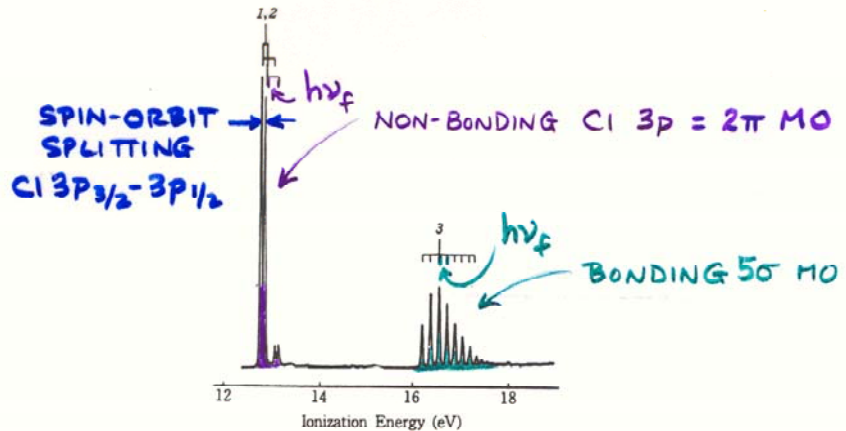
b) We used the bond length reported (A 3) ; symmetry C_{nh} . $E_{SCF} = -112.6672$ hartree. In 4-31G calculations, $E_{SCF} = -112.5524$ hartree and $-\epsilon$ (eV) = 14.93, 17.41, 17.41, and 21.60.

c) CI-II. (9, 8)=1 π . $|N\rangle = 0.98$ (SCF). The results obtained in other CI levels are given in Appendix B.



Kimura et al.,
"Handbook of Hel
Photoelectron Spectra"

THE UV PHOTOELECTRON SPECTRUM OF HCl



KOOPMANS' THEO.			CONFIG. INT. ON FINAL STATE			
Exptl. ^{a)}	SCF MO [4-31 G] ^{b)}		~CI (Ionic State) [4-31 G] ^{c)}			
I_v (eV)	$-\epsilon$ (eV)	MO	Charactor	E (eV)	State	Configuration
1	12.75	12.77	$\left. \begin{array}{l} 2\pi (9,8) \\ n_{Cl} \end{array} \right\}$			
2	12.85	12.77		11.97	$1^1\Pi$	$0.98(9^{-1}) ; 0.98(9^{-1})$
3	16.28	16.50	$5\sigma (7) \quad \sigma_{HCl}$	16.10	$1^1\Sigma^+$	$0.98(7)$

CI
HOLE
WEIGHT-
ING

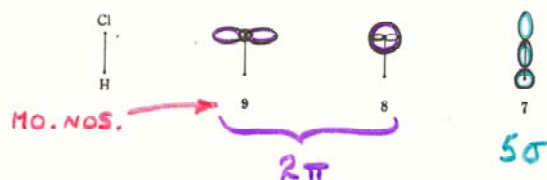
a) The spectrum : this work. The I_v 's : Frost *et al.* (102). See also other works : Lempka *et al.* (150) ; Turner *et al.* (215) ; and Weiss *et al.* (224).

b) We used the bond length reported in Ref. (A 5) : symmetry $C_{\infty h}$. $E_{SCF} = -459.5631$ hartree.

c) Cl-V. $|N\rangle = 0.99$ (SCF).

Cl-V' : E (eV) = 12.01 and 16.11.

Cl-III : E (eV) = 12.60 and 16.79.

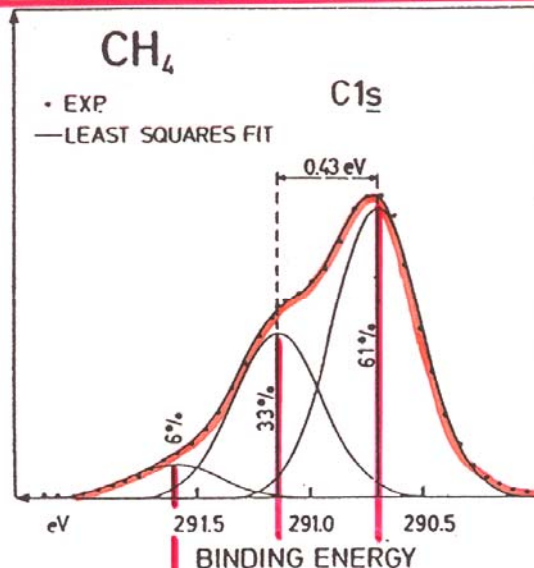


(FROM KIMURA ET AL., "HANDBOOK OF HE I PHOTO-ELECTRON SPECTRA OF FUND. ORGANIC MOLECULES")

VIBRATIONAL FINE STRUCTURE IN CORE SPECTRA

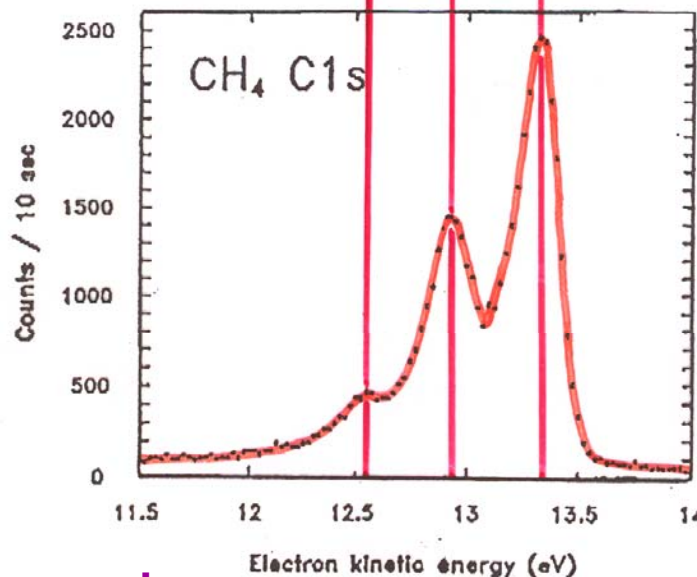
MONOCHROMATIZED
LABORATORY
X-RAY SOURCE

"Basic Concepts of XPS"
Figure 40



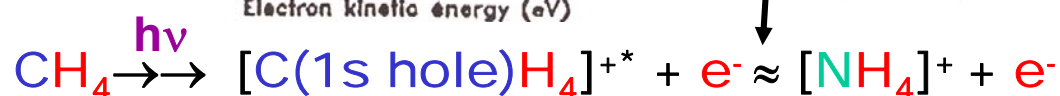
1970
SIEGBAHN,
GELius,
ET AL.

NEW SR
BEAMLINE
AT
BROOK-
HAVEN
(~5-10X
FASTER
@ALS)



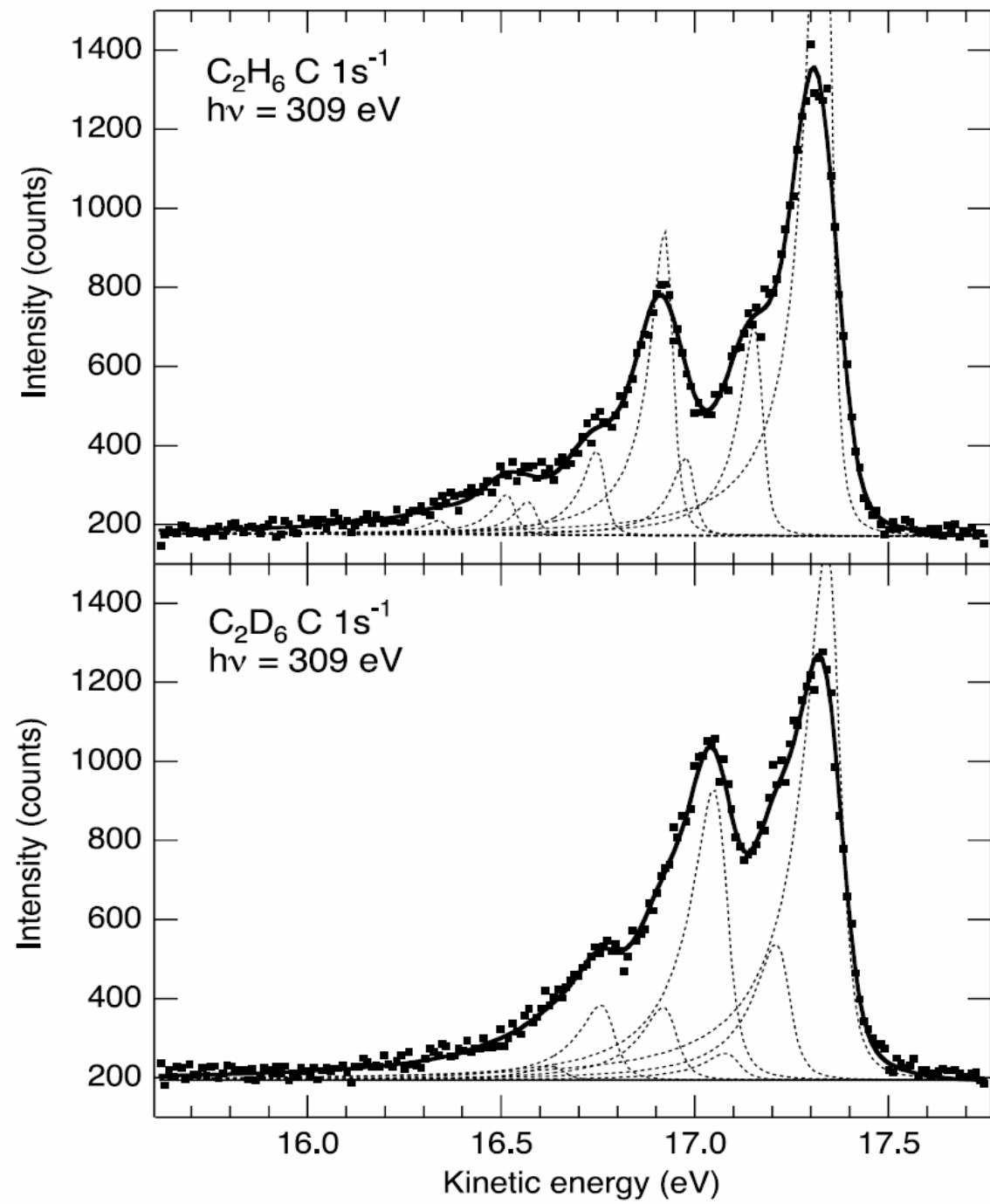
1991
BRADSHAW,
KAINDL,
ET AL.

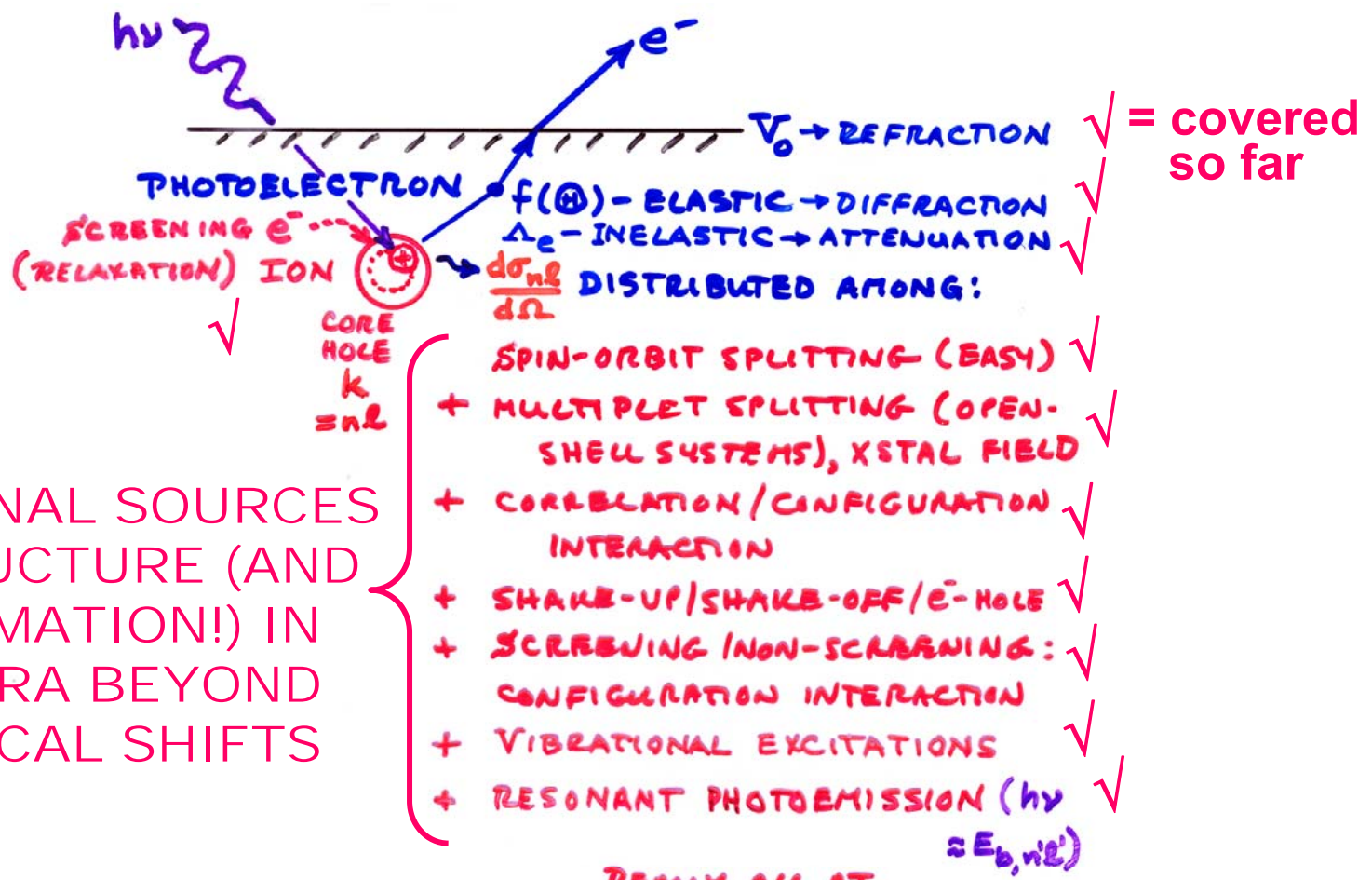
CH distance = 1.10 Å
NH distance = 1.00 Å
Equivalent-core



**Vibrational fine
structure in C 1s
photoemission
from ethane:
two progressions
 v_a at 0.407 eV and
 v_b at 0.176 eV and
various excitations
(v_a, v_b)**

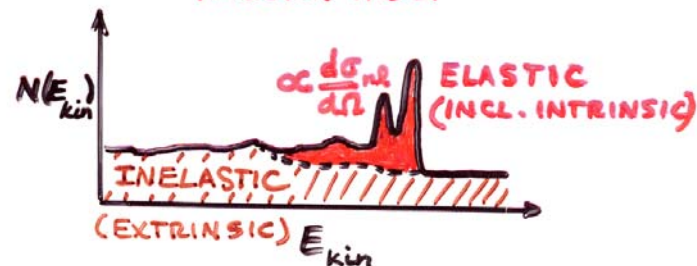
Rennie et al.,
J. Phys. At. Mol. Opt.
Phys. 32, 2691 (1999)





ADDITIONAL SOURCES OF STRUCTURE (AND INFORMATION!) IN SPECTRA BEYOND CHEMICAL SHIFTS

REALLY ALL AT ONCE, BUT SUM RULES + THEORY HELP



Outline

Surface, interface, and nanoscience—short introduction

Some surface concepts and techniques→photoemission

Synchrotron radiation: experimental aspects

Electronic structure—a brief review

**The basic synchrotron radiation techniques:
more experimental and theoretical details**

Core-level photoemission

Valence-level photoemission

 **Microscopy with photoemission:**
**All of the above with lateral spatial resolution
of ca. 20 nm, going down to few nm in future**
(Next lecturers)

Thank you for your attention!